W. A. Davis

NATIONAL ACADEMIES OF SCIENCE AND ENGINEERING

NATIONAL RESEARCH COUNCIL

of the

UNITED STATES OF AMERICA

UNITED STATES NATIONAL COMMITTEE

International Union of Radio Science

National Radio Science Meeting

5-7 January 1983

Sponsored by USNC/URSI
in cooperation with
Institute of Electrical and Electronics Engineers

University of Colorado
Boulder, Colorado
U.S.A.

National Radio Science Meeting
5-7 January 1983
Condensed Technical Program

TUESDAY, 4 JANUARY

1300	
IEEE-GAP AD COM Meeting	Pacific Exchange Room, Broker Inn
2000-2400	
USNC-URSI Meeting	Broker Inn

WEDNESDAY, 5 JANUARY

0900-1200	
A-1 Measurement Principles and Practices-I	CR1-46
B-1 Electromagnetic Theory	CR2-6
F-1 CCIR Special Session on Propagation in Non-Ionized Media	CR2-26
G-1 Ionospheric Modeling	CR1-40
H-1 The Plasma Wave Environment of Jupiter	CR2-28
J-1 Low Noise Receivers for Radio Astronomy	CR0-30
1140-1200	
H-2 General Topics	CR2-28
1330-1700	
A-2 Measurement Principles and Practices-II	CR1-46
B-2 Guided Waves	CR2-6
B-3 Numerical Methods	CR0-14
C-1/J-2 Radar Astronomy	CR0-30
E-1 Noise and Interference - Estimation and System Design	CR0-12
F-2 Effects of Precipation on Microwave Systems - Depolarization, Space Diversity, Backscatter Intensity	CR2-26
G-2 Ionospheric Scintillation	CR1-40
H-3 Wave Emissions From Natural Electron Beams in Space	CR2-28
1645	
Commission A Business Meeting	CR1-46
1700	
Commission C Business Meeting	CR0-30
Commission F Business Meeting	CR2-26
1730	
Commission E Business Meeting	CR0-12
Commission H Business Meeting	CR2-28

United States National Committee

INTERNATIONAL UNION OF RADIO SCIENCE

PROGRAM AND ABSTRACTS

National Radio Science Meeting
5-7 January 1983

Sponsored by USNC/URSI in cooperation
with IEEE groups and societies:

Antennas and Propagation
Circuits and Systems
Communications
Electromagnetic Compatibility
Geoscience Electronics
Information Theory
Instrumentation and Measurement
Microwave Theory and Techniques
Nuclear and Plasma Sciences
Quantum Electronics and Applications

Hosted by:

National Oceanic and Atmospheric Administration
National Bureau of Standards
National Telecommunications and Information Administration
University of Colorado at Boulder
and
The Denver-Boulder Chapter, IEEE/APS

NOTE:

Programs and Abstracts of the USNC/URSI Meetings are available from:

USNC/URSI
National Academy of Sciences
2101 Constitution Avenue, N.W.
Washington, DC 20418

at $2 for meetings prior to 1970, $3 for 1971-75 meetings, and $5 for 1976-83 meetings.

The full papers are not published in any collected format; requests for them should be addressed to the authors who may have them published on their own initiative. Please note that these meetings are national. They are not organized by the International Union, nor are the programs available from the International Secretariat.

MEMBERSHIP

United States National Committee

INTERNATIONAL UNION OF RADIO SCIENCE

Chairman:
Prof. Thomas B.A. Senior*
Vice Chairman:
Prof. Robert K. Crane*
Secretary:
Dr. Thomas E. VanZandt*
Immediate Past Chairman:
Dr. C. Gordon Little*

Members Representing Societies, Groups and Institutes:

American Geophysical Union	Dr. Christopher T. Russell
Bioelectromagnetics Society	Dr. James C. Lin
Institute of Electrical & Electronic Engineering	
IEEE Antennas & Propagation Society	Dr. Alan W. Love
IEEE Communications Society	Prof. Raymond Pickholtz
IEEE Electromagnetic Compatibility Society	
IEEE Information Theory Group	
IEEE Microwave Theory & Techniques Society	
IEEE Quantum Electronics Society	Prof. Herman A. Haus
Optical Society of America	Dr. Steven F. Clifford

Liaison Representatives from Government Agencies:

National Telecommunications & Information Administration	Dr. Douglass D. Crombie
National Science Foundation	Dr. Vernon Pankonin
Department of Commerce	
National Aeronautics & Space Administration	Dr. Erwin R. Schmerling
Federal Communications Commission	Mr. William A. Daniel
Department of Defense	Dr. George L. Salton
Department of the Army	Lt. Col. Roberty Clayton, Jr.
Department of the Navy	Dr. Leo Young
Department of the Air Force	Dr. Allan C. Schell

Members-at-Large: Dr. Sidney A. Bowhill
Dr. Juergen E. Richter
Dr. George W. Swenson, Jr.

*Member of USNC-URSI Executive Committee

Chairmen of the USNC-URSI Commissions:

Commission A	Dr. Helmut Hellwig
Commission B	Prof. Chalmers M. Butler
Commission C	Dr. Andrew J. Viterbi
Commission D	Drs. K.J. Button and A.A. Oliner
Commission E	Dr. Arthur A. Giordano
Commission F	Dr. Earl E. Gossard
Commission G	Dr. Kenneth Davies
Commission H	Dr. Robert F. Benson
Commission J	Prof. Mark A. Gordon

Officers of URSI resident in the United States:
(including Honorary Presidents)

President	Prof. William E. Gordon*
Honorary President	Prof. Henry G. Booker*

Chairmen and Vice Chairmen of
Commissions of URSI resident
in the United States:

Chairman of Commission C	Prof. Jack K. Wolf
Vice Chairman of Commission G	Dr. Jules Aarons

Foreign Secretary of the U.S.
National Academy of Sciences — Dr. Thomas F. Malone

Chairman, Office of Physical
Sciences-NRC — Prof. William A. Fowler

NRC Staff Officer — Mr. Richard Y. Dow

Honorary Members: — Dr. Harold H. Beverage
Dr. Ernst Weber

*Member of USNC-URSI Executive Committee

DESCRIPTION OF THE

INTERNATIONAL UNION OF RADIO SCIENCE

The International Union of Radio Science is one of 18 world scientific unions organized under the International Council of Scientific Unions (ICSU). It is commonly designated as URSI (from its French name, Union Radio Scientifique Internationale). Its aims are (1) to promote the scientific study of radio communications, (2) to aid and organize radio research requiring cooperation on an international scale and to encourage the discussion and publication of the results, (3) to facilitate agreement upon common methods of measurement and the standardization of measuring instruments, and (4) to stimulate and to coordinate studies of the scientific aspects of telecommunications using electromagnetic waves, guided and unguided. The International Union itself is an organizational framework to aid in promoting these objectives. The actual technical work is largely done by the National Committee in the various countries.

The officers of the International Union are:

President:	W. E. Gordon (USA)
Past President:	W. N. Christiansen (Australia)
Vice Presidents:	A. L. Cullen (U.K.)
	A. P. Mitra (India)
	S. Okamura (Japan)
	A. Smolinski (Poland)
Secretary-General:	J. Van Bladel (Belgium)
Honorary Presidents:	G. Beynon (U.K.)
	H. G. Booker (USA)
	W. Dieminger (West Germany)
	I. Koga (Japan)
	J. A. Ratcliffe (U.K.)

The Secretary-General's office and the headquarters of the organization are located at Avenue Albert Lancaster 32, B-1180 Brussels, Belgium. The Union is supported by contributions (dues) from 38 member countries. Additional funds for symposia and other scientific activities of the Union are provided by ICSU from contributions received for this purpose from UNESCO.

The International Union, as of the XXth General Assembly held in Washington, D.C., in August 1981, has nine bodies called Commissions for centralizing studies in the principal technical fields. The names of the Commissions and their chairmen follow.

A. Electromagnetic Metrology
V. Kose (FRG)

B. Fields and Waves
H. G. Unger (FRG)

C. Signals and Systems
J. K. Wolf (USA)

D. Electronic and Optical Devices and Applications
J. Le Mézec (France)

E. Electromagnetic Noise and Interference
S. Lundquist (Sweden)

F. Remote Sensing and Wave Propagation
D. Gjessing (Norway)

G. Ionospheric Radio and Propagation
P. Bauer (France)

H. Waves in Plasmas
M. Petit (France)

J. Radio Astronomy
V. Radhakrishnan (India)

Every three years the International Union holds a meeting called the General Assembly, the next is the XXIst, to be held in Florence, Italy, in August/September, 1984. The Secretariat prepares and distributes the Proceedings of these General Assemblies. The International Union arranges international symposia on specific subjects pertaining to the work of one or several Commissions and also cooperates with other Unions in international symposia on subjects of joint interest.

Radio is unique among the fields of scientific work in having a specific adaptability to large-scale international research programs, since many of the phenomena that must be studied are world-wide in extent and yet are in a measure subject to control by experimenters. Exploration of space and the extension of scientific observations to the space environment are dependent on radio for their research. One branch, radio astronomy, involves cosmic phenomena. URSI thus has a distinct field of usefulness in furnishing a meeting ground for the numerous workers in the manifold aspects of radio research; its meetings and committee activities furnish valuable means of promoting research through exchange of ideas.

Steering Committee

S. W. Maley, Chairman
D. C. Chang
D. Cook
R. Y. Dow
P. L. Jensen
C. G. Little
T. B. A. Senior
T. E. Van Zandt

Technical Program Committee

T. E. Van Zandt, Chairman
R. F. Benson
C. M. Butler
K. Davies
H. Hellwig
M. A. Gordon
E. Gossard
M. Grossi
M. Nesenbergs
A. D. Spaulding
M. Kindren, Secretary to the Committee

MEASUREMENT PRINCIPLES AND PRACTICES - I

Commission A, Session 1, CR1-46

Chairman and Organizer: E. K. Miller, Lawrence Livermore National Laboratory, CA

A1-1 0830 **SPECIAL SESSION ON MEASUREMENT PRINCIPLES AND PRACTICES: INTRODUCTION AND OVERVIEW:** E. K. Miller, Lawrence Livermore National Laboratory, Livermore, CA 94550

The art of making scientific measurements has improved substantially in recent years. In contrast to past relatively limited measurement capability, today's technology offers much greater variety, sensitivity and sophistication to the experimentalist. Among the foremost reasons for the present situation is the computer, which is used not only for data acquisition and control, but for data processing as well. With the increased productivity, innovativity and economy offered by computer-based mneasurement systems, there exists a real challenge to exploit this capability as effectively as possible.

These special sessions are intended to explore various aspects of measurement technology in a coordinated way, beginning with the reasons why measurements are made, proceeding to explore principles, options and trade-offs, and continuing with data interpretation and presentation and concluding with standards and validation. The intent is to emphasize the basic commonality of many kinds of measurements and the interdisciplinary nature of their needs, by approaching the measurement problem from a systems viewpoint. Specific topics to be covered include such areas as:

1. the information aspect of measurements;
2. the cause-effect relationship;
3. the trade-off between information needs and costs;
4. experimental design and strategy;
5. deterministic and probabilistic aspects;
6. modeling of measurements;
7. signal processing and information extraction;
8. data presentation;
9. characterizing large systems from measurements;
10. measurement standards and validation.

A1-2
0845 A PROBLEM-ORIENTED APPROACH TO THE MODELING AND EXTRACTION OF INFORMATION CONTAINED IN MEASUREMENTS: A. S. Willsky, Department of Electrical Engineering and Computer Science, Massachusetts Institute of Technology, Cambridge, MA 02139

In this talk we discuss the problem of describing the information contained in measurements. Since all signal processing algorithms are based either explicitly or implicitly on a model of the way in which the information to be extracted is embedded in the measurement data, we focus our attention on the model. It is our contention that this focus is essential in any fundamental discussior of why one measures and how one assesses the value of a particular measurement collection system.

What a model/problem-oriented perspective makes explicit is what is all too often left implicit. Specifically, formulating a model and a problem requires one to specify precisely what is known a priori about the nature of the data and about the type of information one would like to extract. Obviously such specifications aren't easy to find and once specified would typically be the subject of debate. In fact, this is precisely our point. This perspective forces one to focus attention where it should be focused: on what one knows and what one would like to find out.

As we discuss, there are some extremely useful quantitative tools which in many problems allow one to compute the accuracy with which particular model parameters can be estimated from a given set of data. These tools provide the basis for a systematic, scientific investigation of many questions ranging from assessing the practical utility of particular models for signal processing (given that models and reality typically don't coincide) to determining the adequacy of a particular measurement collection system for a specified set of modest and perhaps immodest objectives. In order to keep the discussion from floating off into the air, we use the problem of tomography to illustrate our points.

A1-3 0930 PHENOMENOLOGICAL ISSUES IN MEASUREMENTS: EXAMPLES FROM REMOTE SENSING Calvin T. Swift and Robert E. McIntosh, University of Massachusetts, Amherst, Massachusetts 01003

Physical interactions allow us to indirectly measure various kinds of information. Understanding the cause--effect relationship between the physical interaction and the measurement is very useful. In many cases of interest, we have only a phenomenological understanding of this relationship. This understanding is useful if a comprehensive amount of empirical data can be obtained that shows how measurements are correlated to the physical interaction.

In this paper we will review how a K-band radar successfully measured the wind speed over the ocean surface from the Sea Sat oceanographic satellite. Here the relationship between the wind speed and the surface scattering cross section had to be carefully determined for a wide variety of wind conditions. We will also discuss how hurricane parameters such as wind speed and rainfall rate have been measured with radiometers and radars mounted in aircraft.

A1-4
1020 THE ROLE OF STATISTICS AND UNCERTAINTIES IN MEASUREMENTS T. H. Lehman, Albuquerque, New Mexico, and Robert M. Mason, Booz-Allen and Hamilton, Inc., Albuquerque, New Mexico 87106

Sources of uncertainty are always present in system level measurement programs. For simple systems, characterized by a small number of degrees of freedom and/or a small number of sources of uncertainty, it is usually possible to control the impact of the uncertainties on the measurement results either through experimental design or analysis. For complex systems, characterized by a large number of degrees of freedom and/or a large number of sources of uncertainty, the validity and usefulness of measurement results are often in question since many of the uncertainties appear to be uncontrollable. In this paper we explore methods for controlling, managing and reducing uncertainties associated with complex system measurements. Emphasis is placed on the requirements for completeness, resolution and experimental efficiency. Methods for evaluating, characterizing and quantifying the uncertainties associated with each of these requirements are discussed. It is demonstrated that "classical" statistical techniques are in most instances inadequate. In particular, it is shown that "unbounded" distributions (normal, log. normal, etc.) do not adequately address the above requiremments and that bounded distributions (beta, extreme value, etc.) are usually more appropriate. As a consequence, system level measurement procedures must incorporate system and physical models of sufficient detail to address these requirements.

A1-5 1050 EXPERIMENTAL DESIGN AND STRATEGY: CONCEPTS AND THEORY Richard W. Mensing, Lawrence Livermore National Laboratory, Livermore, CA 94550

Measurements are accumulated for a variety of reasons, for example, to estimate a physical constant, to estimate the characteristics of a random phenomenon, to estimate, test and/or verify a relationship between variables, etc. Also, measurement situations arise in many environments ranging from a well controlled laboratory environment to the uncontrollable natural environment that exists in the field, thus introducing variability and uncertainty into the measurement process. To assure that the experimental objectives can be met, it is crucial that the procedure for accumulating measurements be well thought out.

Experimental design and strategy deals with planning the pattern of data accumulation. Careful design can assist the experimenter in decreasing the number of measurements and consequent cost, simplify the data processing, and properly handle experimental variation and uncertainty. Concepts of experimental design, such as the appropriate selection of variables, spacing of variables, number of measurements and sequencing of measurements are the topics of this paper. Theoretical concepts along with illustrative examples will be presented.

A1-6 EXPERIMENTAL DESIGN AND STRATEGY: APPLICATIONS
1130 H. S. Boyne, Department of Earth Resources, Colorado State University, Fort Collins, Colorado 80523

Experimental design and strategy are necessary conditions for a successful experimental program. Experimental design is dependent on defining the experimental goals to be achieved. Strategy is concerned with analyzing the most efficient means for achieving the goals. Examples of both well thought out, and poorly thought out, designs and strategies are discussed.

ELECTROMAGNETIC THEORY
Wednesday morning, 5 Jan., CR2-6
Chairman: David A. Hill, National Bureau of Standards, Boulder, CO 80303

B1-1 0920 FOCUS WAVE MODES IN HOMOGENEOUS MAXWELL'S EQUATIONS - TM MODES: James Neill Brittingham, Lawrence Livermore National Laboratory, Livermore, CA 94550

Last year new and unique mathematical formulations were presented [Focus Wave Modes in Homogeneous Maxwell's Equations - TE Modes, J. N. Brittingham, 1982 International Symposium Digest Antennas and Propagation, Vol. 2, pp. 656-659, Albuquerque, New Mexico] of some pulse functions. These mathematical solutions:

- o satisfy homogeneous Maxwell's equations,
- o are three-dimensional pulses,
- o are continuous and nonsingular,
- o propagate in a straight line at light-velocity,
- o remain focused as they propagate,
- o have a far-field identical to that of a stationary dipole in free space.

The terminology Focus Wave Modes [abbreviated FWM] comes from the characteristic that these pulses remain focused for all time. It is obvious that these mathematical solutions represent three-dimensional, source-free, nondispersive electromagnetic pulses which propagates at light-velocity in a straight line.

In the last paper the FWM electric and magnetic fields were presented as TE modes of propagation; the present paper presents the electric and magnetic fields for TM modes of propagation. The TM modes fields are shown to satisfy the homogeneous Maxwell's equations. They are continuous and nonsingular pulses which propagate at light-velocity. The three-dimensional shapes are demonstrated by showing that the pulses' magnitude away from the propagating pulse-centers decrease in front of, behind and transverse to the axis of propagations. These pulses focused nature are discussed along with the asymptotic behavior away from the propagating pulse-centers. By these mathematical proofs it has been demonstrated that these fields represent the TM modes of three-dimensional, source-free, nondispersive electromagnetic pulses which propagate at light-velocity.

---

*Work performed under the auspices of the U. S. Department of Energy by the Lawrence Livermore National Laboratory under contract number W-7405-ENG-48.

B1-2 0940 FOCUS WAVE MODES MIGHT PRESENT NEW REPRESENTATION FOR SINGLE PHOTON: James Neill Brittingham, Lawrence Livermore National Laboratory, Livermore, CA 94550

The TE modes solutions presented at a recent meeting are the first mathematical formulations of three-dimensional, source-free, nondispersive electromagnetic pulses [Focus Wave Modes in Homogeneous Maxwell's Equations - TE Modes, J. N. Brittingham, 1982 International Symposium Digest Antennas and Propagation, Vol 2. pp. 656-659, Albuquerque, New Mexico]. These pulses propagate in a straight line at light-velocity. They are not only nondispersive but the pulses' functional shapes remain fixed for all time as they propagate through free space. It is the focused nature of these functions which explains the terminology Focus Wave Modes [abbreviated FWM]. The pulses' functional values decrease in front of, behind, and transverse to the axis of propagation. The asymptotic behavior away from the propagating pulse-centers decreases as the inverse of the distance from the pulse-centers. This slow functional decline causes the pulses to have infinite electromagnetic energy associated with them. Since these are the first three-dimensional, source-free, nondispersive electromagnetic pulses appearing in the literature it is natural to question if these solutions might represent a single photon as it propagates through free space. The properties of a single photon are listed below:

1. single pulse of electromagnetic energy,
2. contains no charge or mass,
3. propagates nondispersively if undisturbed,
4. propagates at light-velocity in straight line,
5. has a frequency, ω,
6. has an angular momentum, $\pm$ h (normalized Planck's constant),
7. has energy, ω h,
8. has finite energy.

This paper will discuss the strong similarities between the FWM solutions and a single photon.

The basic mathematical structure of the FWM solutions shows that they do obey the first four items listed for the single photon. There are frequencies associated with the FWM solutions; therefore, item five is also satisfied. In classical electromagnetic theory there is a definition for the angular momentum and it can be shown that the FWM pulses do have an angular momentum. If one adjusted the mathematical parameters one could satisfy item six. There is also a net electromagnetic energy associated with the FWM solutions which could be adjusted to satisfy item seven. As has been mentioned above even though the FWM solutions are three-dimensional pulses they do have an infinite amount of electromagnetic energy associated with the wave; therefore, item eight cannot be satisfied with the present formulations. The strong connection between the FWM solutions and single photons are presented here hoping to generate future research into this area. If one could find FWM solutions which have finite energy then those solutions look much like a single photon.

*Work performed under the auspices of the U. S. Department of Energy by the Lawrence Livermore National Laboratory under contract number W-7405-ENG-48.

B1-3
1020

THE CONSTRUCTION OF A VECTOR POTENTIAL

Thomas B.A. Senior
Department of Electrical and Computer Engineering
The University of Michigan, Ann Arbor, MI 48109

For the solution of certain low frequency scattering problems it is necessary to determine a vector potential $\bar{A}$ such that $\nabla \times \bar{A} = \nabla\phi$ where ϕ is a known exterior potential arising from some distribution (charge or dipole) over a surface S. This is a rather classical problem in potential theory and, as shown by Stevenson (Q. Appl. Math. 12, 194-197, 1954), a solution exists if $\nabla^2\phi$ outside and on S and $\int_S \partial\phi/\partial n \, dS = 0$ where $\hat{n}$ is a unit vector normal to the surface.

When S is a closed surface, a method for the construction of $\bar{A}$ has been given by Stevenson. If ϕ is a magnetostatic potential produced by a field incident on the perfectly conducting surface S, ϕ can be expressed as a double layer distribution and $\bar{A}$ is given immediately in terms of the boundary values of $\phi + \phi^{inc}$, where ϕ^{inc} is the incident field potential. The result is also applicable to a curved shell or plate of infinitesimal thickness. On the other hand, if ϕ is an electrostatic potential associated with an isolated conductor, ϕ is naturally expressed as a single layer distribution, and the determination of $\bar{A}$ then requires the solution of a subsidiary (interior Neumann) potential problem, equivalent to the representation of ϕ as a double layer distribution. The construction now fails if S has zero interior volume.

Methods for the construction of $\bar{A}$ in the case of a curved or flat shell (or plate) are discussed. Not surprisingly, each involves the solution of a subsidiary problem, and no way to avoid this has been found. To illustrate the methods, some results for a circular disk are presented.

B1-4 1040 THE T-MATRIX AND MODIFIED GREEN'S FUNCTIONS: R. E. Kleinman, Applied Mathematics Institute, University of Delaware, Newark, DE 19711

The relationship between the so-called T-Matrix approach and a modified Green's function method for scattering problems is derived in the simplest case of acoustic scattering by impenetrable scatterers. First the null field equations are derived by a simple application of Green's theorem and these are then used together with a particular set of expansion functions to arrive at a representation of the solution in terms of the T-Matrix. Then an entirely independent approach is carried out using an integral equation whose kernel is the usual free space Green's function modified by the addition of a linear combustion of radiating multipoles with unknown coefficients. When the coefficients are chosen optimally, in the sense that the modified Green's function is the best least squares approximation to the exact Green's function, the coefficients are shown to be precisely the elements of the T-Matrix. This clarifies the nature of the T-Matrix approach.

CCIR SPECIAL SESSION ON PROPAGATION IN NON-IONIZED MEDIA
Wednesday morning, 5 Jan., CR2-26
Chairman: H.T. Dougherty, NBS, Boulder, CO

F1-1 0900 APPLICATION AND EVALUATION OF THE CCIR RAIN ATTENUATION PREDICTION MODEL FOR EARTH-SPACE PATHS: Louis J. Ippolito, NASA Headquarters, Washington, DC 20546

The CCIR, at its XVth Plenary Assembly in Geneva, approved, for the first time, an empirical global prediction procedure for slant path attenuation caused by rain (Report 564-1 (Mod F), Geneva, 1982). The procedure determines annual (and worst month) attenuation distributions from rain rate distributions, either locally generated or available from a global map of rainfall zones.

The CCIR procedure was modified in June at the RARC SAT-R2 Conference Preparatory Meeting (CPM), based on recommendations of IWP 5/2, which met in May of this year (CPM Doc. A/43 with Addendum, Geneva, 1982). The modifications attempt to improve rain attenuation predictions in tropical climates by adjusting the vertical rain height profile as a function of ground station latitude.

In this paper, the original and modified CCIR models are applied to an extensive set of data observations throughout the world and the mean and standard errors evaluated. Particular emphasis is placed on the 14/12 GHz broadcast satellite bands in Region 2, and the 30/20 GHz fixed satellite bands for the United States, where extensive data sets are available. The advantages and limitations of the CCIR procedure are discussed, and the results are compared to other published rain attenuation models.

F1-2
0920 EVALUATION OF PREDICTION MODELS OF RAINFALL EFFECTS:

H. T. Dougherty and E. J. Dutton, U.S. Department of Commerce, NTIA/ITS, Boulder, CO 80303

There has been sufficient progress in developing the relationships between rainfall and its effects upon microwave signals to also explore those relationships as the bases for predicting the effects of rainfall. Both basic relationship and its adaptation to a prediction method are subject to continuing development and testing, of course. However, a difficulty arises unless one recognizes that the relationship and the prediction method usually do not utilize the same rainfall data nor the same criteria for verification. For example, in the case of rainfall rain rates and their attenuation of microwaves (at a given frequency for a specific locale), one compares observations of microwave attenuation A_o with the attenuation values calculated either:

(a) by the rain rate/attenuation relationship $A_c = f(R_o)$ from observed rain rates R_o to verify the relationship $A = f(R)$

or (b) by the prediction model $A_p = g(R_p)$ from predicted rain rates R_p to verify the prediction methods $A = g(R)$.

Further, for comparison with A_o, the acceptance criteria of A_c and A_p are usually not the same.

F1-3 0940 ATTENUATION DERIVED FROM RADIOMETRIC MEASUREMENTS: W. J. Vogel, EERL - The University of Texas, Austin, TX 78758

The present lack of beacon transmitters on satellites for the determination of space-earth attenuation statistics has revived interest in radiometric measurements. A review of the literature reveals that the interpretation of sky temperatures as an indication of extinction is not straightforward, however, especially as the frequencies of interest are increasing to above 40 GHz.

For this reason a comparison of the various methods of calibration published is made. These are either in terms of sky temperature, or directly in attenuation when simultaneous sun tracker, beacon, or radar measurements were made. With increasing frequency more of the extinction is due to scattering and therefore the impact of scattering on radiometric attenuation measurements has to be considered. Also of importance are antenna characteristics such as beamwidth, sidelobe levels, and polarization as well as the structure of the precipitation, and the drop size distribution.

The impact of all these factors on the quality of the radiometrically derived fade statistics is evaluated.

F1-4
1020

PROPAGATION EFFECTS FOR LAND MOBILE SATELLITE SYSTEMS:

E. K. Smith, JPL, California Institute of Technology, Pasadena, CA 91109; J. F. Cavanagh, Naval Surface Weapons Center, Dahlgren, VA 22448; and W. L. Flock, Department of Electrical Engineering, University of Colorado, Boulder, CO 80309

At the Final Meeting (Geneva, 1981) of CCIR Study Group 5 the U.S. delegation agreed to submit material for an overview report on Land Mobile Satellite propagation effects from 100 MHz to 250 GHz. This preparatory effort has been underway in the U.S. since June of 1982 with a focus on the 800 to 900 MHz band. This paper is a presentation of the current state of affairs. A parallel effort is in progress in the U.S. for propagation effects for maritime mobile satellite systems.

The paper offers an overview of the land mobile satellite problem, including a survey of ionospheric as well as tropospheric effects but concentrates on the latter. The approach is to consider impairments to the direct wave and the behavior of the coherent ground-reflected wave and the diffuse component using the Beckman Spizzichino approach (The Scattering of Electromagnetic Waves from Rough Surfaces 1963, MacMillan).

The general conclusions are that more attention is needed to practical methods for handling terrain and urban multipath for the satellite to mobile vehicle case and that use of the static ground "constants" (dielectric constant and conductivity) is inappropriate when carried to the higher frequencies.

F1-5 1040 DEPOLARIZATION OF EARTH-SPACE MILLIMETER WAVE SIGNALS:

D. L. Runyon, W. L. Stutzman, C. W. Bostian, and T. Pratt, Department of Electrical Engineering, Virginia Polytechnic Institute and State University, Blacksburg, VA 24061

Dual polarized earth-space communication links operating in the millimeter wave region are adversely affected by precipitation. The prediction of attenuation levels that are likely to be encountered during a typical year has received considerable study and can be calculated using one of several reliable models. Such predictions are based on local rain rate statistics or global rain rate models. For dual polarized radio signals the depolarization associated with rain attenuation is important, as well as depolarization introduced by non-attenuating ice clouds along the path. The communication system designer would like to be able to predict depolarization along with attenuation. This is accomplished with a relationship of cross-channel isolation as a function of attenuation. This paper examines the isolation-attenuation relationship. Measured data on a world wide basis are discussed, as well as the theoretical modeling of isolation. The dependence of earth-space communication link performance on rain/ice parameters are examined.

F1-6 1100 DIVERSITY RECEPTION IN SINGLE AND DUAL-POLARIZED 10-30 GHz SATELLITE SYSTEMS: G. C. Towner III, J. M. Gaines, T. Pratt, W. L. Stutzman, and C. W. Bostian, Department of Electrical Engineering, Virginia Polytechnic Institute and State University, Blacksburg, VA 24061

Diversity gain is defined as the difference between the single-site and joint attenuation at a given probability level. As a statistical quantity it provides no information on the time behavior of a diversity receiving system - i.e. on how much lost signal can be recovered through diversity reception at a given instant. This paper introduces a new quantity called instantaneous diversity gain to describe the difference between the single-site and joint attenuations at the same instant of time. The paper presents the results of a theoretical and experimental study of instantaneous diversity gain and compares its behavior with statistical diversity gain. It discusses how diversity gain can best be used in power budget calculations and describes the performance of some hypothetical single and dual-polarized diversity receiving systems.

F1-7 1120 EFFECT OF TERRAIN IRREGULARITY ON GROUND WAVE PROPAGATION:

Alfonso Malaga, SIGNATRON, Inc., Lexington, MA 02173

The effect of terrain irregularities on ground wave propagation depends on a number of factors such as the size of the irregularities relative to the wavelength, ground conductivity, frequency, polarization, etc. When the terrain irregularity is much smaller than the wavelength, small terrain irregularities result in increased attenuation of the ground wave field. When the irregularities are in the order of or larger than the wavelength, terrain obstructions result in a weaker ground wave field at low frequencies and a stronger ground wave field at higher frequencies (vertical polarization). The frequency at which the transition from increased attenuation to enhanced ground wave field occurs depends on the ground conductivity. In this paper results which illustrate the frequency and ground conductivity dependence of the effects of isolated terrain irregularities on ground wave propagation are given.

Commission G Session 1

IONOSPHERIC MODELING
Wednesday morning, 5 Jan., CR1-40
Chairman: C. Rush, NTIA/ITS, Boulder, CO 80303

G1-1
0840 THEORETICAL IONOSPHERIC MODELING: D. N. Anderson, Air Force Geophysics Laboratory, Space Physics Division, Hanscom AFB, MA 01731

A brief overview of theoretical ionospheric modeling is presented with emphasis on the low and midlatitude F region. Ion and electron density distributions are obtained by solving the time-dependent plasma continuity and momentum equations including the effects of ionization production by solar ultraviolet radiation, loss through charge exchange and transport by diffusion, neutral wind and $\overline{E} \times \overline{B}$ drift. The results of a study to improve global maps of monthly median values of the F2-region critical frequency, foF2, using values determined from this theoretical model are presented. This was accomplished by including into the theoretical calculations realistic physical processes along with a realistic geomagnetic field model. An extension of this study to investigate the longitudinal differences in the low latitude F region ionosphere is discussed. Another study addresses the problem of the post-sunset ambient ionosphere at low latitudes and its influence on the formation of equatorial bubbles. It is found that the flux-tube integrated Pedersen conductivity profiles which affect instability growth rates are significantly altered by changes in the assumed F1 region electron density profiles. Modeling total electron content and airglow observations at Ascension Island will also be touched on.

G1-2 0900 MODELING OF THE ELECTRIC FIELD IN THE POLAR IONOSPHERE:
S. Matsushita, High Altitude Observatory, NCAR, Boulder, CO 80307

Ionospheric and field-aligned currents as well as electric fields in the polar region can be theoretically estimated from ground-based geomagnetic data with an electric conductivity model. Birkeland field-aligned current pairs have always been found in the polar region except during unusually quiet periods. Polar ionospheric fields have been estimated for different seasons, IMF sectors, and geomagnetic activity periods. Obtained field distributions show a divergence around early morning - dawn and a convergence around late afternoon - evening at 75°-80° latitudes: eastward fields are predominant in the day side while westward fields are dominative at night. This pattern can be used for the modelling of the polar electric field, although the intensity depends on the amount and gradient of the electric conductivity.

Ionospheric electric potentials have been presented in a perspective manner for quiet and disturbed periods. One example is shown below where α represents the angle in degrees between the line of sight and the colatitude-longitude plane. It can be seen that the electric field of high-latitude origin decays more rapidly with colatitudes in the evening sector than the field in the early morning.

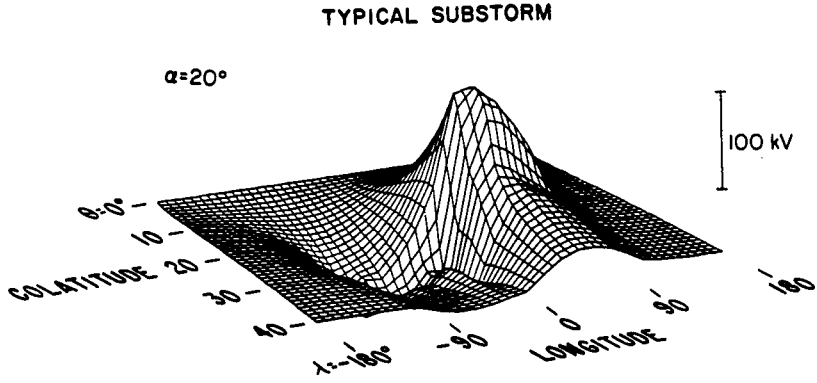

G1-3 0920 IONOSPHERIC MODELS USED BY THE AUSTRALIAN IONOSPHERIC PREDICTION SERVICE: L. F. McNamara, Air Force Geophysics Laboratory, Hanscom AFB, MA 01731

The Australian Ionospheric Service (IPS) routinely provides monthly median MUF and field strength predictions to several hundred organizations in Australia and other countries. The MUF predictions are based on empirical maps of the ionosphere which in some places represent some 40 years of data. Field strength calculations use the Bradley-Dudeney vertical N(h) profile modified to include a finite valley width. IPS can also make predictions of total electron content (TEC) using the IPS maps and the N(h) profile given by the International Reference Ionosphere. IPS is presently developing a model of the ionosphere which can be updated using real-time data from the IPS network of ionosondes. The model will take special account of the mid-latitude trough and will include provision for updating using TEC data from the NAVSTAR Global Positioning System of satellites.

* On leave from the Australian Ionospheric Prediction Service, Sydney, Australia

G1-4
0940 IONOSPHERIC MODELING - U.S. NAVY PERSPECTIVES: John M. Goodman, Ionospheric Effects Branch, E.O. Hulburt Center for Space Sciences, Space Science Division, Naval Research Laboratory, Washington, DC 20375

The U.S. Navy and its Laboratories have had a considerable impact upon the progress in ionospheric research over the years dating from the early experiments of Taylor, Young and Hulburt and the subsequent development of radar. Earliest attention was directed toward application of HF in Fleet communications and target detection and ranging. Nevertheless research has encompassed the frequency zones in the long wave region below HF and in the zones above HF as well. Other applications have included emitter geolocation, navigation, and certain surveillance functions. Satellites have been exploited to satisfy Navy C^3I and Navigation requirements directly and have also provided an opportunity to examine the ionospheric structures in considerable detail. This paper traces the depth and breadth of ionospheric modeling and related research within the Navy Community. Major ongoing R&D activities are outlined in the context of current and future projected Navy requirements.

G1-5 1020 MODELING OF VLF NIGHTTIME SIGNAL VARIATIONS: Maureen O'Brien, IRT Corporation, San Diego, CA 92106

One of the more saluatory features of VLF propagation is its excellent phase and amplitude stability under most conditions. One condition under which this can break down rather drastically is in the vicinity of a propagation null. Nighttime propagation characteristically has narrow, deep nulls—often tens of dB deep and only a few hundreds of kilometers wide. Therefore, changes in the ionosphere profiles which cause the depth or position of these nulls to change can cause enormous changes in signal amplitude at a fixed-site receiver located in one of these regions.

This paper analyzes some data taken by D. Morfitt in 1968 in one such null (NOSC TR 141, Sept. 1977). The data was collected at 28 kHz over five nights and consists of amplitude data only.

Amplitude fluctuations were related to H', an effective ionospheric height used in the NOSC models and statistics are provided. It is shown that to first order, ionospheric height fluctuations can be linearly related to an effective change in receiver position — thus making it possible to approximate signal fluctuations using only one set of propagation constants. The significance of this result for predicting VLF/LF communication link performance is discussed.

Work was done under contract for NOSC (N6601-81-C-0166) on the VLF/LF simulator.

G1-6 1040 LARGE SCALE SEPARATIONS OF FIELD ALIGNED DUCTS: S. H. Gross, Department of Electrical Engineering and Computer Science, Polytechnic Institute of New York, Farmingdale, NY 11735; and D. Muldrew, Communications Research Centre, Department of Communications, Ottawa, Ontario K2H852

Combination mode ducting is one of a number of non-vertical propagation phenomena observed at times by the Alouette and ISIS satellites in sounding the ionosphere. A number of cases were studied for passes over mid- and low latitude regions which exhibited distinguishable, nearly uniformly spaced traces on the ionograms typical of this type of propagation in the frequency range above 1MHz to about 2MHz. Associated extraordinary vertical and ducted traces were evident in all cases. The combination mode traces are interpreted as due to MF ducts below the satellite, whereas the ducted trace is interpreted as due to an MF duct encompassing the satellite at the time of measurement. The simultaneous presence of a ducted echo and combination mode echoes suggests the presence of a parallel system of ducts that are field aligned. On interpreting the ionograms for the events studied by ray tracing, it was found that the ducts are separated as much as 150 km transverse to their alignment. The data indicate that the ducts exist at least down to the order of 700 km altitude and possibly to 400 km and below. A multiplicity of ducts with such large separations was not previously appreciated, and the mechanism for creating them in this fashion is not clear. Whether they are stationary or traveling cannot be determined. Various possibilities range from irregularities resulting from field aligned currents to plasma instabilities and gravity wave excitation at lower altitudes.

G1-7 1100 OBSERVATIONS OF IONOSPHERIC ELECTRON DENSITY IRREGULARITIES BY SATELLITE-TO-SATELLITE, DUAL-FREQUENCY, DOPPLER TRACKING LINK: Robert D. Estes and Mario D. Grossi, Harvard-Smithsonian Center for Astrophysics, Cambridge, MA 02138

We illustrate the low-low, satellite-to-satellite, dual-frequency, Doppler tracking experiment performed by our Observatory on the occasion of the 1975 Apollo-Soyuz Test Project (ASTP), and we analyze the data for irregularities in electron density at the altitude of 221 Km. The differential Doppler data with the relative motion term removed were integrated to obtain a picture of the electron density variation along the satellite path. Well-known large-scale features such as the equatorial geomagnetic anomaly and day/night ionization level differences are clearly observed in the integrated data. The larger crest of the morning geomagnetic anomaly is seen to occur in the southern (winter) hemisphere in agreement with previous observations. In addition, we observe a very sharp peak in the electron density at the day-to-night transition point in two consecutive revolutions. We suggest that this effect may be due to the previously postulated atmospheric shock wave generated by supersonic motion of the terminator. Localized wave structures observed in the differential Doppler data are being further analyzed as possible travelling ionospheric disturbances.
(*)Present address: Massachusetts Institute of Technology, Cambridge, MA 02139

G1-8 1120 REAL TIME UPDATE OF HF PROPAGATION MODELS OF THE MUF USING OBLIQUE SOUNDER INFORMATION: Donald R. Uffelman, E. O. Hulbert Center for Space Sciences, Space Science Division, Ionospheric Effects Branch, Naval Research Laboratory, Washington, DC 20375

The Naval Research Laboratory has an active program which involves an assessment of the HF propagation channel by coupling computer models of the MUF to MOF data obtained from oblique sounders. Currently, this technique draws upon a model of maximum usable frequency encompassed in the Naval Ocean Systems Center PROPHET system (MINIMUF 3.5) and relates this model to real-time measurements of the maximum observed frequency over a reference path. Measurements from the reference path are used to update the model and the driving parameters which are ascertained from this process are used to access the maximum observed frequency over paths disjoint from the reference path.

In the experimental approach, NRL employs a network of oblique sounders to determine the success of the technique. One link in the network is designated the control path and the other links are designated as experimental paths to which the results of the model update are compared. The comparison criterion is RMS error between the modeled parameters and the measurements. Initial results indicate that for F-region propagation near the maximum observed frequency under benign and moderately disturbed conditions, update of the model improves performance by as much as a factor of four. It is suggested that this approach could be utilized in selective calling systems as well as automated frequency control of systems.

THE PLASMA WAVE ENVIRONMENT OF JUPITER
Wednesday morning, 5 Jan., CR2-28
Organizer: James L. Green

PLASMA WAVES IN THE JOVIAN MAGNETOSPHERE

H1-1 0840 W.S. Kurth, Department of Physics and Astronomy, University of Iowa, Iowa City, IA 52242

The Voyager encounters with Jupiter in 1979 provided the first survey of plasma waves in the Jovian magnetosphere. These observations have proven to be important in two respects. First, information on the various plasma waves present is critical in fully understanding the flow of mass and energy in the complex Jupiter-Io system. Second, these data provide the first glimpses of plasma waves in a non-terrestrial magnetosphere and, hence, are an invaluable benchmark in the analysis and interpretation of the terrestrial analogs. In general, the plasma wave menagerie at Jupiter is surprisingly similar to that of the Earth.

We first review the fundamental plasma waves present at Jupiter keeping in mind the importance of wave-particle interactions in understanding the physics of planetary magnetospheres. Starting with the bow shock we see wave turbulence which is responsible for heating the solar wind. The magnetopause and the edge of the plasma sheet in the middle magnetosphere are accentuated by the presence of broadband electrostatic noise indicative of field-aligned currents which link the magnetopause and middle magnetosphere with the high-latitude ionosphere. The Io torus is characterized by whistler-mode chorus and hiss as well as electron cyclotron harmonic emissions, all of which pitch-angle scatter electrons and, hence, play an important role in the loss of energetic particles from the magnetosphere and the deposition of energy into the atmosphere.

In a sense, the Jupiter encounters are continuing at present and in addition to highlighting the major plasma wave phenomena studied heretofore, several new details in the Jovian plasma wave spectrum will be presented which are products of the on-going Jupiter Data Analysis Program. Examples include the first detection of lower harmonic electron cyclotron emissions in the outer magnetosphere, evidence for both ordinary and extraordinary mode trapped continuum radiation, narrowband electromagnetic emissions analogous to terrestrial escaping continuum radiation, and electrostatic bursts near but below the electron plasma frequency which are modulated by a low frequency wave such as chorus. In addition, evidence for a band of emission at the lower hybrid resonance frequency has been found in the Io torus. This band provides a measure of an effective A/Z for the plasma which decreases with increasing radial distance.

H1-2 0900 DECAMETRIC RADIO EMISSIONS FROM JUPITER: A NEW LOOK: J. L. Green, NASA/Marshall Space Flight Center, MSFC, AL 35812; D. Menietti, Southwest Research Institute, San Antonio, TX 78284; F. Six, Western Kentucky University, Bowling Green, KY 42101; S. Gulkis, Jet Propulsion Laboratory, Pasadena, CA 91103; and D. Gurnett, Department of Physics and Astronomy, University of Iowa, Iowa City, IA 52242

The Planetary Radio Astronomy experiment or PRA on Voyager 1 and 2 observed Jovian Decametric (or DAM) radiation from Jupiter for over one month before and after encounter with the giant planet. As measured by the PRA experiment the DAM emissions from 2 MHz to 40 MHz have a characteristic 'arc' like shape in frequency versus time spectrograms. Much work has already been done relating the observation of this emission with the position of the satellite Io. If Io's postion is essential for the emission to be observed, than the arc like structure is a manifestation of the dynamics of the motion of Io and Jupiter as seen by the spacecraft. A reorganization of the PRA data is necessary in order to account for the Io and Jupiter motion and to aid in the analysis of the DAM generation mechanism.

Nearly three months of PRA data were transformed into a coordinate system for which Io and Jupiter remain fixed and the spacecraft is allowed to measure DAM at all System III longitudes. A $1/(Rj)^2$ factor was employed to take into account the radial distance dependence of this emission. The characteristics and generation of the DAM emissions will be dicussed from the results of this data analysis technique and compared with recent ray tracing studies.

H1-3
0920

MODULATED HIGH-FREQUENCY ELECTROSTATIC BURSTS AT JUPITER AND SATURN

L.A. Reinleitner and W.S. Kurth, Department of Physics and Astronomy, The University of Iowa, Iowa City, IA 52242

Recent studies of the wideband plasma wave data taken at both Jupiter and Saturn by the Voyager 1 and 2 spacecraft have shown high frequency electrostatic bursts with some strong modulation effects. These bursts occur at approximately the local plasma frequency, and have a bandwidth of about 1 - 3 kHz. They show a striking similarity to some features investigated in the Earth's outer magnetosphere that are known to be associated with chorus. The bursts in the Earth's magnetosphere have been shown to be produced by enhancements in the electron distribution function at the chorus wave phase velocity. Evidence has been presented that these enhancements are electrons that are trapped in Landau resonance with the chorus wave. These electron enhancements then cause electrostatic bursts at a frequency close to the local plasma frequency by a two-stream type of instability.

Evidence is presented that the observed cases at Jupiter and Saturn are essentially identical to the bursts observed at the Earth. The bursts at Jupiter and Saturn have a time duration of only a few seconds at most, and are observed to be close to the local plasma frequency with a bandwidth of a few kHz. The bursts have a very sporadic nature, and are observed to turn on or to turn off with a time scale on the order of a few tens of milliseconds. Studies of the Voyager waveform data show that some of the bursts are strongly modulated at frequencies in the whistler-mode range. The anticipated whistler-mode waves are not directly observable, however, because of high levels of spacecraft interference at low frequencies. There is some modulation at higher frequencies that is unexplained at present. The plasma parameters for the observed cases at both Jupiter and Saturn are found to be essentially identical to those found at the Earth where similar bursts are observed. All of the similarities lead to the conclusion that these bursts are probably the same in nature and have the same generation mechanism as those observed in the magnetosphere of the Earth.

H1-4 0940 A COMPARISON OF JOVIAN AND TERRESTRIAL CHORUS: U. S. Inan and R. A. Helliwell, Radioscience Laboratory, Stanford University, Stanford, CA 94305; and W. S. Kurth, Department of Physics and Astronomy, University of Iowa, Iowa City, IA 52242

Data from the Plasma Wave Experiment on Voyager I satellite is used to compare the characteristics of VLF 'chorus' emissions observed in the Jovian magnetosphere with known properties of emission phenomena observed in the earth's magnetosphere. Initial comparisons indicate that the phenomena are remarkably similar in terms of normalized occurrence frequency, frequency-time slope, and wave intensity. More detailed comparison in terms of the L-shell of occurrence is complicated by the uncertainties in the magnetic field model for the Jovian magnetosphere. Comparisons in terms of the temporal growth rates should provide information on the parameters of the wave-particle interaction that is thought to stimulate these emissions. Similarities between rapid burst-like emissions (not necessarily to be classified as 'chorus') observed in the Jovian magnetosphere and similar phenomena observed in the terrestrial magnetosphere by the DE-1 satellite are also discussed.

GENERAL TOPICS
Wednesday morning, 5 Jan., CR2-28

H2-1 1040 SHORT-PULSED ATMOSPHERIC MASERS: NONLINEARITIES: M. M. Litvak, JPL/Caltech, Pasadena, CA 91109; and R. R. Anderson, University of Iowa, Iowa City, IA 52242

Terrestrial and Jovian short-pulsed radio emissions exhibit narrow frequency features of high brightness that drift in frequency with time over hundreds of milliseconds. These pulse features indicate power saturation and other nonlinear effects are occuring, effects such as stimulated Thomson (magnetoplasma) scatter. The spectral shapes observed in high-resolution (25 or 50 ms/sweep) spectrum-analyzer results on ISEE 1 & 2 data are consistent with the hyperbolic-secant-type shape expected from these nonlinear effects.

Computer solutions of the simultaneous, coupled, time-dependent equations for the distribution functions of the particles and the waves show pulsed maser behavior for the right-handed, extraordinary mode that agrees with observations at high resolution in time and frequency. The model attributes the pulsing to relaxation oscillations that arise from competition between the maser amplification and the stimulated scatter processes. When a pulse-feature, which resembles a soliton in wavevector space, drifts in frequency sufficiently far from the main maser growth frequency so that interconversion of the waves there with the soliton is weak, then the maser rapidly rebuilds a pulse-feature at that frequency to restart the cycle with another drifting soliton, in the frequency-time domain. The drifting itself is caused by the interconversion (scatter) of waves at one side of the pulse-feature wavevector distribution to the opposite side. Transfer is from high to low values of the wavevector component parallel to the magnetic field, if momentum is being given back to the electrons. The direction and speed of drift is dependent on the velocity distribution slope in the vicinity of the wave group-velocity parallel component.

Terrestrial source regions, about 10 km in latitudinal width, have almost uniform envelope electric field distributions at a given time, owing to the stimulated backscatter that provides feedback within each source and influences its neighborhood. Spatial gradients of the amplification plasma properties cause certain locations to become strong sources at the expense of neighboring locations. A spatial pattern both along and perpendicular to the magnetic field is expected from this nonlinear interaction, according to this model. The whole spatial source region undergoes the time-dependent changes in frequency spectrum, while significant disturbance of the electron distribution along the field occurs. Some cases of formation of cold, accelerated helical beams have been found in the nonlinear calculations.

H2-2 1100 RESONANT ABSORPTION IN A MAGNETIZED PLASMA: J. E. Maggs, G. J. Morales, and A. Banos, Jr., Institute of Geophysics and Planetary Physics, University of California at Los Angeles, Los Angeles, CA 90024

The transfer of energy from electromagnetic waves to electrostatic modes near plasma resonance is investigated in a magnetized warm plasma with a linear density gradient along the magnetic field. Electrostatic mode structure in this plasma environment is complicated. Mode conversion to short wave length Bohm-Gross modes from long wave length electrostatic modes propagating between the plasma and upper-hybrid resonances occurs near plasma resonance. The amount of mode conversion occurring depends upon angle of propagation and also exhibits an asymmetry between sources located in the underdense and overdense regions of the plasma. Wave guide-like modes can be excited from the overdense region of the plasma. The Green's function governing the transfer of energy from a left hand polarized electromagnetic wave to these electrostatic structures is briefly discussed. The discussion focusses on the direct generation of both short and long wave length electrostatic waves, with the subsequent indirect production of short scale lengths through mode conversion.

*Work supported by ONR.

H2-3
1120

EMISSION OF ELECTROSTATIC WAVES BY CURRENT SHEETS OF FINITE THICKNESS

K.S. Hwang, Ernest G. Fontheim, and R. S. B. Ong
Space Physics Research Laboratory, University of Michigan, Ann Arbor, MI 48109

We have investigated the emission of electrostatic ion cyclotron waves and of ion acoustic waves due to current-driven instabilities excited by a cold electron current sheet of finite thickness imbedded in a stationary background plasma. The source current is taken parallel to a steady background magnetic field. A two-dimensional model has been solved with the perpendicular velocity distribution of electrons and ions represented by Maxwellians. The parallel velocity distributions inside the current sheet are taken to be a delta function with drift velocity v_D for the electrons and a stationary delta function for the ions. Thus the current is carried by a cold electron beam. The electron parallel velocity distribution outside the sheet is Maxwellian, while the ion parallel velocity distribution outside the sheet is taken to be a stationary delta function. It is shown that as the sheet thickness increases, the number of potentially unstable wave modes also increases thereby expanding the wave emission spectrum. The variation of the instability threshold with current is also discussed.

H2-4 1140 NIGHTTIME EQUATORIAL F-REGION STRUCTURE AND DYNAMICS INFERRED FROM CORRELATED AE ION COMPOSITION AND GROUND-BASED IONOSONDE N_e MEASUREMENTS: Henry C. Brinton, NASA Headquarters, Washington, DC 20546; and Robert F. Benson, NASA/Goddard Space Flight Center, Greenbelt, MD 20771

Electron density profiles from ionosondes at Manila and Huancayo have been obtained during 3 nighttime overflights of the AE-E spacecraft. These profiles enabled the spacecraft location relative to the F region peak to be determined. Such position information is of fundamental importance to the interpretation of satellite ion composition and density measurements, particularly with regard to investigations of equatorial plasma bubble phenomena. The 3 cases corresponded to the conditions of the spacecraft above, within and below the F peak. The ion composition profiles were relatively smooth when AE was well above or well below the peak. Density bite-outs of as much as 4 orders of magnitude were observed in O^+, however, when AE was near the F peak. Simultaneous molecular ion composition variations imply that such extreme O^+ changes may be the result of a corregated structure to the bottom of the F region, possibly caused by neutral atmospheric gravity waves, which enable the steep bottomside F layer ionized density gradient to oscillate approximately 20 km up to the AE-E altitude. These conclusions are consistent with, and compliment, the radar backscatter results of Tsunoda and White [JGR, 86, 3610, 1981] and re-emphasize the need to use extreme caution in interpreting large in-situ density changes as equatorial plasma bubble encounters.

Commission J Session 1

LOW NOISE RECEIVERS FOR RADIO ASTRONOMY
Wednesday morning, 5 Jan., CRO-30
Chairman: S. Weinreb, National Radio Astronomy Observatory, Charlottesville, VA 22903

J1-1 0900 OWENS VALLEY LOW-NOISE K-BAND MASER RECEIVER: R. L. Moore, A. T. Moffet, and H. E. Hardebeck, Owens Valley Radio Observatory, California Institute of Technology, Pasadena, CA 91125; and D. Neff, Jet Propulsion Laboratory, California Institute of Technology, Pasadena, CA 91109

A low-noise, K-band, reflected-wave ruby maser amplifier has been successfully completed for use on the Owens Valley 40m telescope. The maser follows the design of Moore and Clauss (IEEE Trans. Microwave Theory Tech., MTT-27, 249-256, 1979) and is tunable from 18-24.5 GHz with an instantaneous bandwidth of 400-450 MHz. Net gain is a function of frequency and bandwidth and varies from 28-35 dB. The estimated contribution of the maser to the system temperature is 10-15°K. The maser is pumped with a Siemens backward-wave oscillator. A YIG-tuned Gunn oscillator is used over the entire frequency range as the mixer local oscillator. The maser is cooled to 4.5°K by a closed-cycle refrigerator built by Cryosystems, Inc. A waveguide Dicke switch, designed and built at JPL, provides beam-switching capability at rates up to 10 Hz. The cooled, 4.5°K switch is a significant departure from existing systems which use ambient temperature switching; it contributes only ~1°K to the system noise temperature. Dual, symmetric scalar feeds illuminate ~80% of the antenna surface. The feeds receive left circular polarization from the sky.

The receiver operates at the prime focus of the antenna. System temperatures as low as 40°K at zenith have been achieved at 22.23 GHz; system temperatures are lower at other frequencies. Spillover contributes <10°K to the system temperature. The peak sensitivity of the antenna is 0.1 °K/Jy, giving an aperture efficiency of ~25%. The relative gain peaks at a zenith angle of 40° and decreases to ~0.4 of the peak value at zenith and horizon. The system has been used since February 1982 for VLBI, continuum, and spectral-line observations.

This work has been supported by the NSF, the CIT President's Fund, and the JPL Director's Discretionary Fund. R. Clauss of JPL and C. Moore of NRAO provided valuable assistance.

J1-2 0920 SUB-MILLIMETER WAVELENGTH RECEIVERS--A STATUS REPORT: W. J. Wilson, Jet Propulsion Laboratory, Pasadena, CA 91109

The current status and performance of submillimeter receivers in the 300-1000 GHz frequency range will be reviewed. This review will include descriptions of sub-mm receivers currently in use (or planned) by various research groups. The noise performance of InSb mixers and Schottkey diode fundamental and harmonic mixers will be discussed. The various approaches for local oscillator sources including fundamental sources, such as carcinotrons and lasers, and frequency multipliers will also be covered.

J1-3 0940 A MULTIPLE-MIXER, CRYOGENIC RECEIVER FOR 200-350 GHz: J. W. Archer, National Radio Astronomy Observatory, Charlottesville, VA 22903

A new 200-350 GHz receiver design, incorporating multiple cryogenically cooled Schottky barrier diode, single ended mixers and GaAs I.F. amplifiers will be described. Each mixer is fixed tuned, covering a 30-40 GHz band of the input spectrum; three separate mixers are required for 200-350 GHz, with a fourth centered on 345 GHz. The receiver design allows dual polarization operation in each band. A total of eight mixers is required for complete spectral coverage and polarization diversity. Each mixer, with its I.F. amplifier, is mounted in an individual cryogenic sub-dewar, comprising a separate vacuum chamber and a cold station which may readily be thermally connected to or disconnected from the main refrigerator by a novel mechanical heat switch. Thus any mixer may easily be replaced without affecting the cryogenic operation of the remainder.

A dual polarization Martin-Puplett L.O. diplexer is mounted on a rotary table above the sub-dewars. The two diplexer R.F. output ports may be positioned over a pair of sub-dewars by rotating the assembly to one of four precisely indexed positions spaced 90° apart. The input beam to the diplexer remains precisely on-axis during rotation and the reference polarization planes remain fixed for each of the four positions. Each sub-dewar incorporates a groove-matched teflon lense, which, while coupling power to the mixer corrugated feed from the quasi-collimated beam of the diplexer, also serves as a vacuum window. L.O. power is injected into the diplexer via a lense and feed horn connected directly to a frequency tripler. The plane of polarization of the L.O. beam is set so as to simultaneously provide L.O. drive for both orthogonally polarized channels.

At the time of writing, receiver temperatures of less than 500K SSB have been measured between 210 and 240 GHz. Projected performance is for receiver temperatures of less than 800K SSB to 300 GHz and less than 1000K SSB at 345 GHz.

J1-4 THE BELL LABORATORIES SIS RECEIVER
1040

Antony A. Stark
Bell Laboratories
Holmdel, NJ 07733

A new 2 to 3 mm receiver consisting of a quasi-optical feed system, a superconductor-insulator-superconductor (SIS) heterodyne mixer and a cryogenically cooled FET IF amplifier has been constructed at the Nasmyth focus of the 7 m diameter offset Cassegrain antenna at Bell Laboratories. Its design was a group effort led by R. A. Linke. The quasi-optical feed (T. S. Chu and J. Bally) couples the receiver to the antenna with less than 0.5 dB loss for wavelengths between 1 and 4 mm. Hot and cold load calibration (P. F. Goldsmith), beam chopping, an image sideband rejection filter with cryogenic (17 K) termination of the image sideband (A. A. Stark), and local oscillator injection are all provided. The electronics are in a LHe cooled dewar (R. A. Linke) conveniently mounted on an optical bench in a non-tilting room. The beam enters the dewar through a double window: a plastic vacuum window followed by a coated single crystal quartz window which is maintained at about 70K. On the 4.7 K cold station is a corrugated horn, the SIS mixer, a bias "T," an isolator and the FET amplifier. The SIS junction (R. E. Miller and G. J. Dolan) is a 0.3 μm^2 Pb-In-Au stripline device having a normal resistance of 75 Ω. It is mounted in the mixer (R. A. Linke) across quarter-height waveguide in front of a movable, non-contacting backshort, and is connected to a stripline choke. In normal operation, the junction is biased with 2.4 mV DC and 1 nW of L.O. power from a frequency doubler (G. Knapp) driven by a phase-locked klystron (P. S. Henry). The IF amplifier (A. A. Stark) is based on the NRAO three FET design and has a noise temperature under 10K from 1.25 to 1.75 GHz.

The receiver works exceptionally well. It has been operational for three months without failure, in spite of a dozen coolings from room temperature. The SSB receiver temperature in single sideband mode (20 dB image rejection) measured at the focus of the Cassegrain secondary is under 180 K at 109 GHz over a 400 MHz wide IF passband. At 90 GHz and 135 GHz the receiver temperature rises to about 300K. In use it is a very stable radiometer, well suited to astronomical observations requiring long integration times. In all respects, it is superior to the cooled Schottky-barrier diode receiver it replaces.

J1-5 1100 SIS QUASIPARTICLE MIXING: DEVELOPMENT OF A QUANTUM LIMITED RECEIVER: W. R. McGrath, A. D. Smith, and P. L. Richards, Department of Physics, University of California, Berkeley, CA 94720

The possibility of developing quantum noise limited, near millimeter wave receivers for radio astronomy has been suggested by recent progress in superconductor-insulator-superconductor (SIS) tunnel junction receivers. Photon assisted tunneling theory, worked out by Tucker, quickly led to predictions that the highly nonlinear, quasiparticle current voltage characteristics of the SIS tunnel junction could be used to produce a mixer with unlimited gain and noise levels approaching the quantum photon fluctuation limit. This new technology has the potential of producing heterodyne receivers with sensitivities an order of magnitude better than those currently used in radio astronomy.

Progress in developing SIS mixers has been rapid and widespread. We have made the first measurement of large gain along with a single side-band noise temperature near the quantum limit (2.5K for 36 GHz). Our results for a single tin junction SIS mixer are: Conversion gain = 4.3±1dB, Mixer noise (SSB) = 9±6K, Local oscillator power = 0.8nW, and Input saturation power = 1.5pW.

Higher saturation powers than are attainable with a single junction mixer may be desirable for many receiver applications. By forming a series array of N identical junctions, the saturation limit is increased to N^2 times that of a single junction with the same rf impedance as the array. The conversion efficiency and the noise are predicted to be the same as for the single junction. We have measured the predicted conversion efficiency, but the noise is found to increase as $N^{1/2}$.

The quantum theory also predicts conversion gain and low noise for tunnel junctions made from two different superconductors (SIS' junctions). The inherent negative resistance in SIS' junctions allows for good mixer performance at higher operating temperatures and may ease fabrication requirements. We will discuss mixing experiments with In-Pb alloy SIS' junctions and computer modeling of a number of possible SIS' mixers.

We have constructed a low noise 36 GHz receiver as a prototype for balloon and space astrophysics projects. The receiver is designed to be operated in a vacuum cryostat with a junction temperature of 3K. This temperature limit is set by heat flow along the IF coaxial cable. It is adequate for our lead alloy type junctions which have a T_c near 7.5K. In order to reach temperatures of 1.5K so that tin junctions can be used, a receiver designed to operate in a bath of liquid helium has also been constructed. Single side-band receiver noise temperatures of $\sim$15K are expected for these receivers.

J1-6
1120

REPORT ON THE SIS QUASIPARTICLE RECEIVERS IN OPERATION AT THE OWENS VALLEY RADIO OBSERVATORY

D.P. Woody, Owens Valley Radio Observatory
Big Pine, CA

Superconductor Insulator Superconductor (SIS) quasiparticle receivers have been in operation at the Owens Valley Radio Observatory for more than two years. They are used on the 10 meter diameter millimeter wave telescopes and cover the frequency range from 80 to 300 GHz. They have proven to be low noise ($T_{REC,SSB} \lesssim 200$ K), reliable and easy to use. The receivers have been used for a variety of astronomical projects including single dish spectral line observations, two dish interferometry and 89 GHz VLBI observations.

The principal parts of the receivers are a scalar feedhorn, mixer block, backshort and L-band FET IF amplifier, all of which are cooled to $\sim$4 K. The LO is injected via a 1% reflecting dielectric beam splitter. Several different mixer block structures, including one fourth height rectangular and circular wave guide, have been used. Both liquid helium cryostats and closed cycle refrigerators are used to cool the receivers. Doubled Gunn oscillators, fundamental klystrons and multiplied klystrons are used as LO sources.

The receivers are the result of an extensive development program ranging from theoretical studies of the fundamental limits to mixer sensitivity to monitoring the performance of receivers during astronomical observations. Their noise temperatures have decreased steadily since the initial encouraging laboratory tests three years ago. The receivers presently in use with the millimeter wave interferometer have single-sideband receiver noise temperatures < 200 K. The improvements being incorporated in the next generation of receivers are expected to decrease the noise temperature to < 100 K. The performance should continue to improve as our understanding of the wave guide embedding network and microstructures close to the junction increases. The quantum theory of mixing in quasiparticle tunnel junctions predicts that 100 GHz receivers using the presently available junctions should be capable of reaching the quantum limit of $h\nu/k \sim$ 5K. Performance approaching this limit is likely in the next few years.

MEASUREMENT PRINCIPLES AND PRACTICES - II
Commission A, Session 2, CR1-46
Chairman: H. Boyne, Colorado State University

A2-1 1330 VALIDATING MODELS ON THE BASIS OF INFORMATION VALUE G. C. Corynen, Lawrence Livermore National Laboratory, P. O. Box 5504, L-156, Livermore, California 94550

Most models are developed to reach better decisions, or to improve some estimation process. To decide how much modeling effort should be expended, and how much model validation should be done, a model of the decision maker or estimator should also be developed. Such a model should explicitly account for the value of improved modeling and validation, also called information value.

Models approximate some "reality" of interest. Such approximations can be deterministic in the sense that some metric is used to measure the distance between the model and the object modeled, and values of this metric indicate a quality of the model. Or statistical measures can be used to determine a confidence level that the model faithfully represents reality. This also applies in describing the purposes for a model. A "purpose" may be defined as the decision maker's utility function on the space of model outputs. Roughly speaking, each output has a utility, and the objective of the modeling effort is to find the specific values of model parameters at which the utility function is maximized. These settings represent the optimal decision or the optimal value of the variable being estimated.

This utility function, which can include modeling and validation costs, is itself a model of the decision maker, and subject to similar approximations. Sometimes these approximations are overwhelming because the decision maker is not well known, and there is no point in developing accurate--and expensive--process models.

Our discussion presents a framework and some guidelines to obtain a level of model accuracy which is consistent with the accuracy with which the purposes of the modeling effort and the value of information are known.

A2-2
1400 INVERSE THEORY AND SIGNAL PROCESSING OF OBSERVATIONAL DATA D. W. Oldenburg, Department of Geophysics and Astronomy, University of British Columbia, #129-2219 Main Mall, Vancouver, B.C. V6T 1W5

Inverse theory provides a formulation by which many questions fundamental to signal processing may be entertained. In particular, for linear problems, some of these are: What unique information about a model (system, or transfer function) can be obtained from a finite number of accurate or inaccurate responses? What is the extra information about the model which can be inferred from an additional measurement, and how is this affected by the accuracy with which the observation is taken? Regarding experimental design, what is the optimum rate (or physical spacing) at which data should be collected? I will attempt to illustrate how such questions can be answered by using linear appraisal techniques and funnel function theory.

An alternate approach to extracting information from the recorded signal is to construct models which fit the data. A few techniques, robust to the presence of additive noise, will be introduced.

This talk will be illustrated with practical examples involving deconvolution, extinction of ionospheric current density from ground based magnetometers, and the inversion of laser interferometry data. If time permits, a non-linear problem, involving the estimation of the electrical conductivity of the earth from the ratio of the electric to magnetic fields recorded on the surface, will be presented.

A2-3
1505 DATA REPRESENTATION: GETTING INFORMATION FROM THE NUMBERS Steven P. Frysinger, Bell Laboratories, Whippany Road, Whippany, NJ 07981

Measurement and modelling activities frequently produce enormous quantities of data. Since these data are only as valuable as the information which they convey to the data analyst, maximizing the information extracted is of paramount concern. The type of information one hopes to acquire from a given set of data may be well established by the measurement designer, but more often is only partially understood, with the hope that any relevant information will reveal itself. While data representation methods are responsible for maximizing the flow of information-numeric data to human analyst, they are, in general, poorly understood and less well-developed than their data processing counterparts.

Signal data representation is particularly interesting, both because of the structure of the data and the type of measurements one hopes to obtain. Signal processing has provided many techniques for extracting interesting signals from noise distorted patterns, in the form of models, templates, and functional relationships. But such techniques do not typically provide clues as to unexpected information and are frequently insensitive to such difficult situations as multi-variable relationships and extremely noisy signals.

The human brain, in contrast, is extremely adept at resolving signals from noise or multiple sourse, and is also capable of working with several models at a time, including those which are intuitive and not well defined. However, as a signal processor it is band-limited by its data input function. While its input devices (the senses) are quite versatile, they are also sensitive to data format, and can be misled by poor data representation. The discipline of data representation then, is charged with presenting data to the human brain in a manner which facilitates the extraction of useful information.

In this talk, we first provide an overview of the role of data representation in measurements, identifying our traditional goal as well as some novel modifications. We then survey data representation techniques, introducing new ideas and discussing older ones, so that we may better understand the relevant principles involved. Finally we address the representation of signal data, considering various ways to map its unique characteristics into displayable features. Although no rule for data representation exists, it is hoped that critical examination of existing techniques will provide useful insight to the measurer, and lead to more meaningful, informative displays of measurement.

A2-4
1535 MEASUREMENT CONSIDERATIONS IN DETERMINING SYSTEM PERFORMANCE CAPABILITIES M. L. VanBlaricum, Effects Technology, Inc., 5383 Hollister Avenue, Santa Barbara, CA 93111

Recent trends in the evolution of electronic systems have resulted in systems with very sophisticated electronic equipments which are required to operate in a combination of severe threat and ambient environments. As a result a lot of time and money is spent in attempting to determine the expected system performance in these environments. Many of these environments are such that they cannot be simulated for measurement purposes and if they can be there is not enough time and money available to perform a complete statistical sample of the entire set of scenarios.

Expected system performance is a statistical concept. A system will be characterized by more than one set of performance parameters so the expected value of performance will represent the combination of expected performances of various subsystems under various conditions. These subsystems and conditions may or may not be independent of each other so that interactions and dependencies must be taken into account when measurements are planned.

This paper presents a discussion of how simple tests and modeling as well as system level tests fit into the problem of determining expected system performance. Common misconceptions and pitfalls will be discussed. Cost-tradeoff decision approaches will be presented. Examples will be used from the areas of EMC and EMP system hardening.

A2-5
1605 THE SYSTEMS ASPECTS OF MEASUREMENT ACCURACY: STANDARDS AND VALIDATION Brian Belanger, National Bureau of Standards, Physics Bldg., Room B362, Washington, DC 20234

Measurements are generally made in order to gather data upon which to base decisions. In scientific research, measurements may be made to test a theory or determine the property of a material, device, or system of interest. Measurements may be made by a manufacturer to control the production process in order to produce a product that meets its specifications, or by a buyer to verify that a product meets its specifications. Whatever the purpose of the measurements, incorrect decisions may be made if the data contains specific errors unknown to the measurer. In this paper, examples will be given of situations where a large measurement uncertainty can have adverse consequences.

There is a clear need for measurement consistency, that is, agreement within acceptable limits when two or more laboratories measure the same phenomena or the same device. Such consistency will not come about unless those generating the data agree on measurement reference standards. If the volt as maintained in Boulder, Colorado differs from the volt as maintained in Boston, Massachusetts or in Tokyo, Japan and if the magnitude of such differences is unknown, then obviously data generated in those three locations cannot be directly compared. The role of the National Bureau of Standards (NBS) and its counterparts in other countries is to facilitate this achievement of measurement consistency by providing measurement reference standards and promulgating sound measurement methods.

Statistical quality control techniques developed for industrial production processes can and are being applied to the control of measurement systems in order to produce more reliable data. This paper describes such techniques and illustrates how they can be used to enhance the reliability of data. Data are not truly meaningful unless accompanied by a valid estimate of the upper bounds to the possible measurement errors. Techniques used by NBS to quantify those random error (imprecisions) and systematic error (bias or offset relative to national standards) are described.

GUIDED WAVES
Wednesday afternoon, 5 Jan., CR2-6
Chairman: Dr. Stuart Long, Department of Electrical Engineering, University of Houston, Houston, TX 77004

B2-1 1330 INTEGRAL-OPERATOR FORMULATION OF SURFACE WAVE COUPLING BETWEEN INTEGRATED DIELECTRIC WAVEGUIDES

D. P. Nyquist, Michigan State University

A coupled-mode perturbation theory for non-degenerate surface wave coupling between adjacent, integrated dielectric waveguides is obtained based upon an integral-operator description of the system. The method is applicable to any number of graded-index, integrated guides having cores of (arbitrary) practical cross-section shape.

Guided-wave field $\vec{E} = \vec{e}(\vec{\rho})\exp(-j\beta z)$ supported by a system of N dielectric guides described by refractive-index contrast $\delta n^2(\vec{\rho})$ satisfies coupled EFIE's

$$\left[\overleftrightarrow{I}+\frac{\delta n^2(\vec{\rho})}{n_c^2}\overleftrightarrow{\ell}\right]\cdot\vec{e}(\vec{\rho}) - \sum_{n=1}^{N}\int_{CS_n}\frac{\delta n^2(\vec{\rho}\,')}{n_c^2}\overleftrightarrow{g}_{e\beta}(\vec{\rho}\,|\,\vec{\rho}\,')\cdot\vec{e}(\vec{\rho}\,')dS' = 0$$

for all $\vec{\rho}\in CS$, where $\vec{\rho}$ is the 2-d, transverse position vector, $\overleftrightarrow{\ell}$ is a depolarizing dyadic, and $\overleftrightarrow{g}_{e\beta}$ is a 2-d Green's dyadic which depends upon unknown β and describes uniform layered media of an integrated configuration. If the coupled-mode approximation $\vec{e}(\vec{\rho})\simeq a_n\vec{e}_n(\vec{\rho})$ for $\vec{\rho}\in CS_n$ is invoked, where $\vec{e}_n$ is the isolated eigenfield, the EFIE's lead to the homogeneous matrix equation

$$\sum_{n=1}^{N} C_{mn}(\beta)a_n = 0 \quad \ldots \text{ for } m=1,2,\ldots,N$$

$$C_{mn} = \begin{cases} (\beta-\beta_m)\tilde{C}_{mm} & \ldots \text{ for } n=m \\ \displaystyle\int_{CS_n}\frac{\delta n_n^2(\vec{\rho})}{n_c^2}\,\vec{e}_m(\vec{\rho})\cdot\vec{e}_n(\vec{\rho})dS & \ldots \text{ for } n\neq m \end{cases}$$

where $\tilde{C}_{mm}$ is a normalization constant depending upon eigenfield $\vec{e}_n$ and $\partial\overleftrightarrow{g}_{e\beta}/\partial\beta$ evaluated at isolated eigenvalue $\beta=\beta_m$. The system-mode eigenvalues are those β's which lead to non-trivial solutions which satisfy $\det(C_{mn}(\beta))=0$; relative modal amplitudes are subsequently obtained from the homogeneous matrix equation.

The new coupled-mode theory is applicable to relatively general waveguide systems. It requires approximation of only the waveguide core fields. Results obtained when the perturbation theory is applied to a slab-waveguide system are compared with exact solutions to corresponding eigenvalue equations. Applications to practical integrated configurations are described.

B2-2
1350 COUPLING BETWEEN TWO NON-PARALLEL DIELECTRIC WAVEGUIDES:

M. McHenry and D.C. Chang,
Electromagnetics Laboratory, Department of
Electrical Engineering, University of Colorado,
Boulder, CO 80309

A general theory to analyze the coupling between two non-parallel dielectric waveguides is developed, making the coupled mode approximation. In this approach, all second order terms are retained to give a set of coupled differential equations which are solved numerically. The coupling coefficients are worked out approximately for circularly curved, lossless, single TE-Mode, slab waveguides, allowing analysis of symmetric and nonsymmetric directional couplers formed with combinations of straight and circularly curved slab waveguides.

The results are compared with other theories which assume one-to-one correspondence between the coupled points of curved transmission lines. Differences of 10-20% in the power coupled from one guide to the other are found. In addition, the validity of the coupled mode approximation is seen to break down in some cases because the total power is not conserved. Nonsymmetric couplers are seen to have much larger discrepancies in total power than symmetric couplers at the same frequency and minimum separation.

B2-3
1410 SCATTERING FROM WIRES IN THE CLADDING OF AN INFINITE SLAB WAVEGUIDE: J. S. Bagby and D. P. Nyquist, Dept. of Elec. Eng. and Sys. Sci., Michigan State Univ., East Lansing, MI 48824

An investigation is made of the problem of scattering from several thin, perfectly-conducting wires in the cladding of a monomode, TE0 infinite rectangular dielectric slab waveguide. The wires are positioned in the cladding in such a way as to give the problem the y-invarience shown in the accompanying diagram.

Theoretical results are generated by construction of the appropriate Green's function. The resulting even and odd radiation-mode integrals are evaluated numerically, after accounting for the singularities analytically. The scattered field from the wires is determined by application of the extended boundary condition at the wire surfaces. This scattered field is added to the incident field to obtain the total field.

Experimental results are obtained by utilizing the ground-plane image model of the slab waveguide shown below. Several core refractive indices are used, and the data collected includes SWR, reflection, and transmission coefficients.

The experimental and theoretical results are presented and compared, and the application of the results to the problem of impedance matching of dielectric waveguides is discussed.

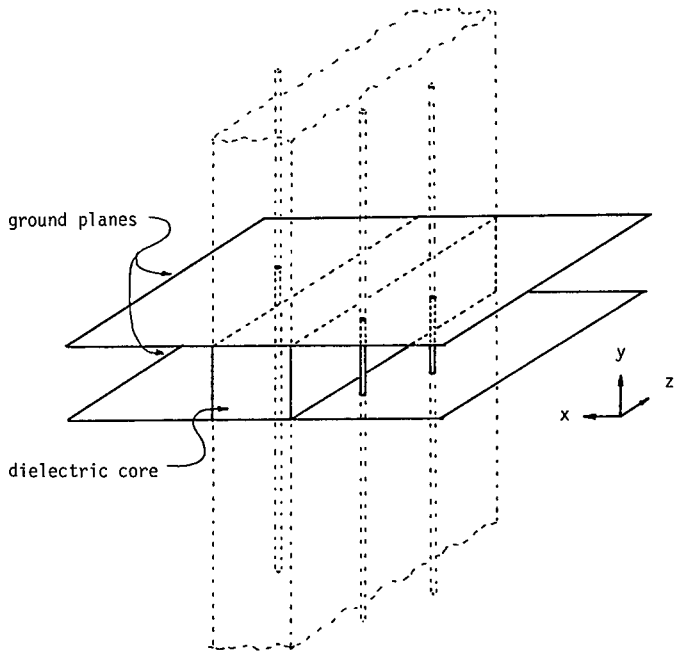

B2-4
1430

ON THE RAY DESCRIPTION OF THE MODES OF A TRIANGULAR-CORE OPTICAL FIBER:

E.F. Kuester, R. Ebrahimian and D.C. Chang, Electromagnetics Laboratory, Dept. of Electrical Engineering, Campus Box 425, University of Colorado, Boulder, CO 80309

Both numerical and asymptotic techniques have been used to study the modes of an optical fiber with a core in the shape of an equilateral triangle. It has recently been suggested that the use of rays repeatedly reflected from the core-cladding interfaces may provide an alternative method for studying this structure. Presumably, this approach would be similar in many ways to Marcatili's well-known analysis of the rectangular-core fiber, which is most accurate far from cutoff. It will be shown that, for a triangular core, the compatibility conditions for the rays are overdeterminate--there are too many equations for the number of unknowns. This has been previously encountered in the case of a rectangular core (J.B. Andersen et al., IEEE Trans. MTT, 23, 555-560, 1975), where a compromise in the form of a weighted least-squares solution was obtained. We will ignore one of the compatibility conditions, and solve the remaining equations by a perturbation procedure suitable to the far-from-cutoff limit. Comparison with other results for the triangular core will be presented, together with some discussion about the approximations made in the method.

B2-5
1510

SCATTERING OF A SURFACE-WAVE MODE INCIDENT OBLIQUELY ONTO A SMALL DIELECTRIC STEP:

Lian Han-Xiong and David C. Chang,
Electromagnetics Laboratory, Department of Electrical Engineering, Campus Box 425,
University of Colorado, Boulder, CO 80309

The canonical problem concerning the reflection and scattering of a surface-wave mode propagating on a two-dimensional dielectric slab with a step discontinuity is an important one for finding guided-mode characteristics of many open dielectric waveguiding structures in an integrated optics or millimeter-wave application. Unlike the previous work of Peng and Oliner (IEEE-MTT, 29, 9, 843-855, 1981), the problem in this paper is solved by a perturbative scheme without first introducing a reflective boundary above the slab. It is shown that the first-order expression for the reflection coefficient is analogous to the so-called equivalent-dielectric-constant (EDC) method. However, unlike the EDC method, the radiation spectrum is fully recovered in the solution process which readily allows us to obtain near-field as well as far-field expressions away from the step. In fact, the approximate field expression can actually reproduce the singular behavior of the field near the step, i.e., the 90° dielectric wedge. Furthermore, because the small parameter involves only the size of the step, the magnitude of the reflection coefficient need not be small and consequently, the total reflection beyond the critical angle can still be observed for the case when the phenomenon of longitudinal wave number of the incident surface-wave parallel to the interface exceeds the wave number of the surface-wave mode on the other side of the step. This of course is important when dealing with guided-modes of a rib guide of finite width. The fact that we can obtain a first-order solution for the field external to the guiding structure also allows us to investigate the coupling problem of two parallel guides, and the problem of radiation loss of a curved guide using a couple-mode type of analysis.

B2-6
1530

THE SLITTED CIRCULAR WAVEGUIDE AS A LEAKY-WAVE ANTENNA:*

K. F. Casey, W. A. Johnson and R. W. Ziolkowski
Lawrence Livermore National Laboratory
P. O. Box 5504, L-156, Livermore, CA 94550

Slitted cylindrical waveguides of separable cross-section shape comprise a class of structures which are representative of certain leaky-wave antennas and whose analysis reduces to the problem of solving a set of dual series equations. In this paper is discussed the slitted circular-cylindrical waveguide operating as a leaky-wave antenna. A variational approach to this problem was described by Harrington (J. Appl. Phys., pp. 1366-1371, November 1953) and Tamir (in Antenna Theory, Part II, pp. 286 ff., McGraw-Hill, 1969). We consider an approach based on the reduction of the dual series equations arising in the formulation of the problem to a set of linear equations in the modal amplitudes. This reduction is carried out using an extension of techniques for the solution of dual series equations arising in potential theory described by Sneddon (Mixed Boundary Value Problems in Potential Theory, North-Holland, 1966). The reduction is exact; approximations in obtaining the solution become those associated with the approximate solution to the linear equations.

We review the analytical procedure employed and present computed numerical results for the complex propagation constant of the dominant (TE_{11}) mode. We also present new approximate analytical expressions for this quantity based on truncation and solution-by-hand of the linear equations, and indicate how one might extend the results to other (non-separable) waveguide cross-sections.

---

*Work performed under the auspices of the U. S. Department of Energy by the Lawrence Livermore National Laboratory under contract number W-7405-ENG-48.

B2-7
1610

RESONANCE IN PLASMA-FILLED ANISOTROPIC RECTANGULAR WAVEGUIDE:

L. Lewin, Electromagnetics Laboratory, Department of Electrical Engineering, University of Colorado, Boulder, CO 80309

The purpose of this study is to investigate the effects of plasma anisotropy on the resonance frequency of the axisymmetric torus mode, with application to fusion machines. Properties of the permittivity tensor are first examined, and it is shown that certain combinations of the tensor elements which determine the transverse field do not exhibit any resonance effects near the plasma cyclotron frequencies. A straight rectangular guide with a uniform anisotropic plasma is examined. The mathematics of this case is exceedingly difficult because of orthogonality problems. A solution is found involving an expansion in terms of the anisotropy, and is probably usable up to about 80% of the ion cyclotron frequency, at which point the anisotropy is seen to have an effect in somewhat reducing the resonance frequency. (This is in sharp contrast to the case of circular waveguide, and indicates a shape effect related to the cross-section form of the waveguide.) The method of the straight rectangular guide case is applied to a combination of curvature and anisotropy in rectangular guide, and is shown to be able to handle the presence of curvature if a very small approximation is made in the equations. The error is less than 1/2% for a ten to one ratio of major and minor torus axes. Up to about 80% of the ion cyclotron frequency, the curvature has a negligible effect on the resonance frequency, although it does affect the field structure in the guide. The influence of curvature in this example is of the same form, and same order, as the effect in non-anisotropic waveguide.

B2-8
1630

ON COUPLING OF TWO TEM CELLS THROUGH A LONGITUDINAL SLOT: Perry F. Wilson and David C. Chang, Electromagnetics Laboratory, Department of Electrical Engineering, University of Colorado, Boulder, CO 80309

Recently, interest has been expressed in coupling together a pair of transverse electromagnetic (TEM) cells in order to perform shielding effectiveness studies. The TEM cell has already established itself as a valuable tool to the electromagnetic interference (EMI) community, by providing a shielded, standardized environment for measuring the emission, and susceptibility properties of electronic equipment. By coupling power from a generating cell through a material laden aperture into a passive, or sensing cell, it is hoped that the same type of uniform environment may be established for shielding studies. Previous efforts to adapt shielded rooms have encountered repeatability difficulties due to the materials proximity to the transmitting antenna's near field. The basic plane wave nature of the TEM cell avoids such complexities.

In particular, we consider a pair of identical cells coupled via a longitudinal slot centrally located in a common broadwall. To gain a qualitative understanding of such a configuration, we consider the simpler problem when no material is present. Because this will be a three conductor system, it will support two TEM system modes, which may be designated as even and odd. The equations governing TEM mode directional couplers require that we know the characteristic impedance of each system mode. The even mode is unaffected by the slot presence, and the odd mode is analyzed via a conformal mapping approach under the assumption that the capacitive effect due to the slot is isolated. One finds a slot perturbation to the local parallel plate capacitance which varies basically as the square of the slot width similar to a pair of shielded coupled strip lines. Numerical data will be presented to demonstrate the system performance as a directional coupler, as well as how the geometry affects the system mode impedance.

NUMERICAL METHODS
Wednesday afternoon, 5 Jan., CRO-14
Chairman: Y. Rahmat-Samii, Jet Propulsion Laboratory, California Institute of Technology, Pasadena, CA 91109

B3-1
1330 THE APPLICATION OF ITERATIVE METHODS FOR THE SOLUTION OF ELECTROMAGNETIC FIELD PROBLEMS

Tapan K. Sarkar
Sadasiva M. Rao
Soheil A. Dianat
Department of Electrical Engineering
Rochester Institute of Technology
Rochester, New York 14623

The approximate methods of solving integral and integro-differential equations of electromagnetics are varied in respect to the ideas lying at their foundation. A number of methods (variational method, Rayleigh-Ritz method, Galerkin's method, method of moments, method of least squares and so on) has been elaborated. At the same time the analysis of these methods, particularly in electromagnetic theory, has not advanced far. Most methods have remained without any theoretical analysis and have only been verified by their effectiveness in individual examples.

A new class of numerical methods is proposed in this presentation for the solution of electromagnetic scattering problems. The principle distinction between the iterative methods and the method of Rayleigh-Ritz, Galerkin's and the method of least squares is that the sequence of approximations is not obtained in a form selected a priori but in a form determined by the problem itself.

It is noted that this class of iterative methods requires considerably less computer storage than the methods of moment formulation using subdomain expansion and testing. Since these are iterative methods, a good guess may considerably reduce the computation time.

B3-2
1350 EFFICIENT COMPUTATION OF NEAR FIELDS AND COUPLING OF ANTENNAS LOCATED NEAR A LOSSY GROUND PLANE:

Jung-Woong Ra* and A. D. Yaghjian
Electromagnetic Fields Division
National Bureau of Standards
Boulder, Colorado 80303

The theory of mutual coupling between any two antennas arbitrarily oriented and separated in free space has been applied to the very efficient computation of antenna coupling and fields versus longitudinal or transverse displacement of the antennas within the near field region (A. D. Yaghjian, IEEE Trans. Ant. and Prop., AP-30, 113-128, 1982). The computer programs require, basically, the electric far fields of the transmitting and receiving antennas and the Eulerian angles of orientation of each antenna. The plane wave sampling theorem and fast Fourier transform are applied in a particularly efficient way to calculate coupling or fields versus transverse displacement, and a newly developed spherical wave representation and sampling theorem for the coupling function are used to obtain the coupling or fields versus separation distance.

When antennas are located near the lossy ground plane, it will be shown that the free space formulation for the coupling or fields can still be used provided that an extra integral around a branch cut due to the Fresnel reflection coefficients can be neglected. And for lossy ground, this branch cut contributes negligibly to the calculation of antenna coupling or fields. Numerical results for a vertical magnetic dipole located in the ground plane compare extremely well with the exact Van der Pol solution.

Since fields calculated by this method require little computer time even for very accurate results, this method is not only powerful in the calculation of mutual coupling and fields of large antennas but also believed to be more efficient than that of evaluating Sommerfeld integrals for fields and mutual impedances of elementary dipoles or wire antennas.

*On leave from the Korea Advanced Institute of Science and Technology, Seoul, Korea.

1909 Sommerfeld
1930 Van der Pol
1936 Norton
1952 Wait (Quasi Static)
1971 Miller
19 Chang
19 Parmi
1982

B3-3
1410 ANALYSIS OF A CYLINDRICAL ANTENNA RESIDING IN TWO CONTIGUOUS HALF SPACES: Chalmers M. Butler and K. A. Michalski, Department of Electrical Engineering, University of Mississippi, University, MS 38677

In this paper are presented the results of the initial phases of a study of a circular cylindrical antenna, which is partially in one half space and partially in another. The half spaces are separated by a planar interface and the cylinder axis is perpendicular to the plane of the interface. Coupled integral equations of the currents on the two cylinder segments are formulated with care that they be amenable to numerical solution. The equations incorporate the exact kernels and special forms of the so-called Sommerfeld integrals. A numerical method for solving the equations is outlined, and data are presented for several cases of interest. An experiment is described in which the input impedance of the antenna is measured, and measured and computed data are compared.

NOSC Support

Hankel Transforms

B3-4
1450 ELECTROMAGNETIC SCATTERING OF ARBITRARILY SHAPED INHOMOGENEOUS CYLINDERS MODELED BY TRIANGULAR PATCHES:

O. M. Al-Bundak and D. R. Wilton, Department of Electrical Engineering, University of Mississippi, University, MS 38677

This paper describes a simple and efficient numerical procedure for determining the polarization current density distributed through the cross-section of an arbitrarily shaped inhomogeneous cylindrical scatterer. The cylinder cross-section is subdivided into planar triangular patches, chosen because of their ability to conform easily to arbitrary cross-sectional boundaries. The formulation for TM illumination is in terms of an ordinary integral equation while TE illumination is in terms of an integro-differential equation for the volume polarization current. From the latter quantity the desired internal fields, absorption, scattered fields, and other quantities of interest can be determined. In the TM case a piecewise-constant current representation is used for determining the current density distribution since no derivatives appear in the integral equation. In the TE case special basis functions defined on the patch domains are used to ensure continuity of conduction-plus-displacement current normal to the interfaces between two patches containing different media. This current representation also has constant divergence (charge density) in each patch. The integro-differential equation is formulated in terms of both vector and scalar potentials, and a testing procedure is used which obviates the need for integration over the potentials yet which properly handles the derivatives in the equation.

B3-5 SCATTERING BY GENERAL THREE DIMENSIONAL OBJECTS: A. Taflove
1510 and K. Umashankar, IIT Research Institute, Chicago, IL 60616; and S. M. Rao, Rochester Institute of Technology, Rochester, NY 14623

General three dimensional electromagnetic scattering problems have been difficult to treat with either analytical and/or numerical methods because of the complicating effects of the scattering geometry due to curvatures, corners, apertures, and dielectric loading of structures. To gain insight into scattering mechanisms using analytical and numerical approaches, generally canonical structures are studied rather than realistic models. Two potential alternate approaches which may permit highly realistic modeling of scattering problems are the finite-difference time-domain (FD-TD) method and the method of moments (MOM) surface patch technique. The goal of this paper is to present new results for an important three-dimensional canonical scattering problem obtained using both the latest FD-TD and MOM triangular surface patch modeling approaches. By comparing the results and the computational resources needed for each method, it is hoped that the range of usefulness of each technique can be better defined. In particular, the range of the scatterer electrical size and the ability of each method to successfully model the physics of wave interaction are key points of comparison discussed in this paper.

The paper will first briefly review the basis of the latest FD-TD and MOM triangular surface patch approaches for modeling three dimensional scattering problems. Results of these two methods for surface currents (magnitude and phase) and for far-scattered fields are then compared for the caseof a metalcube illuminated by a plane wave at normal incidence to one face. The paper concludes with a discussion of the implication of these results for the modeling of more realistic scattering problems by these two approaches.

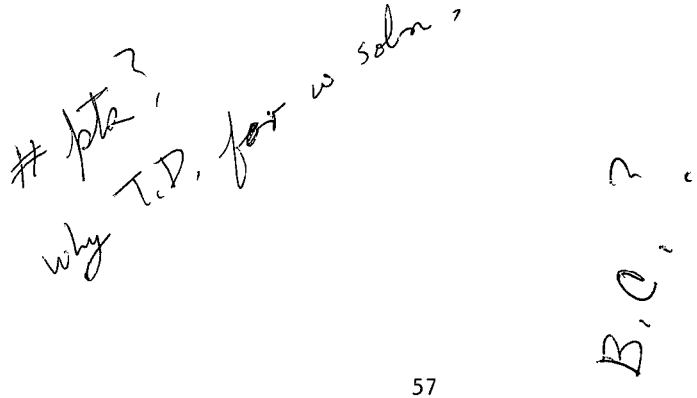

B3-6 1530 ALTERNATE APPROACHES TO THE PROBLEM OF H-POLARIZED PLANE WAVE SCATTERING FROM AN AXIALLY SLOTTED INFINITE CYLINDER:

W. A. Johnson, R. W. Ziolkowski, and K. F. Casey, Lawrence Livermore National Laboratory, Department of Electrical Engineering, Livermore, CA 94550

The azimuthal current induced on an axially slotted cylinder by an H-polarized plane wave at an arbitrary angle of incidence may be computed by a variety of techniques. Morris (1982 IEEE AP Symposium Digest, Vol. 2, pp. 511-512) solved integral equations with highly singular kernels using the Hadamard finite part interpretation of the integral to obtain this current.

Two alternate approaches will be considered in this paper. The dual series technique, a technique originally developed to treat problems in potential theory, has recently been applied by Casey to the analysis of irises in waveguides. This technique is analytical in nature, and the behavior of the current near the edges may be extracted from the solution. Application of the dual series technique to the present problem will be discussed. A purely numerical solution employing the method of moments will also be presented. This solution, based on vector and scalar potentials, is analogous to that of Glisson and Wilton (IEEE Trans. Antennas and Progagat., Vol. AP-28, No. 5, Sept. 1980, pp. 593-603).

Comparison of results obtained using each of these techniques will be made to identify their strengths and weakness.

---

*Work performed under the auspices of the U. S. Department of Energy by the Lawrence Livermore National Laboratory under contract number W-7405-ENG-48.

B3-7
1610

STABILITY CONSIDERATIONS FOR THE FINITE DIFFERENCE REPRESENTATION OF ELECTROMAGNETIC EQUATIONS

D. J. Riley and W. A. Davis
Department of Electrical Engineering
Virginia Polytechnic Institute and
State University
Blacksburg, VA 24061

Explicit finite difference schemes typically are used for the time-domain representation of electromagnetic equations. The numerical stability of these schemes is dependent on the ratio of the time and spatial sampling distances used in the finite difference approximation. For a stable solution, this ratio must be bounded by some real number which is dependent on how the discretization is implemented. The theoretical, and widely known upper bound for this ratio of unity is only applicable for some difference formulations; several formulations require an upper bound of lesser value, while some formulations are unstable for any value. It is desirable to know a priori the particular value of this upper bound that will yield a numerically stable solution for an arbitrary difference formulation.

Two methods exist for the stability analysis of linear difference schemes. These are known as the Fourier and matrix stability methods. The intent of this paper is to present the theoretical foundations of these methods and demonstrate their applicablity to various finite difference formulations of the time-domain electromagnetic equations.

Send Pages on Stab.
to Don Wilton

H. MIERAS
100 NORTH RD
SUDBURY MA 01776
SPERRY RESEARCH CENTER

Commission C Session 1
Commission J Session 2

RADAR ASTRONOMY
Wednesday afternoon, 5 Jan., CRO-30
Chairman: R. F. Jurgens

C1/J2-1 1330 REMOTE-SENSING OF THE TERRESTRIAL PLANETS BY GROUND-BASED RADAR: R. F. Jurgens, Jet Propulsion Laboratory, Pasadena, CA

Radar exploration of the terrestrial planets has been a steadily developing science since the early 1960s. The first observations provided information on the orbital dynamics and spin states of these objects. Fortunately, radar sensitivity increased rapidly with as the Arecibo, Haystack, and Goldstone instruments were completed and upgraded. This added sensitivity permitted more detailed studies and increasingly higher resolution mapping projects. Most of the planetary radar observations have been made at wavelengths between 3.5 and 70 cm, however, some data exist to the meter wavelengths. In recent years, a major effort has been placed on the imaging of the Venusian surface and on the construction of detailed maps of Mars from the altimetry and reflectivity profiles. The highest resolution maps of Venus have been made by the Arecibo radar group with some images having a resolution of roughly 4 km. Most of the Goldstone images have resolutions near 8 km for both the reflectivity and altimetry. A large number of geological forms can be observed in both data sets. Both radar systems employ delay-Doppler and interferometry techniques to provide much greater resolution than can be obtained from the single antenna which provides no appreciable resolution. Since 1977, a three-station interferometer has been in use at Goldstone. This system provides images of reflectivity and altimetry simultaneously. Radar studies of Mars also utilize the delay-Doppler technique, however, due to the large rotation rate, only the region within about 70% of the subradar point can be studied. Radar maps of Mars show altitude, dielectric constants and surface roughness for about 5% of the surface area with 35% more coverage being possible in the future. Little work has been reported on Mercury in recent years, however, most of the effort has been directed toward the measurement of topographic profiles and the removal of topography from the ranging data set to provide an improved ephemeris and a measurement of the effect general relativity on the orbit. All three planets are currently viewed as a broad collection of variegated surfaces having differing dielectric constants and roughness properties. The relationship of these to geological surface types is being studied by several groups. Future work requires more quantitative measurements, i.e., absolute as opposed to relative calibration. These data, when combined with other remote-sensing data and appropriate theoretical models, should provide a greatly improved understanding of the surfaces and geological processes that formed them.

C1/J2-2
1350

FURTHER RESULTS FROM THE PIONEER VENUS RADAR EXPERIMENT

P. G. Ford and G. H. Pettengill
Department of Earth and Planetary Sciences,
Massachusetts Institute of Technology,
54-426, Cambridge, MA 02139

In almost daily operation from December 1978 to March 1981, the Pioneer Venus radar mapper experiment has yielded some 240,000 measurements of time-resolved echoes at near-normal incidence covering the entire planetary surface between 75°N and 65°S latitude, and 2 million measurements of side-looking radar brightness (at angles of incidence between 20° and 60°) covering an equatorial belt between 45°N and 5°S latitude. With the data processing now essentially completed, the four data sets (planetary radius, surface reflectivity, meter-scale surface roughness, and radar brightness) have been compared and contrasted to isolate "anomalous" areas and to provide suggestions of the geological and surface properties of the planet.

In the areas of geological and tectonic analysis, the relatively large surface footprint corresponding to the planetary radius data (40-200 km. per line pair) has nevertheless proved sufficient to identify several large-scale rift features suggesting a degree of lateral crustal motion. Surface properties have been studied by a bi-variant analysis of surface reflectivity and meter-scale roughness: one striking result is the presence of certain features (e.g. Theia Mons and Ozza Mons) that combine average smoothness (rms. surface slopes $< 4°$) and extremely high intrinsic reflectivity, higher than any dry terrestrial surfaces except those that contain a high percentage of electrically conductive mineral inclusions.

C1/J2-3 1410 GROUND-BASED RADAR RECONNAISSANCE OF ASTEROIDS:

Steven J. Ostro, Department of Astronomy, Cornell University, Ithaca, New York 14853

As a class of planetary objects, asteroids are genetically related to both meteorites and comets, and therefore hold important clues to the origin and evolution of the solar system. Nearly a third of the catalogued minor planets have been categorized according to disk-integrated, broad-band, VIS/IR observational parameters. However, with few exceptions, the physical properties of asteroids are not well known.

Radar observations can provide useful constraints on an asteroid's size, shape, spin vector, topography, centimeter-to-meter-scale morphology, composition, and density. Radar techniques for resolving a target in Doppler and/or delay are invaluable when applied to asteroids, which generally remain unresolved by groundbased VIS/IR methods. By virtue of the wavelengths employed, dual-polarization radar measurements can provide information about structural scales in between those probed by optical polarimetry and the scales of asteroid diameters.

In 1980, a program of dual-circular-polarization, λ12.6-cm radar observations of minor planets was initiated at the Arecibo Observatory. Although most of the observations have been simple CW experiments, binary phase coding was used to achieve delay resolution of echoes from Iris and Apollo. A twin-maser front end receiver facilitates determination of the ratio, μ_C, of echo power in the same sense of circular polarization as transmitted to that in the opposite sense. Estimates of μ_C have been obtained for the mainbelt asteroids Pallas, Iris, Flora, and Psyche, and the Earth-approaching asteroids Toro, Apollo, Quetzalcoatl, and Ra-Shalom (Ostro, D. B. Campbell, and I. I. Shapiro, in preparation; see abstracts in Bull. Amer. Astron. Soc. vols. 12, 13, 14). The average value of μ_C for the smaller, Earth-approaching objects exceeds that for the larger, mainbelt objects. For several objects, variations in μ_C as a function of rotational phase suggest heterogeneous surface structure at centimeter-to-meter scales. The sharply peaked spectral signature of quasispecular scattering, which dominates echoes from the Moon and inner planets, is absent in the asteroid echo spectra.

Commission C Session 1
Commission J Session 2

C1/J2-4
1450

LUNAR RADAR STUDIES: T. W. Thompson, California Institute of Technology, Jet Propulsion Laboratory, Pasadena, CA 91109

Starting in the mid 1960's and continuing today, radar mapping of the moon and subsequent study of these measurements has contributed to our general knowledge of the Earth's satellite. High resolution radar maps of the moon were produced in the 1960's with the goal of aiding Apollo landing site selection via radar detection of surface roughness. This Apollo impetus led to surface mapping of 1-3 Km at 3.8 cm wavelength using the 7840 MHz radar at the Haystack Observatory. In addition, a radar program at the Arecibo Observatory produced a surface mapping with 5-10 Km resolutions at 70 cm wavelength with a high power 430 MHz radar. These two radar programs used delay-Doppler techniques where narrow antenna beams resolved the inherent ambiguity of this technique. Also, there were other radar observations of the moon at wavelengths of 8 cm, 23 cm, and 7.5 m during this period. These radar results of the moon are now being supplemented with a new observing program with the 430 MHz (70 cm wavelength) radar at Arecibo - a program which will produce radar maps of 2-3 Km resolution, comparable to the high reoslution Haystack 3.8 cm maps.

These radar maps have been used in a number of geologic studies in the last decade. Some of these studies have shown that radar echo stengths of different mare units and the Aristarchus Plateau are modulated by differences in the chemical compositions of the lunar soil. Areas with higher concentrations of iron have higher electrical losses which attenuates volume scattering in the first few meters of the soil.

Other studies of lunar radar data have concentrated on surface roughness on meter and centimeter scales associated with lunar craters. The youngest craters have abundant rocks which produce ehnanced radar echoes. The oldest craters have average echoes. The evolution of young to older craters is driven by meteoritic bomabardment which gradually erases the excess rocks. Various aspects of this meteoritic bombardment can be verified by correlating radar signature with geologic age classifications of lunar craters. The youngest craters on the moon have a distinct radar signature which permits radar maps to be a useful tool estimating lunar crater history in the last one or two billion years.

Also, radar maps of the moon show that some craters have a bright-ring appearance like Venusian radar features. This may indicate that the bright ring features on Venus are impact craters. Thus continued study of the lunar radar maps may contribute to our understanding of Venus as well as other planets.

Commission C Session 1
Commission J Session 2

C1/J2-5 VOYAGER RADIO SCIENCE EXPERIMENTS IN THE SATURN SYSTEM
1510

G. Leonard Tyler
Center for Radar Astronomy
Stanford University

The Voyager Radio Science Experiment at Saturn included dual-frequency (2.3 & 8.4 GHz) occultation observations of the atmosphere of Titan, the atmosphere, ionosphere, magnetic field, and rings of Saturn, and radio tracking determination of the gravity field of Saturn and the masses of several satellites. These experiments required a number of innovations in spacecraft hardware, design, and operational strategies which ultimately led to very large measurement signal-to-noise ratios ($P_T/N_o > 50$ db, $\Delta f/f_o < 2 \times 10^{-12}$) and dynamic range.

Radio occultation studies of Saturn's rings represent entirely new spacecraft technique. The data include simultaneous observations of the attenuated line-of-sight signal propagating directly through the rings and the near-forward scatter from the ring particles. The results contain sufficient information to map the structure of the rings, to determine the distribution of particle sizes for several different locations, and to estimate the total mass of the ring system.

The numbers of various size particles are obtained by a combination of two methods. Differential extinction measurements at the 3.6 and 13 cm-λ give a measure of the integrated cross-sectional area of particles in the cm-size range. The power spectra of the near-forward scattered waves gives the collective forward-scatter phase function of the particle ensemble; use of the phase function in the inverse-scattering problem then yields the size distribution for supra-meter particles. Combination of the extinction and scattering results leads to the size distribution from cm to ~ 50 m. Additional information on sub-cm particles is obtained from the transmitted phase. Although the size distribution is found to vary with location in the ring system, it can be roughly characterized as an inverse power law type with index ~ 3, and an upper size cut-off of about 5 meters radius.

C1/J2-6
1530

REMOTE SENSING WITH SPACEBORNE SYNTHETIC APERTURE RADAR

J. C. Curlander, Jet Propulsion Laboratory,
California Institute of Technology,
Pasadena, CA 91109

The SEASAT experiment launched in 1978 marked the first synthetic aperture radar operated from space. This instrument was designed primarily to image the oceans, however, the data has found numerous land applications and is currently being utilized by geologists, oceanographers and scientists studying polar ice formations. Following the success of SEASAT, a Shuttle Imaging Radar (SIR-A) was carried by the orbiter in 1981. This instrument, designed for land applications, contained an optical tape recorder and could therefore, collect data from areas previously inaccessible to the SEASAT SAR. This data which is still being analyzed, has revealed surface characteristics not previously seen by optical sensors. A follow-on to SIR-A is currently in the design stage and a 1984 launch is planned. This instrument will be more sophisticated than its predecessors with the capability of variable incidence angle and onboard data digitization. The SIR-B experiment will provide valuable information on the variation of scattering coefficient with incidence angle and the feasibility of generating stereo SAR maps. The improved geometric resolution and radiometric calibration should greatly enhance the utilization of the data.

NOISE AND INTERFERENCE - ESTIMATION AND SYSTEM DESIGN
Wednesday afternoon, 5 Jan., CRO-12
Chairman: A. A. Giordano

E1-1
1330 THE STANFORD UNIVERSITY ELF/VLF RADIOMETER

A.C. Fraser-Smith, R.A. Helliwell, E.W. Paschal and B.R. Fortnam, Radioscience Laboratory, Stanford University, Stanford, CA 94305

As part of a project aimed at improving radio communication in the ELF/VLF (10 - 32,000 Hz) range, Stanford University is preparing to monitor global ELF/VLF noise levels and spectra using a network of up to seven ELF/VLF radiometer stations. The instrumentation for each station consists of two dual-channel receiving systems, each of which is linked to two crossed loop antennas (E-W, N-S); one of these systems covers the frequency range 10 - 500 Hz and the other the range 200 - 32,000 Hz. Both analog and digital recording are to be used, the latter covering 16 narrowband (5% bandwidths) channels distributed throughout the range 10 - 32,000 Hz. The system as a whole, which we are referring to as an ELF/VLF radiometer to emphasize the quantitative nature of the measurements, is controlled by a microcomputer, thus enabling its performance to be monitored and also changed, if desired, via a video terminal. The digital radiometer data will be particularly useful for statistical studies of the global ELF/VLF noise distribution, and the waveform data will allow detailed studies of the spectral properties of the noise and the identification of different noise sources. It is anticipated that the results of the study will help in the identification of optimum frequencies, modulation patterns, and signal processing techniques for ELF/VLF communication systems.

E1-2 1350 MODELING AND FIELD TEST VERIFICATION OF ELECTROMAGNETIC INTERFERENCE BETWEEN OVERHEAD POWER TRANSMISSION LINES AND RAILROAD COMMUNICATIONS AND SIGNALLING SYSTEMS:

K. Umashankar and A. Taflove, IIT Research Institute, Chicago, IL 60616

Many restraints have been placed on the co-location or sharing of existing railroad rights-of-way with existing or new ac power transmission lines, since railroad systems usually have integral communications and signal facilities that can be inductively interfered by an overhead electric power line. This has called for proper characterization, modeling, and mitigation of the electromagnetic interference between overhead power transmission lines and railroad communications and signal systems to assure compatible, normal operation.

This paper describes coupling models which have been developed both for parallel and nonparallel rights-of-way to predict analytically induced voltages and currents along sections of the railroad track and the associated communication lines. The method is based upon a coupled multiconductor transmission line approach taking into account interactions between power lines and rail conductors along with associated communication and signalling systems. Two different models have been developed to predict interference: one for coupling during normal operation; and the other for coupling during fault current situations. Simple Nortons type equivalent circuits are obtained for the coupling models which are suitable for treating non-parallel rights-of-way

Representative field test results are presented showing the electromagnetic interference and coupling in a typical experimental right-of-way. Theoretical results of the induced railroad currents and voltages are also presented verifying the field tests.

E1-3
1410

TORNADO RADIO EMISSIONS

J. B. Smyth, Smyth Research Associates
3555 Aero Court
San Diego, CA 92041

It is assumed that stepped-leader type lightning discharges take place within the tornado cloud. Field parameters of the process are derived. These data provide information for designing optimum filters for detecting these electromagnetic transients. In addition, polarization information required for designing receiver antennas is presented.

Several interesting electromagnetic phenomena observed during tornado events are described by the mechanism postulated: These include ball-lightning and T V interference.

E1-4 1450

ADVANCES IN ATMOSPHERIC NOISE MAPPING BY NUMERICAL METHODS

D. B. Sailors,
Ocean and Atmospheric Sciences Division
Naval Ocean Systems Center, San Diego, CA 92152

Recent progress made at the Naval Ocean Systems Center to improve numerical methods for mapping and predicting atmospheric noise characteristics used in telecommunications is presented. One major problem is considered - the tendency of maps to smooth out physical properties of the atmospheric noise, particularly at low latitudes where the gradient in atmospheric noise maximizes due to a concentration of noise sources in that region. As the number of harmonics in the numerical map are reduced to make the model usable on a minicomputer, the high level contours begin to disappear, enhancing the problem.

Significant improvement is made in solving the problem by the use of a "modified latitude" coordinate. By making a transformation so that the latitude input into the latitude function $G_{j,k}(\lambda)$ in the numerical mapping process is spread further away from the equator than the actual latitude, there will be a more uniform variation of atmospheric noise as a function of the modified latitude. The transformations chosen had a built-in constraint at the geographic poles ($\lambda = \pm 90^0$) in that the modified latitude was to equal the actual latitude, thus preserving the stability of the latitude function $G_{j,k}(\lambda)$ at the poles. The transformations being considered include: $\lambda_1 = \tan^{-1}(\lambda/\sqrt{\cos\lambda})$; $\lambda_2 = \tan^{-1}(\tan\lambda/\sqrt{\cos\lambda})$; $\lambda_3 = (\pi/2)\sin\lambda$; $\lambda_4 = \pm\pi/2 - \tan^{-1}[(\pm\pi/2-\lambda)/\sqrt{\cos(\pm\pi/2-\lambda)}]$; and $\lambda_5 = \pm\sin^{-1}(\sqrt{\pm 2\lambda/\pi})$. The negative sign is taken when λ is negative. The first two transformations are similar to the modified dip utilized in ionospheric mapping (W. B. Jones, R. P. Graham, and M. Leftin, NBS Tech. Note 337, May 12, 1966). The third transformation was considered by W. B. Jones and R. M. Gallet (J. Res. NBS, 66D, 1962) in their representation of diurnal and geographic variations of ionospheric data by numerical methods. They found the representation to be improved around the equator, but significant geographic variation in the temperate latitudes was squeezed into the poles and so lost. The fourth transformation is a variation of the first. The last transformation is the arc sin distribution function.

A general description is given of the new procedures for forming numerical maps, including a number of illustrations showing the results from using the transformations in the development of atmospheric noise numerical maps.

E1-5 1530 LOCALLY OPTIMUM AND SUB-OPTIMUM DETECTOR PERFORMANCE IN NON-GAUSSIAN NOISE, A. D. Spaulding, National Telecommunication and Information Administration, Institute for Telecommunication Sciences, Boulder, CO '80303

The real-world noise environment is almost never Gaussian in character, yet receiving systems in general use are those which are optimum for white Gaussian noise (i.e., linear matched filter or correlation detectors). Usually, very large improvements in the performance of systems can be achieved if the actual statistical characteristics of the noise and interference are properly taken into account. The usual means of deriving a "better" detector is to assume the derived signal is suitably "small" and that the number of independent samples from the received waveform is quite large. These detectors are usually termed "locally optimum Bayes detectors" or LOBD's. This paper summarizes the results from an extensive set of Monte Carlo computer simulations for the CPSK system, using various detectors (including the LOBD detector) and also using Rayleigh fading signals as well as constant signals including situations where the signal is not particularly "small" and the number of independent samples is not particularly "large." It is demonstrated that, under proper conditions, the usual analytical performance estimates (which are reviewed) are valid. It is also demonstrated that non-Gaussian noise which is tremendously non-Gaussian" does not necessarily result in "tremendous" improvement over a linear receiver being attainable.

E1-6 1550 CANONICALLY OPTIMUM THRESHOLD SIGNAL AND PARAMETER ESTIMATION: David Middleton, New York, NY 10028

Optimum threshold estimation of signal waveforms and parameters is considered, where it is demonstrated that both locally optimum (LO) and asymptotically optimum (AO) Bayes estimation may be canonically constructed. This requires suitable termination of the various likelihood ratios of the associated detection problem, in order that asymptotic optimality may be preserved. The canonical theory is developed here for the simple cost function (i.e., unconditional maximum likelihood estimators) and for the quadratic cost function (least mean square estimators). Furthermore, upper bounds on input signal strength are established, for which the LO and AO estimators retain their optimal character. The general results are illustrated by the derivation of optimum threshold estimators for input signal amplitudes. Various general questions and problems needing further exploration here are also described. The above results are believed to be new.

E1-7 1610 CANONICAL LOCALLY (LO) AND ASYMPTOTICALLY (AO) OPTIMUM COMPOSITE THRESHOLD DETECTORS: David Middleton, New York, NY 10028

When there is sufficient phase(or epoch) information at the receiver to permit at least partially coherent detection in highly nongaussian noise and interference,it is possible to obtain significant improvement O(3-10+ db) in minimum detectable signal by employing a suitably designed composite LO and AO threshold detector. Similar orders of improvement are also obtainable by certain composite suboptimum detectors,in particular,a combination of coherent and incoherent clipper-correlators employing hard limiting.

Since the added complexity of such detectors is essentially nil:one needs both for signal detection and subsequent processing,important gains can be made by employing a suitably optimized composite detector. Analytic and numerical examples of the processing algorithms and performance,in Class A interference,are provided,with quantitative comparisons with coherent reception alone,for both optimum and suboptimum detection algorithms and situations.

E1-8
1650

A FAST ALGORITHM FOR FREQUENCY ESTIMATION:

Allan Steinhardt and R.A. Roberts,
Department of Electrical Engineering,
University of Colorado, Boulder, CO 80309

Currently there is much interest in techniques for estimating the frequencies of sinusoidal/narrow band signals buried in broadband noise. Linear prediction (maximum entropy) is known to offer resolution advantages over the Periodogram, particularly for short data records. However this approach suffers from a rapid decline in performance as the SNR decreases. Because of this many improvements to linear prediction have been proposed. Recently Kumaresan (Proc. IEEE August 1982) has proposed a superior method using a sparse linear predictor (i.e. one for which most of the coefficients are constrained to be zero). This method offers both speed and precision. As with standard linear prediction, once the predictor polynomial is found its roots must be computed in order to obtain the frequency estimates. Normally this is a slow iterative procedure, and claims a large fraction of the overall computation time. However we shall show that when the number of sinusoids (M) is known an algorithm exists whereby the sparse predictor polynomial can be more quickly rooted. When M = 1 the algorithm is very fast and is non-iterative. The CPU time required to obtain frequency estimates using this algorithm, in conjunction with Kumaresan's method, was found to be 1-2% of that required by other linear prediction and periodogram estimators.

This research supported by the Army Research Office under contract #ARO DAAG 29-80-K-0062.

E1-9 1710 RECEIVER PERFORMANCE SIMULATIONS IN MEASURED WIDEBAND ATMOSPHERIC NOISE: J. R. Herman and F. M. Hsu, GTE Products Corporation, Strategic Systems Division, Westborough, MA 01581

Performance simulations using extant analytical atmospheric noise models (e.g., the truncated Hall model) suggest that nonlinear receivers offer considerable improvement over linear receivers for digital communications in the presence of noise. However, the improvement is less pronounced when measured noise is used in the simulation. Several nonlinear receiver models have been investigated, including a bandpass limiter, an inverse weighted correlator, a log correlator, and a soft clipper, among others. In all cases, the improvement is less in measured noise than in simulated noise. It appears that the non-stationary character of measured atmospheric noise leads to second order (pulse occurrence) statistics which are quite different from those of a truncated Hall model, to cause a reduction in expected performance improvement. The improvement factor can be recovered through use of spread spectrum techniques with proper interleaving in the digital transmission.

Commission F Session 2

EFFECTS OF PRECIPITATION ON MICROWAVE SYSTEMS - DEPOLARIZATION, SPACE DIVERSITY, BACKSCATTER INTENSITY
Wednesday afternoon, 5 Jan., CR2-26
Chairman: Louis J. Ippolito, NASA Headquarters, Washington, DC

F2-1
1330 A POLARIZATION-DIVERSITY, 35-GHz METEOROLOGICAL DOPPLER RADAR

F. Pasqualucci, R.A. Kropfli, W.R. Moninger,
NOAA/ERL/Wave Propagation Laboratory, Boulder, Colorado 80303

A Doppler radar operating at a frequency of 35 GHz (8.6-mm wavelength) and having polarization-diversity capability is discussed. The system is bistatic and uses two Cassegranian 1.2-m-diameter antennas for the transmitter and the receiver. A switchable polarizer in the transmitter antenna allows the selection of either circular (right-hand or left-hand) or linear polarization. A similar polarizer in the receiver antenna allows the reception of both circular or both linear polarizations, and an orthomode transducer is used to separate the two polarization components of the backscattered signal.

In order to increase the unambiguous Doppler velocity measurable with the system, the radar operates in the double pulse mode. The spacing between the first and second pulse can be varied between 32 μs and 500 μs, changing the unambiguous velocity from ±67 m s^{-1} to ±4.3 m s^{-1}. The receiver has six channels: linear in-phase and quadrature co-polarized and cross-polarized components, and logarithmic power co-polarized and cross-polarized components.

The data acquisition and processing system includes a microprocessor-controlled pulse pair processor for the real-time estimation of the received Doppler spectral parameters and a NOVA-3 minicomputer with magnetic tape recorders.

F2-2
1400 THE UTILITY OF CIRCULAR DEPOLARIZATION RATIO IN THE IDENTIFICATION OF TROPOSPHERIC SCATTERERS

R.A. Kropfli, W.R. Moninger, and F. Pasqualucci
NOAA/ERL/Wave Propagation Laboratory, 325 Broadway,
Boulder, CO 80303

The new NOAA/WPL K-band, dual-polarization Doppler radar was used extensively during the Cooperative Convective Precipitation Experiment (CCOPE). Data from this experiment indicates that the circular depolarization ratio (CDR) measured with this radar responds to changes in ice crystal type just above the melting layer. This reponse is observed in the magnitude of CDR as well as its aspect dependency. These data along with Doppler velocity data suggest that future experiments of a similar nature may further improve our understanding of microphysical processes near the melting layer. In addition to these data, CDR data in the planetary boundary layer and in severe convective storms will be discussed.

F2-3
1420 FIRST-ORDER CALCULATIONS OF INCOHERENT INTENSITY DUE TO RAIN*:

R. Woo and D.C. Blackman, Jet Propulsion Laboratory, California Institute of Technology, Pasadena, CA 91109.
A. Ishimaru, Department of Electrical Engineering, University of Washington, Seattle, WA 98195.

In multiple scattering studies based on the equation of transfer, it is important to compare the first-order and exact solutions in order to determine the merit of the considerably simpler first-order solution. In this paper, we present first-order calculations of incoherent intensity due to rain carried out at 30 GHz. The incident wave is linearly polarized, and both vertical and slant paths are considered. The non-spherical shape of the raindrops is that described by Pruppacher and Pitter, for which single particale scattering calculations are available (Yeh et al., Radio Science, 17, 757, 1982). The drop sizes are distributed according to the Laws-Parsons distribution. The first-order calculations for Pruppacher-Pitter raindrops are compared with first-order and exact (Ishimaru et al., Radio Science, in press) results for spherical raindrops. It is seen that while the first-order copolarized incoherent intensities represent a good approximation at 30 GHz for low values of copolarized attenuation (CPA), they could substantially underestimate the exact results at the higher values of CPA (>20 dB). The crosspolarized incoherent intensities are significantly underestimated by the first-order solutions for all values of CPA. Some results for spherical raindrops at 120 GHz will also be presented.

*This paper presents the results of one phase of research carried out at JPL under contract NAS7-100 sponsored by NASA.

F2-4
1440 SPACE DIVERSITY DEPENDENCE ON PATH ANGLE, FREQUENCY, AND DROP SIZE DISTRIBUTION USING RADAR MODELING TECHNIQUES, Julius Goldhirsh, Applied Physics Laboratory, Johns Hopkins University, Johns Hopkins Road, Laurel, Maryland 20707

A radar data base of the reflectivity environment at Wallops Island, Virginia is injected into a path attenuation modeling program and both single and joint probability cumulative fade distributions are computed at variable path angles ranging from 20 to 90 degrees at frequencies of 19.04 and 28.56 GHz and site spacings up to 50 km. The diversity gains for the various cases are computed and criteria are established associated with variable path angles and frequencies. In addition, the effect of assuming various drop size distributions are examined. These include measured drop size spectra using a disdrometer system and the Marshall-Palmer case.

The data base was amassed over a three year period during which simultaneous COMSTAR beacon data was received. Radar reflectivity coupled with simultaneous disdrometer data over 16 rain days covering all seasons are included in the modeling program.

Preliminary results have demonstrated that the "relative diversity gain" defined as the diversity gain at any site spacing divided by the respective saturated value is approximately invariant with single terminal probability, frequency, and drop size distribution.

F2-5
1540 PREDICTION OF SPACE DIVERSITY IMPROVEMENT USING THE TWO-COMPONENT RAIN MODEL

R.K. Crane, Thayer School of Engineering, Dartmouth College, Hanover, New Hampshire 03755

The newly developed two-component rain model for the prediction of attenuation statistics was extended to provide predictions of the joint occurrences of specified or higher attenuation values on closely spaced earth-satellite propagation paths. The joint statistics provide the information required for the estimation of diversity gain or diversity advantage.

The model for the prediction of space diversity improvement was tested using available diversity data. The two-component model performed well for baselines shorter than about 15 km. The prediction error increased as the separation between the paths increased. For shorter baselines, less than 12 km, the maximum observed differences between the predicted and observed attenuation values at a preselected set of occurrence probabilities was 42 percent (root mean square deviation), a result comparable with the expected performance of single path attenuation estimation models. For longer paths, the estimation error was larger but so was the difference between observations in the same rain climate region.

F2-6
1600

DUAL POLARIZATION RADAR FOR SLANT PATH PROPAGATION RESEARCH

T. Pratt, R. E. Marshall, C. Ozbay, J. H. Andrews,
Electrical Engineering Department, Virginia
Polytechnic Institute and State University,
Blacksburg, VA

Dual polarized radars can provide range-gated data about hydrometeors along a slant path in support of propagation studies. The relationships between backscatter from a volume of hydrometeors and the parameters measured by an S-band dual polarized radar have been derived using Rayleigh scattering theory. The hydrometeor model includes distributions for particle size, shape and canting angle as well as rainfall rate to provide a realistic model of a rain or ice storm. Measurement of differential reflectivity, ZDR, in several planes is shown to give information on the particle orientation.

Radar data has been obtained during rainstorms on a low-angle slant path to the SIRIO satellite and used to predict the forward attenuation at 11.7 GHz with encouraging results.

F2-7
1620

DROP-SIZE DISTRIBUTION MEASUREMENTS IN CONVECTIVE STORMS WITH A VERTICALLY POINTING 35-GHz DOPPLER RADAR

F. Pasqualucci, NOAA/ERL/Wave Propagation Laboratory
Boulder, Colorado 80303

Measurements at vertical incidence in convective storms with a 35-GHz pseudo-noise coded high-resolution radar at Johannesburg, South Africa, are discussed. The radar is bistatic and has the capability to measure targets at very short ranges ($\simeq$19 m). This capability is used to derive an accurate experimental mean velocity-reflectivity ($\bar{v}$-Z) relationship in convective storm systems. It is shown that at an altitude of 19 m the standard deviation of the data points from the mean $\bar{v}$-Z relationship is about 0.25 m s^{-1}, indicating that the contribution of the vertical air velocity at the low altitude of 19 m is less than about $\pm$0.5 m s^{-1} (95% confidence limit). The experimental $\bar{v}$-Z relationship is then used to derive drop-size distributions from the measured Doppler spectra in convective rainfall with high time resolution (10 s). Some of the measured drop-size distributions, and the departure from the exponential model, are discussed and related to specific kinematic features of the storm under study. For example, drop-size distributions measured in a severe squall line show a large abundance of smaller drops (<1.5 mm in diameter) in regions of wind shear near the edges of the main downdraft core. A possible explanation of this large concentration of smaller drops is sorting of the hydrometeors caused by shear in the horizontal wind that is generated by the divergence of the downdraft at the ground. These observations show the usefulness of this radar measurement technique to detect features of drop-size distributions in convective systems and relate them to storm structure and kinematics.

IONOSPHERIC SCINTILLATION
Wednesday afternoon, 5 Jan., CR1-40
Chairman: E. J. Fremouw, Physical Dynamics, Inc., Bellevue, WA 98009

G2-1
1340

DRIFT CHARACTERISTICS OF THE EQUATORIAL SCINTILLATION OF SATELLITE SIGNALS

M. R. Paulson
Electromagnetic Propagation Division
Naval Ocean Systems Center
San Diego, California 92152

Limited spaced-receiver measurements made at Guam in 1976 of the equatorial scintillation of satellite signals showed very good correlation between the eastward component of drift velocity, measured at the ground, and the intensity of the scintillation. This suggested that it might be possible to use this drift velocity as a measure of ionospheric movement to further study equatorial scintillation.

Two vhf/uhf receivers have been set up in Guam with an east-west separation of 1500 feet and are monitoring the broadcast channel of the Pacific Fleet Satellite. In addition one L-Band receiver is monitoring the beacon of the Pacific Marine Satellite. Cross correlations between the two uhf receivers are used to get a measure of the drift velocity and the standard deviation divided by the mean is used as an indication of scintillation intensity.

Diurnal variations of the east-west component of drift velocity are shown as well as night-to-night differences. Scintillation intensities and drift velocities are compared for both the uhf and the L-band data. Examples of uhf scintillation and drift velocities near sunrise are also shown.

G2-2
1400

A MORPHOLOGICAL STUDY OF GIGAHERTZ EQUATORIAL SCINTILLATIONS IN THE ASIAN SECTOR:

D. J. Fang, Propagation Studies Department, COMSAT Laboratories, Clarksburg, MD 20871 and C. H. Liu, Ionospheric Radio Labs, University of Illinois, Urbana, IL 61801

Concerted efforts were made from 1978 to 1980 for monitoring ionospheric scintillations in the Asian sector. Two geostationary satellites (INTELSAT IV F8 POR satellite and IV-A F1 IOR satellite) and five earth stations (Hong Kong, Singapore, Thailand, Hawaii, and Sri Lanka) with a total of eight up-/down-link signals at 4/6 GHz, respectively, were involved. The twenty-nine month measurement period coincided with the solar maximum period of the current solar cycle 21. Intensity scintillations with peak-to-peak fluctuations up to 14 dB were recorded. This paper is devoted to studying the morphological aspect of scintillation in the Asian sector, including the equinoctial occurrence pattern, diurnal onset characteristics, relationship between scintillations along the eastward link and westward link during sunset, correlation with sunspot numbers, etc. These findings, complementary to information already available from American and Europe-African sectors, provide an essential element in understanding the global behavior of gigahertz ionospheric scintillations.

This paper is based upon work performed under the sponsorship and technical direction of the International Telecommunication Satellite Organization (INTELSAT). Any views expressed herein are not necessarily those of INTELSAT.

G2-3
1420

STUDIES OF VHF AND GHZ AMPLITUDE SCINTILLATION CAUSED BY IRREGULARITIES ASSOCIATED WITH PLASMA BUBBLES IN THE EQUATORIAL ANOMALY REGION

S. J. Franke and C. H. Liu, University of Illinois at Urbana-Champaign, Urbana, IL 61801

Multifrequency scintillation data collected at Ascension Island in early 1981 have been studied and the results will be discussed. Power spectra and scintillation index (S_4) will be presented for signals received from the geostationary satellite MARISAT along a propagation path oriented within a few degrees of the magnetic meridian plane. The data will be interpreted using existing scintillation theory and computer model calculations based on a one dimensional phase screen. The high frequency asymptotes of the amplitude power spectra and the frequency dependence of S_4 will be shown to be consistent with a rather steeply sloped power law irregularity spectrum. In addition, aspects of the temporal signature of the scintillating signals which are believed to be due in part to the special propagation geometry, will be presented. In particular, the effects of refraction on structure associated with equatorial plasma bubbles will be discussed. Observations of the time shift between similar features in the scintillation patterns are shown to be consistent with a simple model of refraction on the "walls" of the depleted plasma bubbles. Other special features of the temporal signature of the signal will also be discussed.

G2-4 1440 GIGAHERTZ SCINTILLATIONS OF EQUATORIAL PATCHES: J. Aarons, Department of Astronomy, Boston University, Boston, MA 02215; J. Al Klobuchar and H. E. Whitney, Air Force Geophysics Laboratory, Hanscom AFB, MA 01731; J. Austen, University of Illinois, Urbana, IL 61801; A. L. Johnson, Avionics Laboratory, WPAFB, OH 45433; and C. L. Rino, SRI International, Menlo Park, CA 94025

In a program designed to compare measurements of scintillation activity in the equatorial anomaly region, observations were made of satellite beacon signals transmitting at frequencies ranging from 137 MHz to 7 GHz. Recordings were made at Ascension Island in January-February 1981, during a month of very high solar flux and a high occurrence of scintillations. Saturation was noted in the VHF-UHF range with levels of 8 dB peak to peak at 4 GHz and 3 dB peak to peak at 7 GHz. Statistics of occurrence of various levels for 1.5 and 4 GHz are given in the paper.

The hypotheses of vertical or horizontal irregularity sheets within the patches of irregularities were examined with data from the GPS satellites. Vertical sheets were eliminated as a possibility. A comparison of scintillations with 6300A airglow images, which map regions of depleted electron density over the entire sky, showed that in the anomaly region, maximum scintillation activity occurs within the patch and not at the walls of the patch.

G2-5
1500

VHF AMPLITUDE SCINTILLATIONS AND ASSOCIATED ELECTRON CONTENT DEPLETIONS AS OBSERVED AT AREQUIPA, PERU

A. DasGupta[1,5], Santimay Basu[2], J. Aarons[3], J.A. Klobuchar[1], Sunanda Basu[2], and A. Bushby[4]

Results of observations on occurrences and behavior of 137 MHz VHF amplitude scintillations and associated ionospheric electron content depletions obtained at Arequipa, Peru (16.4°S, 71.5°W, Geogr.; 9°S Dip) during the recent solar maximum period 1979-80 are presented. The seasonal variation of scintillations shows the usual deep minimum during May-July and a prominent maximum in December, when scintillations also persist for a long period of time, sometimes even beyond sunrise. Ionospheric irregularities have been found to occur in distinct patches whose extent varies with season. During the December solstice the average VHF scintillation patch duration is about 6 hours, while numerous patches of much shorter duration are observed in equinoctial months. The depletions in the height integrated ionospheric electron content associated with scintillations have a typical duration of 10-15 mins and amplitude less than 5×10^{16} el/m^2, although depletions with amplitude as large as 20×10^{16} el/m^2 and with duration more than 30 mins are sometimes encountered. The pre-midnight amplitude scintillations and associated electron content depletions could be identified with range type spread-F, as established earlier, while the association of post-midnight VHF scintillations with frequency type spread-F is found to be a special feature observed during years of very high solar activity. The seasonal dependence of irregularity patch dimensions is examined in terms of variations of drifts in the post-sunset equatorial ionosphere.

1. Air Force Geophysics Laboratory, Hanscom Air Force Base, MA 01731, USA;
2. Emmanuel College, 400 The Fenway, Boston, MA 02115, USA;
3. Department of Astronomy, Boston University, Boston, MA 02215, USA;
4. Instituto Geofisico del Peru, Huancayo, Peru;
5. NRC/NAS Senior Resident Research Associate on leave from the University of Calcutta, India.

G2-6
1540

SPECTRAL BEHAVIOR OF PHASE SCINTILLATION IN THE SUB-AURORAL ENHANCEMENT REGION

E.J. Fremouw, J.A. Secan, and J.M. Lansinger
Physical Dynamics, Inc.; P.O. Box 3027
Bellevue, WA 98009

Enhancement of phase and intensity scintillation as the radio line of sight scans through grazing incidence on the local L shell in the nightside diffuse-auroral ionosphere has been well documented by means of data from the Wideband satellite. In this paper, we describe a recently noticed systematic behavior of the phase spectrum in the enhancement region. Routine Wideband processing included spectral analysis of 20-sec ($\approx$ 60-km) segments of VHF and UHF phase records and log-linear fits thereto. Tabulation of the resulting power-law spectral indices, p, disclosed increased values in the scintillation-enhancement region. Recently, it has been established that the increase in p is the signature of a physically real phenomenon and not merely an artifact of statistical non-stationarity arising from the narrowness of the scintillation strength enhancement. Moreover, it has been found that p is not increased in strength enhancements occurring close to the magnetic zenith. Indeed, in some cases, it is substantially decreased. A possible source of these unexpected spectral behaviors is size-dependent anisotropy (an idealization of the irregularities responsible being small-scale field-aligned rods imbedded in large-scale shell-aligned sheets). In this paper, the collective behavior of p will be described, representative individual spectra will be presented, and the hypothesis of size-dependent anisotropy will be explored.

G2-7
1600

INTENSITY AND PHASE SPECTRAL CHARACTERICS UNDER STRONG SCATTER CONDITIONS

C.L. Rino and J. Owen
Radio Physics Laboratory
SRI International, Menlo Park, CA 94025

We have used the power-law phase-screen model to calculate the intensity scintillation index, the intensity and complex-signal decorrelation times, and the frequency decorrelation of radio-wave scintillation. Predictions from our model agree well with data from the Wideband satellite. More recently, we have performed numerical simulations using the power-law phase-screen model to study the detailed structure of intensity and phase spectra. We verified the model by comparing the results to theoretical predictions obtained using asymptotic approximations. We then analyzed the measured intensity and phase spectra to identify features that reveal unambiguously the spectral characteristics of the in situ irregularities, particularly discontinuities in the spectral index.

G2-8 1620 IONOSPHERIC EFFECTS OF THE APRIL 1981 MAJOR MAGNETIC STORM AT MIDLATITUDES: A. Das Gupta and J. A. Klobuchar, Air Force Geophysics Laboratory, Hanscom AFB, MA 01731; H. Soicher, U.S. Army Communications-Electronics Command, Fort Monmouth, NJ 07703; and Santimay Basu, Emmanuel College, Boston, MA 02115

Ionospheric electron content (TEC) data obtained by the Faraday rotation technique at a number of stations around the 75°W longitude meridian showed two remarkable features during the major magnetic storm of 11-15 April 1981. The maximum storm activity occurred in the pre-dawn hours of 13 April 1981. During this period a large build up of TEC was observed at the low mid-latitude stations, which was nearly identical to a normal sunrise TEC increase, except that it was observed approximately 90 minutes earlier than the normal sunrise.

The Faraday rotation records at all stations also exhibited occasions of fast polarization fluctuations (FPF), which are normally peculiar to stations situated only near the crests of the Appleton anomaly. We observed FPF at stations from a magnetic dip of 45°, to the sub-auroral location at Hamilton, Massachusetts. Dynamical ionospheric effects associated with the magnetic disturbance are examined to explain the observed phenomena.

* NRC/NAS Resident Research Associate. Permanent address: University of Calcutta, India.

Commission H Session 3

WAVE EMISSIONS FROM NATURAL ELECTRON BEAMS IN SPACE
Wednesday afternoon, 5 Jan., CR2-78
Chairman: W. Calvert

H3-1
1340

CURRENT QUESTIONS ABOUT AURORAL KILOMETRIC RADIATION

W. Calvert, Department of Physics and Astronomy
The University of Iowa, Iowa City, Iowa 52242

Over the past few years, it has been shown that auroral kilometric radiation (AKR) originates within a transient cavity of decreased plasma density, mostly as X-mode waves perpendicular to the magnetic field and at frequencies just above the electron cyclotron frequency. It has been found to consist of temporally-drifting discrete spectral components and also to sometimes exhibit what appears to be ion cyclotron modulation. Surprisingly, the AKR can sometimes be triggered by external waves. The basic mechanism for generating AKR seems to be the doppler-shifted cyclotron resonance instabilility, probably driven by loss cone free energy. Quite recently, a new feedback model has been proposed for the AKR source, which requires saturated wave oscillations inside local density enhancements. This can account for the discrete components, including their drifts, and it would require less gain than that previously believed necessary. At this stage, the pertinent observational and theoretical questions about AKR seem to be the following: (1) How strong and prevalent are the emissions in other wave modes and at harmonics, and are they really independent of the primary X-mode signals? (2) What is the temporal relation between AKR, auroral arcs, and the cavity, in view of the cavity's transient nature and the possibility of external triggering? (3) What causes the cavity? (4) How does the triggering occur? (5) What simultaneous direct evidence can be found for loss cone free energy and ion waves at the AKR source? (6) Is the predicted wave growth still sufficient when refraction, feedback, and saturation are included in the theories?

H3-2
1400

AURORAL KILOMETRIC RADIATION/AURORA CORRELATION:

Robert F. Benson, NASA/Goddard Space Flight Center, Greenbelt, MD 20771
S. -I. Akasofu, Geophysical Institute, University of Alaska, Fairbanks, AK 99701

A dozen high-altitude, high-latitude, nighttime ISIS 1 satellite passes have been used to deduce contours of the electron density N_e from the satellite position to the peak of the F region throughout the auroral kilometric radiation (AKR) source region. The latitudinal extent of the electron density depletions ($N_e < 100$ cm^{-3}) associated with AKR generation is quite variable from pass to pass, ranging from a few degrees to 25°. AKR sources are often associated with steep latitudinal N_e gradients. Some of these passes corresponded to overflights of Alaskan auroral all sky camera stations. While the correlation of individual features between the two data sets is difficult to achieve, the general activity levels of a larger data base including more than 100 all-sky camera station overflights are well correlated. In this correlation, however, the intensity of AKR activity often exceeds that of the aurora, i.e., intense AKR can often be observed even when little auroral activity is detected. Such a difference suggests that the AKR has a lower threshold for excitation. One possible explanation is that the higher altitude AKR phenomena can be generated by lower energy particles than are required to excite the lower altitude phenomena of the visual aurora.

H3-3
1420 "Auroral Zone Wave Emissions Observed with Dynamics Explorer", Stanley D. Shawhan, Donald A. Gurnett and Richard L. Huff, Department of Physics and Astronomy, The University of Iowa, Iowa City, Iowa 52242

In the first year of operation, the Dynamics Explorer-1 spacecraft has covered the northern auroral zone region from 1 to 3.7 R_E in altitude and the southern region from 0.1 to 3 R_E in altitude. Three types of auroral zone emissions are predominant--Auroral Kilometric Radiation (AKR), Auroral Hiss (AH) and low frequency electrostatic noise, possibly Electrostatic Ion Cyclotron Emissions (EIC).

Through use of an on-board correlator, AKR and AH are found to be righthand polarized and propagating away from the earth above 1 R_E altitude. AKR is often observable on the dayside at high altitudes; but it is not always present when auroral zone field lines are crossed; it is correlated with auroral arcs as seen with the DE Spin Scan Auroral Imager and is correlated with geomagnetic substorms. Auroral hiss is almost always present whenever auroral field lines are crossed. It exhibits spatial structure with several strong emission regions across the auroral zone. A ray tracing analysis for one case requires that the emission altitude not be below 5,000 km. The electrostatic noise emission is intense in the cusp region as well as the auroral zone and it occurs sporadically over the polar cap. Frequenices extend from a few hertz up into the kHz range. Detailed wideband spectrograms have shown evidence of wavelengths short compared to the 200 meter electric antenna. These observational features are to be illustrated and implications for the source mechanisms to be discussed.

H3-4
1440

ORDINARY MODE AURORAL KILOMETRIC RADIATION - WITH HARMONICS - OBSERVED BY ISIS 1:

Robert F. Benson, NASA/Goddard Space Flight Center, Greenbelt, MD 20771

Many theories have been proposed to explain auroral kilometric radiation (AKR) - the most intense emission of natural origin from the terrestrial magnetosphere. The main theoretical challenge has been to explain this great emission intensity which indicates that a particle to wave energy conversion process with an efficiency as large as 1% is involved. The propagation mode and harmonic components of the radiation are among the most important theoretical parameters amenable to observational confirmation. One theoretical approach, based on direct amplified cyclotron emission, predicts radiation in both extraordinary and ordinary modes, both with harmonics, with the fundamental x-mode being by far the dominate signal in the low density source regions of intense AKR (Melrose et al., JGR, 87, 5140, 1982]. Most observations have inferred that the main radiation is in the x-mode, e.g., see the recent high latitude DE-1 observations of Shawhan and Gurnett [GRL, 9, 913, 1982]. Oya and Morioka (private communication, 1982), however, observed the dominate AKR emission to be in the o-mode from the lower latitude Jikiken satellite (EXOS-B).

The present ISIS 1 topside-sounder receiver observations also reveal examples of o-mode AKR observed equatorward of the low density source region of intense AKR x-mode emission. The propagation modes are identified by comparing the natural radiation wave cutoffs with the local resonant and wave cutoff phenomena stimulated by the sounder transmitter. The o-mode AKR is the dominant emission in these regions of relatively high electron density, but it is considerably weaker than the intense x-mode AKR observed to emanate from the low density cavities found by Benson and Calvert [GRL, 6, 479, 1979]. In addition to the fundamental o-mode, 2nd and 3rd harmonic bands of radiation have also been detected. Based on the few examples which have been identified to date - these o-mode harmonics are less intense than the harmonics (up to the 4th) of x-mode AKR [Benson, GRL, 9, 1121, 1982]. These results indicate the importance of extending future theoretical investigations to treat the limiting conditions of higher plasma density conditions (plasma frequency as high as the electron cyclotron frequency) in order to predict the behavior of the weaker emissions which can be, and are, observed - in addition to the dominant emissions generated within AKR density cavities.

H3-5
1500

EVIDENCE FOR ORDINARY MODE AURORAL KILOMETRIC RADIATION FROM THE MODE - COUPLING MECHANISM:

Robert F. Benson, NASA/Goddard Space Flight Center, Greenbelt, MD 20771

One of the first mechanisms proposed to explain auroral kilometric radiation (AKR) involved the conversion of wave energy from a longitudinal electrostatic mode to the transverse electromagnetic ordinary mode [Benson, GRL, 2, 52, 1975]. A number of workers have pointed out that such a wave-mode coupling process lacks the efficiency to explain the AKR intensity. In addition, observational evidence from a number of satellites indicate that the intense AKR signals are predominately in the extraordinary mode. A weak wideband signal is occasionally observed on ISIS 1 high-latitude nighttime ionograms, however, with characteristics which are consistent with the mode-coupling mechanism. This signal is observed to be associated with the narrowband noise signal near 2MHz observed under similar conditions on ISIS ionograms which has been interpreted in terms of o-mode waves resulting from a 3-wave interaction occuring in the auroral region below the satellite at the level where $f_T = 2f_H$ where f_T is the upper hybrid frequency and f_H is the electron cyclotron frequency [James et al., AGARD, CP #138, 24-1, 1974]. The upper frequency cutoff of the proposed o-mode AKR noise band is typically 1.65 MHz which corresponds to the plasma frequency f_N at the level identified by James et al where $f_T = 2f_H$. This cutoff frequency is in exact agreement with the value predicted by the mode-coupling mechanism. Since it is greater than the local value of f_T, the wide band noise signal cannot be in the whistler or z-modes. In addition to the upper frequency cutoff being consistent with the remote f_N value when $f_T = 2f_H$, the lack of an observed low frequency cutoff at the local cutoff for the x-mode argues in favor of the o rather than the x mode for this weak wideband signal. While lower frequency, higher signal intensity o-mode AKR waves consistent with the direct amplified cyclotron emission mechanism are also observed on ISIS 1 ionograms [Benson, this conference, 1982], the present observations appear to be the first convincing evidence of o-mode AKR waves produced by the mode-coupling mechanism.

H3-6 1540 COMPUTER SIMULATION OF AURORAL KILOMETRIC RADIATION: J. S. Wagner and T. Tajima, Institute for Fusion Studies, University of Texas; L. C. Lee, Geophysical Institute, University of Alaska; C. S. Wu, Institute for Physical Science and Technology, University of Maryland

We are working on a self-consistent relativistic, electromagnetic particle simulation of auroral kilometric radiation. We assume two electron populations, a cold maxwellian background and a hot loss cone component. This configuration has been shown to be unstable to cyclotron wave instability. We can follow the linear growth and saturation of all important radiations including the X,O, and Z-modes, as well as the whistler. We find the X-mode saturates by turbulent scattering of hot electrons into the loss cone at higher power levels in general agreement with observation.

H3-7 The Generation of Auroral Kilometric Radiation
1600 P. B. Dusenbery, Department of Astro-Geophysics, University of Colorado, Boulder, CO 80309

Auroral kilometric radiation (AKR) has a peak intensity at 250 kHz and is associated with discrete aurora in regions where $\omega_p/\omega_c<0.2$. There are two high frequency electromagnetic wave modes in which AKR could propagate, the L mode and the R mode. Most observations of AKR are inconsistent with the characteristics of L-mode radiation. However, the characteristics of the upper frequency branch of the R-X mode are consistent with most AKR observations. We therefore look at the following free-energy sources in the auroral electron distribution function as possibilities for exciting the R-X mode: (1) the accelerated, precipitating electrons and, (2) the upgoing loss cone associated with the electrostatically trapped electrons. Solving the relativistic resonance condition exactly gives contours in velocity space that are elliptical. We are able from this condition, to determine the maximum value of ω_p/ω_c for which resonance exists for the first three harmonic emissions. Diffusion of precipitating electrons which develop $\partial f/\partial v_\perp>0$ due to the magnetic mirroring force and diffusion of trapped electrons in the upgoing loss-cone with R-X waves are towards decreasing energies so that wave growth is possible. To determine which frequency and wave vector (k,θ) is associated with each resonant contour we solve the cold plasma dispersion relation for ω_R, k and θ where $\omega_R>\omega_x$, the right-hand cutoff frequency. Growing waves will be associated with those contours which pass through regions of velocity space where $\partial f/\partial v_\perp>0$ is large. A simple criteria is given to show which R-X waves will have large positive growth rates. Finally, we calculate the group velocity of R-X waves and show that R-X waves with large, positive growth rates also have small group velocities ($V_g/c<<1$) implying a very small convective growth length $\sim$10m. The intense wave generation should occur at wave frequencies just above harmonics of the electron-cyclotron frequency and have wave normal angles $75^o<\theta\lesssim 105^o$. Wave growth maximizes in regions where ω_p/ω_c is small ($\lesssim$0.07). On the other hand, for $\omega_p/\omega_c \sim$0.3-1.0, no growth of the fundamental emission should occur but growth rates of the second harmonic emission should be less than, but comparable to, the maximum growth rate of the fundamental for $\omega_p/\omega_c \lesssim 0.07$. Maximum growth rates for the third and higher harmonic emissions were found to be generally much less than that for the first two harmonic emissions.

H3-8 1620 SCATTERING OF ION BEAMS ASSOCIATED WITH AURORAL KILOMETRIC RADIATION AND OTHER WAVE ACTIVITY AS WELL AS STRONG DC ELECTRIC FIELD TURBULENCE: Eigil Ungstrup, R. D. Sharp, Space Sciences Laboratory, Lockheed Palo Alto Research Laboratory, Palo Alto, CA 94304; C. Cattell, Space Sciences Laboratory, University of California, Berkeley, CA 94720; R. R. Anderson, Department of Physics and Astronomy, University of Iowa, Iowa City, IA 52242; and R. J. Fitzenreiter, NASA Goddard Spaceflight Center, Greenbelt, MD 20771

The ISEE-1 Ion Mass Spectrometer was operated in a high time resolution mode on 2 out of 5 passes over the auroral oval from the fall of 1980 until the spring of 1982 and accumulated data from 95 passes over the auroral oval during that period. The data set obtained from this mode, the Auroral Search Mode, has been searched for signatures of local instabilities occurring at or close to the satellite. Over the auroral oval one frequently observes upflowing field aligned beams of O^+ or H^+. These beams are typically collimated to within 20 to 30 degrees of the magnetic field direction, but at times the beams are suddenly scattered and become almost isotropic over the upper hemisphere still maintaining the upward flow direction. Scattered beams are observed on 34 of the 95 passes accumulated.

The electrons show strong variations in flux and pitch angle as well as in density during the ion beam scattering events. The broadenings or scatterings of the ion beams are also associated with strong auroral kilometric radiation and strong wave activity below the local plasma frequency as well as by turbulent DC electric fields. The scattering of the ion beams seems to be the signature of a plasma instability at or near the satellite. A likely candidate for the instability is the ion cyclotron instability which will preferentially scatter the beam normal to the magnetic field direction because of its polarisation. The observations seem to support the hypothesis that there is a connection between electrostatic ion cyclotron waves and the generation of auroral kilometric radiation (C. L. Grabbe et al. JGR, 85, 3337, 1980).

H3-9 1640 STATISTICAL STUDY OF AURORAL ROAR: Paul J. Kellogg and Steven J. Monson, School of Physics and Astronomy, University of Minnesota, Minneapolis, MN 55455

A total of about 60 auroral roar events (Kellogg and Monson, 1979) have been found in data obtained during three campaigns at Churchill, Manitoba. No events have been found in a similar period at Poker Flat near Fairbanks, Alaska. Data on frequency range (near 3 MHz), time (around local midnight) and length will be presented.

Kellogg, P. J. and S. J. Monson, Geophys. Res. Lett. 6, 297-300 (1979)

MICROWAVE AND FIELD MEASUREMENTS
Commission A, Session 3, CR1-46
Chairman: N. S. Nahman, NBS, Boulder, CO

A3-1 0900 REMOTE TEMPERATURE SENSING BY MEANS OF ACTIVE MICROWAVE IMAGING: J. Ch. Bolomey, L. Jofre, and G. Peronnet, Groupe d'Electromagnetisme, Laboratoire des Signaux et Systemes, Ecole Superieure d'Electricite, Plateau du Moulon, France

This communication is devoted to the possible use of active microwave imaging for remote temperature sensing. Such a possibility results from the temperature dependence of the complex permittivity of the objects to be observed.

Active microwave tomography (J.Ch. Bolomey et al., Microwave diffraction tomography for biomedical applications, to be published in IEEE-MTT Transactions, Nov. 1982) allows the reconstruction of the equivalent currents which are related to the complex permittivity. Microwave images can then be interpreted in terms of temperature from a more or less straigth forward manner.

Some basic experiments conducted in water at 3 GHz illustrate the temperature sensitivity as well as the spatial resolution capabilities of this imaging process. Its limitations are discussed in view of applications to microwave heating in biomedical (hyperthermia) or industrial domains. The discussion includes a comparison with classical microwave thermography.

(*)Sponsored by DGRST [TLB 81.M.0909], in collaboration with Société d'Etude du Radant (Orsay) and Laboratoire de Thermologie Biomédicale (Strasbourg).

A3-2
0920

SURFACE CURRENT ANALYSIS ON FLAT PLATES

Ronald M. Sega and Robert W. Burton
Department of Electrical Engineering
University of Colorado, Colorado Springs, CO 80933

This report focuses on an infrared measurement technique for determining the magnitude of surface currents. A comparison is made with magnetic field probe measurements and theoretical solutions for metallic flat plates illuminated with a normally incident, plane electromagnetic wave.

The surface currents induced by electromagnetic radiation incident on conductive bodies produce joule heating measurable by infrared techniques. Qualitative studies have shown that surface current amplitude information can be determined from the surface heating pattern. A quantitative analysis, via infrared techniques, of microwave induced surface current amplitude distributions on the flat plates is presented.

This correlation study of infrared obtained surface current amplitude distributions compared with electromagnetic computer code calculations and probe measurements on flat plates is an essential step toward the infrared measurement of current distributions on more complex shapes.

A3-3
0940

MICROWAVE MEASUREMENT OF THE COMPLEX PERMITTIVITY TENSOR OF ANISOTROPIC SLAB MATERIALS

R. J. King, Lawrence Livermore National Laboratory
Livermore, CA 94550 (on leave from the University of Wisconsin, Madison) and
Y. H. Yen, Bell Telephone Laboratories
Homdel, NJ 07733

A microwave (4.8 GHz) system has recently been developed for measuring the amplitude, phase and polarization of plane waves transmitted through slabs of uniaxial anisotropic media [King and Yen, IEEE Trans. MTT-29(11), 1225-2231, 1981]. Here it will be shown how these measured electrical parameters can be used to infer the complex dielectric tensor. In turn, these data are correlated with the physical parameters (e.g., specific gravity, moisture content and the macroscopic grain direction). These nondestructive testing techniques were used to study the electrical and physical properties of several species of dimension lumber. Some typical results for Douglas Fir are shown in the figure, where $\perp$ and $\parallel$ refer to when the incident electric field is perpendicular or parallel to the grain, respectively. The results are in good agreement with published data obtained using shaped specimens inserted into a cavity or waveguide.

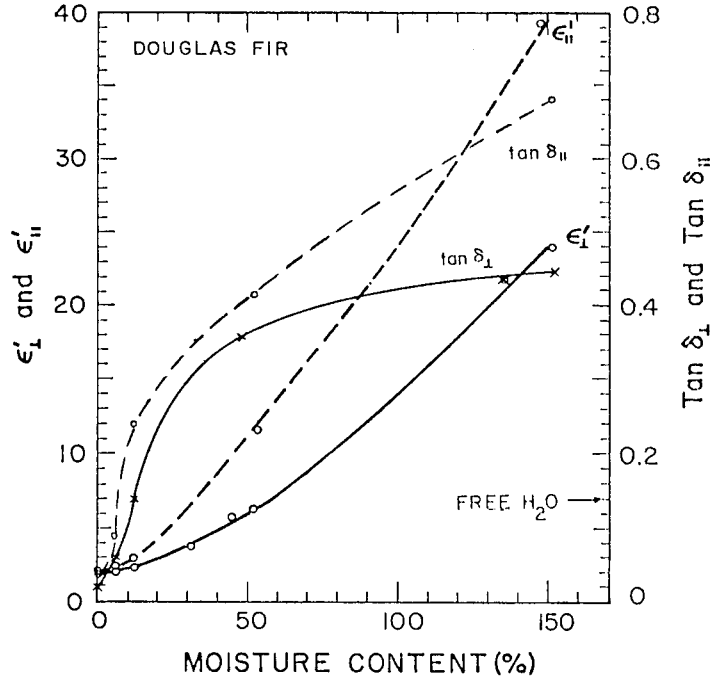

A3-4
1020

Preliminary Results from Measurements of 800 MHz Radio Transmission into Residential Buildings

D. C. Cox, R. R. Murray and A. W. Norris,
Bell Laboratories, Crawford Hill Lab,
Holmdel, New Jersey 07733

The attenuation of radio signals propagating into buildings has a significant effect on the performance of portable radiotelephone systems. An experiment has been implemented to provide 800 MHz attenuation information needed for refining the configuration and design of portable systems that will accomodate low-power portable sets. The measurements are made using an instrumentation van that can be parked at different locations to simulate different Portable Radiotelephone Terminals, i.e., different fixed radio terminals that could provide attachment points to the telephone network. The van has an erectable 25 foot high omnidirectional antenna. Attenuation is measured in and around houses in suburban residential areas. The experiment and attenuation statistics measured in a few residential buildings are described. Building attenuation for a house that has metal foil insulation ranges from -10 dB to 25 dB when referred to the average signal level outside the house. Small scale signal distributions are approximately Rayleigh distributed. Large scale distributions of the small scale signal medians are approximately log-normally distributed.

A3-5
1040 MEASUREMENT OF THE INPUT IMPEDANCE OF A CYLINDRICAL ANTENNA WHICH RESIDES IN TWO CONTIGUOUS HALF SPACES:

Cecil A. Harrison and Chalmers M. Butler, Department of Electrical Engineering, University of Mississippi, University, MS 38677

In this paper is described the initial phases of an experimental study of a circular cylindrical antenna, which is partially in one half space and partially in another. The half spaces are separated by a planar interface and the cylinder axis is perpendicular to the plane of the interface. The two media are water and air, and the measurements are made in a tank (16' x 16' x 4'). The antenna is a sleeve "monopole" constructed from semi-rigid coaxial line which is fed by means of a high-quality coax attached to the tank bottom and having a feed-through to the tank exterior. The water is sufficiently lossy that the portion of the antenna in the water appears to be of infinite length and that the feed line does not perturb the field in the water radiated by the antenna. Input impedance is measured over a range of frequencies about 600 MHz for various parameters of interest including radius and length-above-water of the cylinder and displacement of feed point above water. In order that the measurements may be placed in proper perspective, the water properties are measured at the frequencies of interest. Measured data are compared with calculated data.

A3-6 1100 THE VLF EMF MEASUREMENTS: H. Trzaska, Institute of Telecommunication and Acoustics, Technical University of Wroclaw, Poland

Lately in Poland were introduced new environmental regulations establishing permissible levels of EMF at frequency 50 Hz as well. It creates new formal need in EMF measurements.

Taking into account higher harmonics of 50 Hz, e.g., in multiphase rectifiers or thyristor regulators, were designed and published meters for frequency range about 50-200 Hz. However, it is necessary to remember, that there is a problem of EM radiation hazard in vicinity of other VLF power sources / inductive heaters, ultrasonic equipment / which work in the frequency range from several hundred hertz to several hundred kilohertz. It could be supposed that work safety standards will be introduced in this frequency range in the near future as well. Disregarding this, today exists need for measurements in the frequency range in research on the VLF EMF bioeffects. Another problem here is the measurement of the VLF EMF radiated by living bodies and tissues. The measurement is important in "in vivo" noninvasive investigations of electrical phenomena of live.

In two above cases are used wideband methods of measurements in the frequency range of few decades. Sensitivity should sometime exceed used in EMF measurements at RF and microwaves.

The paper presents theoretical basis of the VLF EMF meter designing, discusses necessary measuring accuracy and ways to its realization and shows two designs of meters for different VLF EMF measuring purposes. Each of them contains electrically small antenna, wideband amplifier and the output voltage processing system.

A3-7
1120

PROTOTYPE OF A REFERENCE MAGNETIC-FIELD RADIATOR:

L. D. Driver, National Bureau of Standards, Electromagnetic Fields Division, Boulder, CO 80303

A stable, self-contained magnetic-field radiator has been designed and built for use in the evaluation and characterization of new and varied electromagnetic (EM) measurement systems, facilities, and techniques. This H-field radiator operates at any one of five rf frequencies (2, 4, 6, 8, or 10 MHz). This provides corresponding rf loop currents of 400 to 180 mA, and an effective radiator Q which varies from 1 to 6. Preliminary evaluation of the radiator has been performed.

The single-turn radiating loop was fabricated using standard 1-1/8" copper pipe and 90° elbows. Two sides of the 23 cm (9") square loop contain a rechargeable 8 cell battery pack. A third side houses a circuit board which contains (1) a dc voltage regulator; (2) an rf signal source composed of a crystal controlled oscillator, a buffer amplifier, a power output stage, and a tuned output circuit; (3) an rf loop current detector cicuit; and (4) the appropriate switches, indicators, measurement test jacks, and battery recharging terminals. The fourth side of the loop contains a 1.58 mm (1/16") gap which allows the loop to be driven by the internal rf signal generator. The dc output of the rf loop current detector can be measured using an external metering system. This calibrated dc output voltage provides information as to the magnitude of the rf loop current. The measured rf loop current can readily be converted to field strength units and/or to radiated rf power by using the appropriate formulas.

This prototype reference H-field radiator will be modified, improved, and/or updated as required to meet future needs. Also, additional prototype models of this H-field radiator will undoubtedly be forthcoming as size, operating frequency, radiated power, and other radiator parameter requirements change. It is expected that this effort will lead to the development of a standard H-field radiator(s) which will be capable of emitting stable, repeatable, predictable, and well-defined fields. The radiation characteristics of such a standard radiator would (1) be analytically predictable and (2) have good correlation with experimental measurement results.

Commission B Session 4

TRANSIENTS
Thursday morning, 6 Jan., CR2-6
Chairman: Dr. D. R. Wilton, Department of Electrical Engineering, University of Mississippi, University, MS 38677

B4-1
0850 CONVOLUTION OF SYNTHESIZED RADAR SIGNALS FOR SINGLE- OR ZERO-MODE EXCITATION WITH EXPERIMENTAL RADAR RETURNS: Lance Webb, Byron Drachman, K.M. Chen, D.P. Nyquist, C-I Chuang; Michigan State University, E. Lansing, Mich. 48824 and Bruce Hollmann; Naval Surface Weapons Center, Dahlgren, VA 22448

In the study of the radar waveform synthesis for target identification, the required waveforms for the incident radar signal, which is aspect-independent, to excite single-mode backscatters or zero backscatter (K-pulse) in the late-time period of the radar return are synthesized for various simple targets based on the SEM principle. Instead of radiating these required incident signals to the targets, we store them in the computer, and convolve them with radar returns from the targets excited by a smoothed impulse signal. The objective of this study is to examine the applicability of these theoretically synthesized incident signals to the practical situations simulated by experiments.

The radar returns from wire and spherical targets excited by a smoothed impulse signal were measured on a time-domain range. The measured returns were deconvolved with the impulse response of the receiver to obtain the impulse responses of the targets. For this purpose, a deconvolution technique which gives stable results was developed. The impulse responses of the targets were then convolved with the required signals for single-mode or zero-mode excitation. The late-time responses of the convolved, output signals were examined.

B4-2
0910

ANTENNA RESPONSE OF A CYLINDER GROUNDED BY A THINNER COLLINEAR CYLINDER:

A.W. Biggs, Remote Sensing Laboratory, CRINC
University of Kansas, Lawrence, KS 66045

Analysis of the transient response of a monopole antenna, made from a metal cylinder connected to a ground plane by a thinner collinear metal cylinder, is presented along with experimental results. The antenna consists of a copper metal cylinder, 7.5 cm diameter and 1.0 m long, and a copper metal cylinder, 2.5 cm diameter and 25 cm long, capped at the larger cylinder. The smaller cylinder fits into a 2.5 cm thick aluminum plate which rests on the ground plane.

The antenna was radiated with electromagnetic pulses (EMP) at the Air Force Weapons Laboratory's ALECS facility in Albuquerque, NM. The risetime varied from 3 to 10 ns with peak amplitudes for the electric field from 70 to 90 kV/m.

The "dumbbell" antenna was originally made to simulate the transition between a B-52 aircraft and a refuelling boom from a KC-135 aircraft or a trailing wire antenna. It was also made ti observe current transitions along a changing wire diameter.

Simplex Algorithm

B4-3
0930 TWO METHODS TO DECONVOLVE: L_1 - METHOD USING SIMPLEX ALGORITHM AND L_2 - METHOD USING LEAST SQUARES AND A PARAMETER? Byron Drachman, Dept. of Mathematics, Michigan State University, East Lansing, Michigan 48824

If $r(t)$ is the linear, scatter response of an object to an excitation waveform $e(t)$, then $r(t) = (e * h)(t)$. One would like to deconvolve and solve for $h(t)$, the impulse response. It is well-known that this is often an ill-conditioned problem. Two methods are discussed. The first method replaces the discretized matrix form $E \cdot H = R$ by the following problem: minimize $|h_1|+\cdots+|h_n|$ subject to $R-\lambda \leq E \cdot H \leq R+\lambda$ where λ is a column vector chosen sufficiently small to yield acceptable residuals, yet large enough to make the problem well-conditioned. This problem is converted to a linear programming problem so that the Simplex Algorithm can be used.

The second method is to minimize $||E \cdot H-R||^2 + \lambda||H||^2$ where again λ is chosen small enough to yield acceptable residuals and large enough to make the problem well-conditioned.

The method will be demonstrated with a Hilbert matrix inversion problem and also the deconvolution of the impulse response of a simple target from measured data.

Phillips, ACM Vol. 8-9, 1961 Pp. 84-97

Rheinhardt

B4-4
0950

KILL-PULSE SYNTHESIS USING TIME-DOMAIN SEM:

D. P. Nyquist and K-M Chen, Dept. of Elect. Eng. and Sys. Sci., Michigan State Univ., East Lansing, MI 48824

The intriguing new K-pulse (kill-pulse) concept recently advanced by Kennaugh provides a potential scheme for radar target discrimination. It is found that an optimal incident waveform of finite duration T_e can be synthesized, for a preselected target, which excites no late-time scatter field when it illuminates that target. Since a different target maintains nonzero late-time backscatter when illuminated by the K-pulse, the preselected target is discriminated. Kennaugh used primarily frequency-domain transmission-line and circuit analogies to implement his original K-pulse. We find, based upon a simple time-domain SEM technique, that the aspect-independent K-pulse arises as a special case of our incident-waveform synthesis for monomode scattering.

Unknown K-pulse waveform E_K^i satisfies the integral equation

$$E^s(t) = \int_0^{T_e} E_K^i(t')h(t-t')dt' = 0 \quad \text{... for } t>T_e+2T$$

where E^s is the scatter field, $h = h_f + h_n$ is the target impulse response where the forced component $h_f = 0$ for $t > 2T$, T is the maximal one-way transit time for an impulsive wavefront to traverse the target, and $t > T_e + 2T$ defines the late-time period of the scatter field. Natural component h_n of the impulse response has the SEM representation

$$h_n(t) = \sum_{i=1}^{N} a_n(\theta,\phi)e^{\sigma_n t}\cos\{\omega_n t + \psi_n(\theta,\phi)\}$$

where $s_n = \sigma_n + j\omega_n$ are the target natural frequencies while $a_n(\theta,\phi)$ and $\psi_n(\theta,\phi)$ are aspect-dependent amplitude and phase factors. Expansion of E_K^i in an appropriate basis set leads to an aspect-independent, homogeneous matrix equation of order 2N with elements $M_{nm}(T_e)$ depending upon T_e. Characteristic K-pulse durations are determined by the condition $\det(M_{nm}(T_e)) = 0$, which leads subsequently to non-trivial K-pulse waveforms.

Results presented include K-pulse waveforms for thin-wire and spherical targets. Uniqueness of the K-pulse is established by demonstrating that it is independent of the basis set chosen to represent E_K^i and insensitive to the number N of SEM modes retained in the expansion for h_n.

B4-5
1030

IMPULSE RESPONSE OF COUPLED WIRES BY SEM:

C-I Chuang, D. P. Nyquist and K-M Chen, Dept. of Elect. Eng. and Sys. Sci., Michigan State Univ., E. Lansing, MI 48824

The impulse response of a relatively general, skew-coupled wire system is computed by the Singularity Expansion Method (SEM). For the purpose of determining the transient response of a scatterer, it is desirable to compute its impulse response. Once computed, any transient response can be obtained by convolving it with the incident waveform. If this impulse response is convolved with the required waveform obtained from single-mode or kill-pulse synthesis, the expected response can be observed.

The impulse response of a system of coupled wires is obtained by applying SEM and the moment method to the coupled integral equations. Both E-field and Hallen-type integral equations are derived. Hallen's integral equation is used to determine the natural modes of this system, while the E-field integral equation is used to compute the coupling coefficients. Both "class 1" and "class 2" coupling coefficients are obtained and their physical implication will be illustrated. Current and scattered electric field impulse responses are constructed based upon these coefficients and natural mode currents. Special cases of current step responses are compared with results in the existing literature. Various approximations to the backscattered E-field impulse response of an isolated wire target are compared.

The impulse response is convolved with the required E-field synthesized previously to implement monomode scatter or K-pulse behavior. The potential of these schemes for radar target discrimination is thus confirmed. Computed impulse responses are compared with those measured on our time-domain range.

B4-6
1050 TRANSIENT REFLECTED FIELD DUE TO A PULSED LINE SOURCE ABOVE A CONDUCTING, DIELECTRIC HALF-SPACE:

E.F. Kuester, Electromagnetics Laboratory, Department of Electrical Engineering, Campus Box 425, University of Colorado, Boulder, CO 80309

Except in certain special cases, the computation of transient fields in the presence of layered, dispersive media requires Fourier inversion of a frequency-domain solution, itself expressed as an infinite integral over the wavenumber (a Sommerfeld integral). For the case of a pulsed line current located above a finitely conducting, dielectric half-space, there is presently no other solution than the doubly-infinite integral which results from this Fourier inversion. Since the error involved in numerically evaluating a doubly-infinite integral can be hard to estimate, and because a large amount of computing time may be necessary, we present a modification of a method originally proposed by P.E. Doak (Proc. Royal Soc. (London), A215, 233-254, 1952) which allows us to write the exact solution as a finite double integral. This integral can be quickly and efficiently evaluated on a computer. We will present numerical results and compare them with an early-time (Cagniard-de Hoop) approximation, as well as with a late-time approximation due to Ollendorff (Elek. Nachr.-Tech., 7, 393-407, 1930) and Peterson (Bell Syst. Tech. J., 9, 760-769, 1930). There is a significant time-interval where neither approximation is numerically accurate, making our method of computation a valuable one.

Commission C Session 2

INFORMATION THEORY
Thursday morning, 6 Jan., CR1-42
Chairman: A. J. Viterbi

C2-1
0850

RANDOM ACCESS COMMUNICATIONS

J. K. Wolf, Department of Electrical and Computer Engineering, University of Massachusetts, Amherst, MA 01003

Some recent results on random access communications will be discussed. Emphasis will be on results obtained by information theoretic arguments.

C2-2
0910

AN INFORMATION THEORETIC APPROACH TO MITIGATION OF TONE JAMMING IN NONCOHERENT MFSK CHANNELS

A. J. Viterbi, M/A-COM Linkabit, Inc.,
3033 Science Park Road, San Diego, CA 92121

It is well known that a tone or partial-band noise jammer can so choose his jamming strategy as to cause the bit error rate of a frequency-hopped MFSK transmission system, to be an inverse linear function of $E_b/N_o = (W/R)/(J/S)$, where W is the total available bandwidth available to the communicator, R is the bit rate and J/S is the jammer-to-signal power margin. This situation can be greatly improved by the use of coding, but with hard decisions, performance is still significantly worse than in additive Gaussian noise, unless sufficient time diversity (hops/bit) are employed to thwart such jammers - but at a cost in performance due to coherence loss. This paper investigates use of a simple robust technique which generates a "quality" bit based on the ratio of the maximum filter output to the second largest filter output. This improves coded system performance by as much as 6 dB for a tone jammer and makes lower redundancy (time diversity) more desirable. Performance is measured by E_b/N_o level required to operate at a given rate equal to cutoff rate r_o for the jammed channel at the minimax operating point.

C2-3
0950

DISTRIBUTED ALGORITHMS FOR RADIO NETWORKS

R. G. Gallager, Massachusetts Institute of Technology, Department of Electrical Engineering and Computer Science, Cambridge, MA 02139

Suppose a radio network is modelled by a graph in which the nodes represent radio transmitter/receiver pairs and an edge between two nodes denotes that the two radios are in reception range of each other. The edges of the graph change slowly in time due to changing propagation conditions and possible mobility of the radios. We discuss a number of approaches to routing data in such networks. Particular attention is given to algorithms in which each node maintains a routing table associating each destination with two next edges, either of which can be used to reach the destination. Upon an edge failure, these tables revert immediately to one edge per destination, routing around the failure, and then a distributed algorithm, using communication between the nodes, rebuilds the alternate path.

REMOTE SENSING OF SURFACES - I: THE SEA
Thursday morning, 6 Jan., CR2-26
Chairman: Leonard Fedor, Wave Propagation Laboratory, ERL/NOAA, Boulder, CO

F3-1
0830 AMPLITUDE OF HF RADIOWAVES NEAR A LAND-SEA INTERFACE

R.M. Jones
NOAA/ERL/Wave Propagation Laboratory
Boulder, CO 80303

Groundwave modes have propagation characteristics that depend on the surface impedance of the ground. At a land-sea interface, groundwave mode conversion takes place. The conversion coefficients have been known for several years (D.A. Hill and J.R. Wait, IEEE Trans. Geosci. Remote Sensing, GE-19, pp 210-216, 1981, and the references they cite). However, the usual representation, in which the radiowave amplitude is represented by a sum of groundwave modes appropriate to the sea above the sea and a sum of groundwave modes appropriate to the land above the land, yields field discontinuities above the land-sea interface, possibly because the sum of groundwave modes above the land (for sea-to-land propagation) may not converge.

Insight into the behavior of the radiowaves near a land-sea interface comes from recognizing that each sea-type groundwave mode does not stop at the vertical plane above the land-sea interface, but extends beyond the interface for an elevated observer. The shadow boundary for each groundwave mode is a plane that includes the land-sea interface and is made up of complex rays tangent to the caustic associated with the groundwave mode. For an observer at a given height, the shadow boundary of lower order modes extends farther across the interface than that of higher order modes. Further, the groundwave modes excited at the land-sea interface also have a shadow-boundary associated with them in the same way, so that an elevated observer above the land may be in the shadow zone of all but the highest order land-type groundwave modes that were excited at the land-sea interface by groundwaves incident from the sea.

A complete description of the field would require calculating the field of each mode across its shadow boundary. However, an approximate representation of the field can be found by simply cutting off each mode in its shadow region. This representation divides the space above the land (for sea-to-land propagation) into three regions: (1) a sea-type groundwave region where all of the significant (lower order) groundwaves incident from the sea are in their lit regions, (2) a transition region, where some of the incident (lower order) sea-type groundwave modes and some of the interface-excited (higher order) land-type groundwave modes are in their lit regions, and (3) a land-type groundwave region, where all of the land-type groundwave modes are in their lit regions. The transition region is larger and farther over the land for higher observers.

F3-2
0900

DISTRIBUTION FUNCTIONS OF SMALL FOOTPRINT RADAR SEA RETURN

R.K. Moore, R.L. Vaughn and R. Lawner,
Remote Sensing Laboratory,
University of Kansas Center for Research, Inc.,
Lawrence Kansas 66045

When taking measurements of radar backscatter from a tower in the North Sea, it was observed that the return signal in general consists of two components: a reflected component and a scattered component. This is probably caused by the fact that the antenna footprint is small. As a result, the reflected component of the measured signal must be filtered out before determining the distribution function for the scattered component. This paper deals with some methods for removing the reflected component and subsequent testing of the scattered power data versus standard distribution functions.

F3-3
0920

TOWER MEASUREMENTS OF RADAR BACKSCATTER FROM SEA AT X- AND KU-BAND

R.K. Moore and A.H. Chaudhry,
Remote Sensing Laboratory,
University of Kansas Center for Research, Inc.
Lawrence, Kansas 66045

In September 1979 tower measurements of radar scattering coefficient (σ°) were made at platform Noordwijk in the North Sea 10 km off the Dutch coast. These measurements were made together with Dutch and French investigators as part of Project MARSEN. Our measurements were made at VV and HH polarization, frequency band of 8-17 GHz, incidence angle range of 0° to 70°, wind speed variation of 2 m/s to 22 m/s and look directions of upwind, downwind and crosswind. This paper presents results for σ° for these radar and ocean parameters and comparisons are made with a two-scale sea scatter theory and other available data.

F3-4
0940

SHORT GRAVITY AND CAPILLARY WAVE SPECTRA FROM TOWER-BASED RADAR

by
R.K. Moore, R. Lawner and R. Vaughn
Remote Sensing Laboratory
University of Kansas Center for Research, Inc.
Lawrence, Kansas 66045

Measurements of radar backscatter taken at approximately the same wind speed from a tower in the North Sea over a frequency range from 9 to 17 GHz on an incident angular range from 20° to 70° have been used to estimate a portion of the sea spectrum based on the Bragg scatter theory. This means that the spatial wave number covered lies in the range 1.289 - 6.692 1/cm. This is done for wind speeds ranging from 6 - 14 m/sec. Comparisons are made with the water wave spectrum measured under laboratory conditions by Mitsuyasu and Honda. It is found that the sea spectrum decrease with increasing spatial wave number, K, in the order $K^{-3.60}$ and $K^{-4.30}$.

F3-5
1040

EXTRACTION OF MODULATION ON CAPILLARY WAVES

R.K. Moore, S. Barkeshli, R. Vaughn, T. Lam
Remote Sensing Laboratory
University of Kansas Center for Research, Inc.
Lawrence, Kansas 66045

An experiment was designed to determine information about the modulation of capillary waves by underlying large waves on the sea. Since the Bragg resonance of a radar wave with the capillary waves is the cause of most radar backscatter from the sea, knowledge of this modulation is important in describing operation of other radar systems. This is particularly true for synthetic-aperture radar imagers, since the location of the predominant scatterers on the large waves determines the appropriate Doppler frequency to use in describing distortions caused by wave motion. The experiment was performed in 1979 as part of Project MARSEN on the Noordwijk Tower. Analysis to date appears to indicate that the capillary waves are not uniformly distributed over the front and back side of the large underlying waves. In particular, the capillary waves seem to have a peak near the trough of the large wave, but slightly upwind from it and another peak on the back side of the crest of the large wave.

F3-6
1100

THE INFLUENCE ON OCEAN WAVE RADAR MODULATION TRANSFER FUNCTIONS OF ENVIRONMENTAL CONDITIONS AND WAVE PARAMETERS:

W.C. Keller and W.J. Plant
Naval Research Laboratory
Washington, D.C.
D.E. Weissman
Hofstra University
Hempstead, New York 11550

Recent measurements of the ocean wave-radar modulation transfer function (MTF) from fixed ocean platforms, over a period of several years, have demonstrated that the local hydrodynamic modulation of short centimetric waves is affected by the air-sea interaction. Results from widely separated ocean regions also show different individual properties, that make detailed measurements necessary. An X-band radar with vertical polarization was mounted on a platform in the Gulf of Mexico during Nov-Dec 1978. An analysis of this data has been conducted on the separate, independent influence of wind speed, air-sea temperature difference and wave slope on the MTF. Dependence of the MTF on all of these environmental parameters was observed.

In most situations the modulation transfer function decreases with wind speed in an inverse manner. The effect of a strong drop in the air-sea temperature difference, to create an unstable boundary layer, is to reduce the modulation. Also noted was a dependence on wave slope. This represents the first time that a dependence of the MTF on the latter two parameters has been reliably detected. This is probably a result of the wider range of these parameters encountered during this experiment then during previous measurements.

F3-7
1120 CORRECTION OF SAR DERIVED WAVE SPECTRA FOR THE EFFECTS OF OCEAN SURFACE MOVEMENT, Frank Monaldo, Applied Physics Laboratory, Johns Hopkins University, Johns Hopkins Rd., Laurel, Md. 20707

The azimuth or along tack position of a scatterer in a SAR image is estimated by evaluating the Doppler shift associated with a scatterer. The random radial velocity or acceleration of an ocean facet during the SAR integration time can introduce a positional ambiguity that results in an effective loss of SAR image azimuth resolution. This resolution loss has been quantitatively modelled (Monaldo and Beal, Wave Dynamics and Radio Probing of the Ocean Surface, to be published in 1983). The effect of this resolution loss on the spectrum is to impose a Gaussian-shaped falloff in the azimuth wavenumber direction. This falloff tends to reduce the wavenumber of the spectral peak and rotate it towards the range direction.

A method for correcting SAR spectra for this azimuth falloff is presented. Revised spectra are generated and the new positions of the spectral peaks are determined. These revised spectral peaks are shown to be much more consistent with the known spatial and temporal location of the storm system which generated the waves.

F3-8
1140 OVERVIEW OF NRL REMOTE SENSING EXPERIMENT (July 1982) IN THE NANTUCKET SHOALS:

G. R. Valenzuela, D. T. Chen, J. A. C. Kaiser and W. D. Garrett, Naval Research Laboratory, Washington, DC 20375

The NRL Remote Sensing Experiment was conducted during July 6-25, 1982 off Nantucket Island, Massachusetts near Phelps Bank. The experiment was the outcome of the originally proposed, much more ambitious, SEBEX exercise (Valenzuela & Chen, 1980) to delineate the hydrodynamic process responsible for the surface expressions of bathymetry in shallow water in coastal areas. Among others, the purpose of the present experiment was to investigate shear current front/tidal interactions with the surface wave field, and their effect on radar imagery, including the atmospheric stability and the wind field. Deep sea measurements were also included at the Gulf Stream during transit of the research ship, T-AGOR 16 USNS HAYES, toward the shoals.

The NRL Remote Sensing Experiment involved the already mentioned USNS HAYES and several aircraft, among them, the NRL P-3 and two US Marine Corps RF-4's. Simultaneous and coordinated "in-situ" and remote sensing measurements were performed for correlation of the hydrography, surface waves and meteorology. The remote sensors were an X-band ROWS (remote ocean wave spectrometer), X-band SAR, Laser profilometer, I.R. thermal scanner and photography. An additional L-band ROWS and dual-frequency radar were on board USNS HAYES.

Preliminary assessment of the quality of the data obtained is beyond original expectation and seemingly we should have quantitative information on some very interesting phenomena. In this presentation an overview and preliminary results will be given of the July 1982 NRL Remote Sensing Experiment.

IONOSPHERIC PROPAGATION
Thursday morning, 6 Jan., CR1-40
Chairman: John C. Schlobotin, SRI International,
Menlo Park, CA 94025

G3-1
0840

WHY ADAPTIVE HF?

Georgellen Smith, Radio Physics Laboratory
SRI International
333 Ravenswood Avenue
Menlo Park, CA 94025

By an adaptive HF system, we mean a two-way communication system that can select its own operating parameters on the basis of real-time measurements of propagation conditions over the desired path. This requires some form of path sounding, with feedback from the opposite end of the link. For an HF system, the most important parameter to be determined from the sounding is the operating frequency. However, data rates, modulation schemes, and transmitted power can also be adapted to prevailing ionospheric conditions.

The greatest improvement in performance, relative to a conventional HF system, will be achieved during periods of ionospheric disturbance, either natural or man-made. Although even an adaptive HF system cannot overcome the intense D-region absorption caused by a severe solar flare or a high-altitude nuclear detonation, adaptive techniques can significantly reduce the duration of the outage. The most important advantage of an adaptive system, however, is its ability to operate successfully in the presence of large oscillations in F-region critical frequency and height, such as those that occur during an ionospheric storm or for many hours after a high-altitude nuclear explosion.

G3-2
0900

FIRST BISTATIC OBLIQUE-INCIDENCE IONOGRAMS BETWEEN DIGITAL IONOSONDES:

J.W. Wright, NOAA/ERL*, Boulder, CO 80309
R.I. Kressman, Natural Environment Research Council, British Antarctic Survey, Cambridge, England

Recently consideration has been given to the practicality of global ionospheric monitoring by a thoughtfully deployed network of about 90 modern digital ionosondes. An essential feature of that notion, by which an adequate spatial resolution is maintained despite this relatively small number (there are about 160 ionosondes operating today) is the use of more sophisticated instruments in both vertical and bistatic oblique measurements modes. Identical Dynasondes were established at NOAA's research site at Brighton, Colorado, and at the White Sands, New Mexico, Missile Range (WSMR) operated by the U.S. Army Atmospheric Sciences Laboratory. The instruments were 866 km apart. During a September 1981 opportunity we used these nominally vertical-incidence instruments in an oblique bistatic mode. This paper shows the typical ionograms and fixed-frequency sequences obtained, identifies the propagation modes observed, and discussed prospects for improvement.

G3-3
0920

TWO-WAY CHANNEL MEASUREMENTS FOR PRE-TRANSMIT EQUALIZATION OF MEGAHERTZ-BANDWIDTH HF RADIO SYSTEMS;

B.D. Perry, MITRE Corp., Bedford, MA 01730

Megahertz-bandwidth coherent signaling over 2000 km one-hop F layer paths has been achieved using a transversal filter as an adaptive channel equalizer. The equalizer coefficients (viz; transversal-filter tap weights) are derived from periodic channel measurements at the receiving terminal of a communications link. The equalizer is used to correct the received signal. As an alternative the equalizer can also be used to pre-distort the transmitted signal, yielding the following advantages: (1) only one equalizer per communications link is required, (2) any special channel-measuring probe signal need only be transmitted from one terminal, and (3) if the inverse-filter equalization is used, pre-transmit equalization provides a higher average signal-to-noise ratio than equalization in the receiver.

The ability to achieve pre-transmit equalization based on channel measurements in the receiver depends on the degree of reciprocity exhibited by the channel. To explore reciprocity, we measured the complex channel-transfer function using a bi-direction path between Massachusetts and Florida during September 1982. The accompanying figure shows an example of measurement magnitude at both receivers. $|C(\omega)|$ is the magnitude of the channel transfer function. $|c(t)|$ is the magnitude of the channel's band-limited impulse response and is obtained by taking the discrete Fourier transform of $C(\omega)$.

These data are presently being analyzed in order to quantify the degree of path reciprocity and establish a method for achieving pre-transmit equalization over one-megahertz coherent bandwidths.

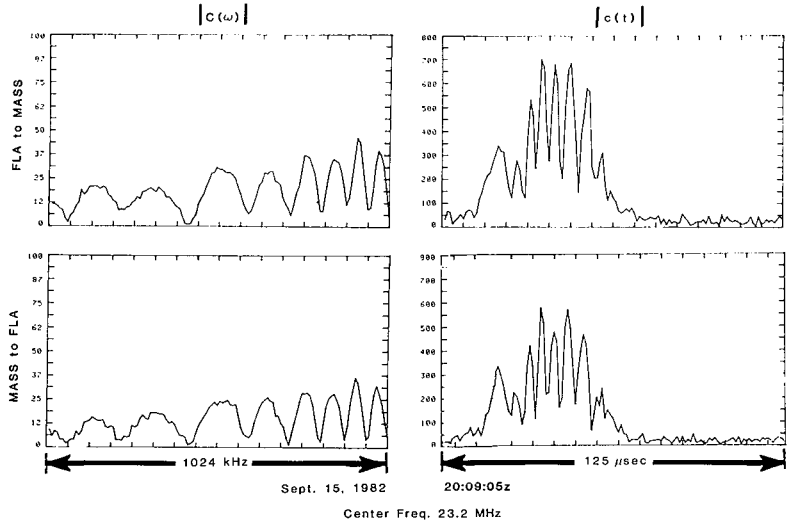

G3-4
0940 WAVE SCATTERING BY IRREGULARITIES IMBEDDED IN A STRATIFIED MEDIUM -- APPLICATIONS TO PROPAGATION IN THE IONOSPHERE

Yean-Woei Kiang and C. H. Liu, Department of Electrical Engineering, University of Illinois at Urbana-Champaign, Urbana, IL 61801

Plane wave scattering by an irregularity slab imbedded in a linearly stratified isotropic medium is studied. The irregularities are assumed to be characterized by two-dimensional Shkarofsky spectrum. In addition to regular reflection from the stratified background, the wave is randomly scattered by the irregularities. Both the incident and reflected waves will interact with the irregularities producing scattered fields. The behavior of the unperturbed field in the neighborhood of the turning point is accurately taken into account by using the full wave solution. Several statistical characteristics of the scattered field, such as average scattered field intensity, correlation functions, etc., are examined. The results are compared with those obtained for Gaussian irregularity spectrum. Applications to the problem of HF propagation in the ionosphere in the presence of small-scale irregularities will be discussed. Moreover, this approach is also employed to investigate radio wave scattering by large-scale ionospheric inhomogeneities, such as traveling ionospheric disturbances.

G3-5
1020 ESTIMATES OF IONOSPHERIC EFFECTS ON SYNTHETIC APERTURE RADARS: E.P. Szuszczewicz, M. Singh, P. Rodriguez and S. Mango, E.O. Hulburt Center For Space Research, Naval Research Laboratory, Washington, DC 20375

Accumulating data are making it increasingly evident that major plasma irregularities populate a substantial portion of the Earth's F-region ionosphere. In fact, the frequency of occurrence of such structures is so high as to suggest that smooth, slowly-varying ionospheric models are of limited use in calculations intended to define the characteristics of transionospheric electromagnetic wave propagation. In considering the imaging capability of satellite-borne synthetic aperture radars (SAR), it is generally assumed that the ionosphere is uniformly layered and unchanging under the orbiting SAR...an assumption relevant to imaging integrity requiring constant phase path length from the satellite-to-ground over the full aperture width. Analysis of plasma irregularity structures on the S3-4 satellite[1,2] suggests that this assumption can be substantially violated (e.g., phase path variations can be several times the wavelength of the probing radar) over specific segments of a given orbit. Initial estimates of ionospheric effects based on S3-4 satellite measurements of the F-region structure can be summarized as follows:

(i) There should be little problem (phase path variation) in the dayside hemisphere at equatorial and midlatitude domains;

(ii) There should be little problem across nightside midlatitudes;

(iii) There are potentially serious problems in the nighttime equatorial domain...that is, roughly inside $\pm$ 20° of the magnetic equator and between 7 P.M.-to-2 A.M. local time; and

(iv) There are potentially serious problems at high-latitudes most of the time.

1. "The S3-4 Ionospheric Irregularities Satellite Experiment: Probe Detection of Multi-Ion Component Plasmas and Associated Effects on Instability Processes", E. Szuszczewicz, J. Holmes and M. Singh, Astrophysics and Space Science (in press).
2. "An Atlas of Ionospheric F-Region Structure as determined by the NRL-747/S3-4 Ionospheric Irregularities Satellite Investigation, E.P. Szuszczewicz, et al., NRL Memo Rept. #4862, July 1982.

G3-6
1040 TURBULENT ENERGY DISSIPATION, WINDS AND IONOSPHERIC STRUCTURE:

J.W. Wright, The Cooperative Institute in Environmental Sciences, University of Colorado, Boulder, CO 80309
R.D. Hunsucker, Geophysical Institute, University of Alaska, College, Alaska

A sample of Dynasonde observations of the daytime E-Region, in Ionogram and Kinesonde observing modes, is shown to satisfy analysis criteria leading to winds and turbulence. The wind effects on the ionization distribution in the E-Region are shown to be consistent with the 'wind shear' process for the Sporadia E phenomenon at this large magnetic dip (76.5°). The lifetime of neutral atmospheric density fluctuations is deduced using standard phase-screen diffraction arguments, and is shown to yield plausible values for the energy rate of turbulent eddy diffusion. This suggests that value of a more systematic and long-term Dynasonde measurement program dedicated to studies of the turbopause.

G3-7 F-Region Variability
1100

Adolf K. Paul, Code 5321
Naval Oceans Systems Center
San Diego, CA 92152

Fast sequences of ionograms permit the observation of F-region variations in the periodicity range of gravity waves. Directly observed and derived parameters, e.g., virtual heights, MUF(3000), foF2, etc. show that those oscillations are present most of the time with widely varying magnitudes. No correlation between magnetic and gravity wave activity could be found. There is some indication that high gravity wave activity is originated by severe weather systems and extends over distances of 1000 km and more.

G3-8 1120 SIMULATED IONOGRAMS FOR IONOSPHERICALLY DUCTED HF PROPAGATION: Eli J. Tichovolsky, Rome Air Development Center, Electromagnetic Sciences Division, Hanscom AFB, MA 01731

Adiabatic invariant theory, (A.V. Gurevich, Ye. Ye. Tsedilina, Sverkhdal'neye Rasprostraneniye Korotkikh Radiovoln, Publishing House "Nauka", Mascow, 1979, pp. 1-246.) for predicting the potential for ionospheric ducting of HF radiowaves has been applied, using the ITS IONCAP median ionospheric model, in order to determine optimum ducting paths to a low-altitude orbiting satellite. Global maps of adiabatic invariant, maximum launch angle, and optimum transmitter and receiver altitudes were used to prepare input parameters for 3-dimensional ray tracing in order to simulate ionograms seen by this satellite. The propagation modes were limited to daytime F1/F2 region ducting, nightime F-layer chordal modes and classical ground/F-region multihop.

Commission H Session 4

WAVE EMISSIONS FROM ARTIFICIAL ELECTRON BEAMS
Thursday morning, 6 Jan., CR2-28
Chairman: P. M. Banks, Stanford University, Stanford, CA 94305

H4-1
0840 REVIEW OF WAVE EMISSIONS FROM ARTIFICIAL ELECTRON BEAMS IN SPACE

K.J. Harker and P.M. Banks, Radioscience Laboratory, Stanford University, Stanford, CA 94305

One of the most interesting and puzzling type of experiments conducted in the space program has been the injection of electron beams into space and the study of their interaction with the surrounding plasma medium. We review here the theory and experiment for the generation of waves by artificial electron beams, extending from the early rocket experiments through recent experiments conducted on the space shuttle.

We discuss first the incoherent spontaneous emission process characterized by a radiated power varying linearly with particle density. We then consider the coherent spontaneous emission processes, where the radiated power varies as the square of the particle density. Coherent radiation can arise from organized motion of electrons, such as occurs, for example, in the helical beam associated with charged particle flow through a magnetized medium. We then proceed to stimulated emission processes, for both electrostatic and electromagnetic waves, which arise from beam plasma interaction. These include various combinations of the Cerenkov and cyclotron instabilities. The role of beam size, beam temperature, and nonlinear effects will be considered.

Finally, consideration will be given to the character of the beam flow itself and its relation to wave excitation. This includes the range from simple structured helical flow through a magnetized medium to the diffuse flow associated with beam plasma discharge. Related topics such as return current and flow randomization will also be considered.

H4-2
0900

OBSERVATIONS OF PLASMA WAVES AND CHARGED PARTICLE PHENOMENA FROM ELECTRON BEAM EXPERIMENTS ON STS-3

P.M. Banks, P.R. Williamson, Radioscience Laboratory, Stanford University, CA 94305
W.J. Raitt, Physics Department, Utah State University, Logan, UT 84322

Electron beam experiments conducted aboard STS-3 provide a wealth of new information about beam-plasma interactions. The present data were gathered during D.C. operation of a 50 mA, 1 kV electron emitter. Photographic and TV observations accurately define the geometrical shape of the emitted beam, while wave and particle measurements provide information about interactions between the beam and the ambient nighttime ionosphere. Plasma waves observed included plasma oscillations, cyclotron emission and lower frequency waves which may reflect intense whistler mode generation. When the electron beam escapes the vehicle strong ion heating occurs in the range of 10-20 eV, while electrons span the range from low energies to slightly above the gun energy.

H4-3
0920 "Wave Emissions from the FPEG Electron Beam Measured with the PDP", Stanley D. Shawhan and Gerald B. Murphy, Department of Physics and Astronomy, The University of Iowa, Iowa City, Iowa 52242 and Peter Banks, Stanford University, Stanford, California

The Utah State University Fast Pulse Electron Generator (FPEG) has been operated in the Johnson Space Center Space Plasma Simulation chamber (March 1981) and in space as part of the STS-3/OSS-1 Shuttle Mission (March 1982). Waves and fields generated by the 1 keV, 100 ma beam interaction with the plasma and waves stimulated by modulating the beam in the ELF to HF frequency range have been measured with the University of Iowa Plasma Diagnostics Package (PDP).

In the plasma chamber electrostatic waves near the plasma and gyrofrequencies were found to be more intense ~ 10 V/m than on orbit ~ 1 V/m probably due to better beam confinement in the chamber. Electromagnetic wave fields were stronger on orbit with the peak in the kHz range since the chamber dimensions were less than a typical wavelength and the fields were "shorted out". Electric and magnetic fields were clearly detected when the beam was on/off modulated in the kHz range. These emissions suggest that the modulated beam may be an efficient method for launching VLF waves in the ionosphere.

H4-4
0940

THEORY FOR PULSED ELECTRON BEAM RADIATION IN SPACE

K.J. Harker and P.M. Banks, Radioscience Laboratory, Stanford University, Stanford, CA 94305

A theoretical study has been made of the electromagnetic radiation from a pulsed electron beam traveling in an idealized helical path through a space plasma. If the electrons in the beam maintain their respective positions within the beam, then a coherent spontaneous emission radiation pattern is produced due to the organized motion of the electrons. The theory determines the total radiation by adding coherently the radiation from each individual electron in the helix. The radiation per unit frequency interval is determined, as well as the radiation per unit solid angle as a function of both propagation and ray angles. Radiated power is determined as a function of the electron pulse length, pulse separation, and the total number of pulses in the beam. The radiated power varies as the square of the beam current, as expected for a coherent process. For one pulse of a 1000 V 100 ma beam a possible radiated power per unit solid angle at selected angles and frequencies is predicted in excess of 1% of the total beam power.

H4-5 1020 BEAM PLASMA DISCHARGE PHENOMENA UNDER IONOSPHERIC CONDITIONS: K. Papadopoulos* and K. Ko, Science Applications, Inc., McLean, VA 22102

Rocket and laboratory experiments injecting energetic electron beams in the pressure range of 5×10^{-5} - 10^{-7} torr have produced a variety of phenomena indicating that strong collective plasma processes might be dominating the energy deposition. A numerical model has been developed which solves the particle and energy balance equations, including impact ionization and excitation, in the presence of collisional and collisionless energy deposition due to the beam. The model has been applied to the EXCEDE SPECTRAL experiment and to the NASA Johnston S.F.C. tank experiments. It is shown that most of the surprising results (Kofsky, et al 1981; Kellogg et al, 1981) can be quantitatively understood by properly incorporating nonlinear phenomena caused by beam plasma interactions.

Kofsky et al, "Artificial Particle Beams in Space Plasma Studies" p. 217, Ed. B. Grandal, Plenum Press (1981).
P. Kellogg et al. ibid p. 289.

*Permanent Address: University of Maryland

H4-6
1040 LABORATORY OBSERVATIONS OF ELECTROSTATIC WAVES IN SPACE-SIMULATION BEAM-PLASMA INTERACTIONS: D.N. Walker and E.P. Szuszczewicz, E.O. Hulburt Center for Space Research, Naval Research Laboratory, Washington, DC 20375

Plasma density profiles in laboratory-based space-simulations of electron beam-plasma interaction processes have been found to show rather large-scale fluctuations. With kilovolt beams in magnetoplasmas ($B \sim 1$ gauss) of densities spanning the 10^4-$10^7 cm^{-3}$ range, the fluctuation spectra generally show a dominance at the low frequency end ($1 \text{ Hz} \lesssim f \lesssim 50 \text{ Hz}$) with relatively constant levels of intensity. While observed frequencies can extend to 250 Hz with an f^{-3} behavior (higher frequency components have not been studied as yet), the region at or near the ion cyclotron frequency appears to contain the highest frequency components of substantial spectral intensity. While the experimental configuration did not provide the wave number measurements to complement the frequency spectrum results, the domain of contributing wave phenomena was isolated by focusing on the more intense frequencies and on wavelengths compatible with the size of the beam-plasma system. Within these guidelines we conclude that there are two likely contributions:

(i) the longitudinal ion cyclotron waves branching into the ion acoustic mode, and

(ii) the lower branch of the drift wave mode which in itself covers all frequencies in the current set of observations.

The measurements support both possibilities, but in a number of cases the existence of substantial gradients in density and temperature favor the drift wave mode.

H4-7
1100

THE ELECTRIC DIPOLE AS AN ARTIFICIAL BEAM SOURCE:

H.G. James, Communications Research Centre,
Department of Communications,
P.O. Box 11490, Station 'H',
Ottawa, K2H 8S2, Canada

Sounder-accelerated particles (SAP) are detected by the soft-particle spectrometer aboard the ISIS spacecraft when the sounder transmits at medium frequencies in the ionospheric plasma. The electrons are thought to be energized nonlinearly because their trajectories take them through the intense, inhomogeneous near field of the dipole antenna. Peak SAP fluxes appear at frequencies near, but not at, the principal resonances: the plasma frequency, the gyrofrequency and the upper hybrid resonance frequency. Both electrons and ions are accelerated by the rf near field. Fluxes and energies of up to 10^8 cm^{-2} $ster^{-1}$ eV^{-1} sec^{-1} and 1 keV, respectively, have been measured.

Peak SAP electrons are observed at pitch angles, α, between 60° and 120°. The α-spread of electrons suggests that considerable SAP flux escapes the spacecraft during the sounder pulse (length = 100 μsec; peak power = 400 W). This is partially confirmed by the observation on ISIS-I of SAP electrons 4.7 msec after the rf pulse. The evidence indicates that SAP electrons retain the phase of the original rf field. They may therefore resemble waves as far as receiving antennas are concerned. SAP may have application to electrodynamic probing of the ionospheric plasma near a spacecraft.

H4-8 1120 ANTENNA-PLASMA INSTABILITIES: Paul J. Kellog, School of Physics and Astronomy, University of Minnesota, Minneapolis, MN 55455; and Pierre Couturier, Section d'Astrophysique, Observatoire de Paris, 92190, Meudon, France

Under certain conditions, an antenna immersed in flowing plasma may become electrically unstable. The physics is similar to a beam-plasma instability where the antenna replaces the beam. Observations and calculations for an instability near the lower hybrid frequency will be discussed, together with possible other cases.

Commission J Session 3
Commission F Session 4

ATMOSPHERIC EFFECTS AND RADIO ASTRONOMY
Thursday morning, 6 Jan., CRO-30
Chairman: M. A. Gordon, Chairman, National Radio Astronomy Observatory, Tucson, AZ 85745

J3/F4-1 0830 ATMOSPHERIC WINDOW TRANSPARENCIES NEAR 35, 90, 140, 220 GHz, AND HIGHER

H. J. Liebe, National Telecommunications and Information Administration, Institute for Telecommunication Sciences, Boulder, CO 80303

New requirements for high-data-rate communication links, for active and passive sensors, and in radio astronomy have kindled growing activity in the millimeter and submillimeter wavelength regions of the spectrum. In general, atmospheric propagation limitations dominate all considerations in the advancement of these applications. Transparency of atmospheric windows in the frequency range 30 to 400 (1000) GHz is obscured by precipitation (rain, wet snow), by suspended particles (fog, cloud, haze, dust), and by water vapor. Useful models are discussed for calculating transfer characteristics of a radio path based upon measurable meteorological variables: rain rate, concentration of suspended matter (hydrosol), humidity, pressure, and temperature (Liebe, IEEE Trans. Ant. Prop. AP-31 (1), 1983). Emphasis is on recent advances in formulating the physical basis for modeling transparency and on a discussion of some of the principal remaining uncertainties.

Commission J Session 3
Commission F Session 4

J3/F4-2
0900 GROUND-BASED RADIOMETRIC MEASUREMENTS OF ATMOSPHERIC ABSORPTION AT 20.6 and 31.65 GHz: F. O. Guiraud, D.C. Hogg, and E. R. Westwater, Wave Propagation Laboratory/ERL/NOAA, Boulder, CO 80303

Sets of ground-based radiometric measurements of atmospheric absorption (ν = 20.6 and 31.65 GHz) were made at Sterling, Virginia and at Denver, Colorado. Clear sky measurements of atmospheric absorption, obtained by the tipping curve method, were compared with calculations based on National Weather Service radiosonde observations. Both Van Vleck-Weisskopf and Zhevakin-Naumov-Gross line shapes were compared. Preliminary results indicated that the dependence of the non-resonant water vapor absorption on total pressure significantly departs from conventional theory.

J3/F4-3
0920

GROUND-BASED RADIO SPECTROSCOPY OF H_2O IN THE EARTH'S MIDDLE ATMOSPHERE

R. Bevilacqua, P.R. Schwartz, D.L. Thacker,
E. O. Hulburt Center for Space Research,
Naval Research Laboratory, Washington, D. C. 20375
J.J. Olivero, Department of Meterology,
Pennsylvania State University,
University Park, PA 16802

Molecular absorption and emission lines may be regarded as either a problem for radio astronomy or as an opportunity to sense atmospheric constituents using radio astronomy techniques. Atmospheric emission from the $6_{16} - 5_{23}$ H_2O transition at 22.2 GHz has been observed on a seasonal basis for the last three years using the high resolution spectrometer at Haystack Observatory in Westford, MA. Altitude profiles in the range 50-80 km have been recovered by inversion of the observed emission line. At these altitudes (a) a peak in H_2O mixing ratio is often found near 60-65 km, (b) the mixing ratio drops rapidly above 70 km and (c) the H_2O profile shows pronounced changes from season to season and, sometimes, over periods of a few days.

Commission J Session 3
Commission F Session 4

J3/F4-4
0940

PREDICTION OF PATH DELAY BY RADIOMETRIC SENSING OF WATER VAPOR:

D. E. Hogg and P. J. Napier
National Radio Astronomy Observatory
G. M. Resch
Jet Propulsion Laboratory

To support very long baseline interferometric experiments, the Jet Propulsion Laboratory has developed a microwave radiometer which provides a basis for estimating the path delay introduced by water vapor. The device consists of dual microwave radiometers, one operating at 20.7 GHz and the other at 31.4 GHz. Comparison of the brightness temperatures of the sky measured at these two frequencies yields the estimate of the amount of precipitable water present in both vapor and droplets.

In order to explore the accuracy with which the devices predict path delay, a series of observations was undertaken in which the difference between the outputs of two water vapor radiometers is compared with the phase observed with two connected elements of the Very Large Array. The results show: (1) it is indeed water vapor fluctuations that dominate the residual phase of the interferometer; and (2) the water vapor radiometers are capable of reducing these effects. The rms error in the phase after correction for the differential delay in the troposphere is typically 15 degrees at a wavelength of 6 cm, corresponding to an uncertainty in the path delay of 0.25 cm. The technique is less successful under conditions of heavy cloud.

The work at JPL was carried out under contract NAS 7-100, sponsored by NASA. The NRAO is operated by AUI, under contract to the NSF.

Commission J Session 3
Commission F Session 4

J3/F4-5
1020

COHERENCE LIMITS IMPOSED BY ATMOSPHERIC AND FREQUENCY-STANDARD PHASE NOISE IN VLBI OBSERVATIONS AT 3mm WAVELENGTH:

A.E.E.Rogers, Haystack Observatory, Westford, MA 01886, A.T. Moffet, Owens Valley Radio Observatory, Caltech, Pasadena, CA91125, and D.C. Backer, Radio Astronomy Lab., University of California, Berkeley, CA 94720

Recent VLBI experiments at a frequency of 89GHz (3.4mm wavelength) using hydrogen maser frequency standards show that under good atmospheric conditions coherence of the recorded signals can be maintained for times up to 700 seconds, corresponding to an Allan standard deviation of approximately 5×10^{-15}. While the observations appear to be largely limited by the phase noise resulting from fluctuations in delay through the troposphere, a group of observations taken with an older-generation hydrogen maser at one of the stations is clearly limited by phase noise in that frequency standard.

Atmospheric phase fluctuations observed at 3 millimeters and in other VLBI experiments at longer wavelengths show large variations with atmospheric conditions and an increase proportional to the square root of the cosecant of the elevation when the source elevation is low at one of the stations.

Commission J Session 3
Commission F Session 4

J3/F4-6 ATMOSPHERIC PHASE FLUCTUATION AT THE VLA
1040 R. A. Sramek, National Radio Astronomy Observatory
P. O. Box O, Socorro, New Mexico 87801

The N.R.A.O. interferometer in central New Mexico, the VLA, has been used to measure differential atmospheric phase fluctuations on scale lengths from a few hundred meters to 35 kilometers. The resulting two-dimensional structure functions, power spectra, and cross-correlation functions are described.

J3/F4-7
1100 INTERFEROMETRIC MEASUREMENTS OF ATMOSPHERIC PHASE NOISE USING THE 86 GHz SiO MASER EMISSION IN THE ORION NEBULA: W.J. Welch, J. Morgan, and J.H. Bieging, Radio Astronomy Laboratory, University of California, Berkeley, CA 94720

We have analyzed a large body of observations of the 86 GHz silicon monoxide maser emission from the Orion Nebula to determine the atmospheric contribution to interferometer phase noise. The observations were made with the Hat Creek millimeter-wavelength interferometer. A large range of interferometer baselines is included in the data. Since the maser emission consists of two strong features of nearly equal intensity and separated in frequency by only 6 MHz, a comparison of the measured phases in the two features allows us to separate the instrumental and atmospheric phase noise contributions.

A plot of the rms atmospheric phase noise vs. projected interferometer baseline shows a rather large scatter of points, but with a well-defined lower envelope. This lower envelope can be well-represented by a straight line through the origin with a slope of 5 milliradians/kilolambda, out to at least 50 kilolambda. Mean values for rms phase noise are typically about 3 times this lower limit.

Comparison of these 86 GHz results with earlier measurements made at 22 GHz at Hat Creek indicates that the atmospheric phase noise does scale approximately linearly with frequency, at least for this frequency range. We discuss the implications of these results for the design of millimeter synthesis instruments.

Commission J Session 3
Commission F Session 4

J3/F4-8 ESTIMATION OF TROPOSPHERIC SCINTILLATION
1120 EFFECTS FOR LARGER APERTURE ANTENNAS

R.K. Crane, Thayer School of Engineering,
Dartmouth College, Hanover, New Hampshire
03755

Turbulence induced refractive index irregularities produce the amplitude, phase, and angle-of-arrival fluctuations described as scintillation. Low elevation angle observations of scintillation made at the Haystack Observatory using satellite beacons at 7.3 GHz show that the fluctuations are adequately described by the weak scintillation model developed by Tatarski (The Effect of the Turbulent Atmosphere on Wave Propagation, 1967, translation available from the US Dept. of Commerce, Springfield, VA, 1971) when the turbulence is assumed to occur in a thin layer at a height of 1 killometer.

A simplified model for the estimation of amplitude, phase and angle-of-arrival fluctuations as a function of frequency, antenna aperture size, and elevation angle was developed using the Haystack observations. The model was tested against amplitude fluctuation observations made using large aperture antennas at different frequencies in Japan and elsewhere in the United States. In each case the predicted median value closely approximated the observed median value for the variance of the logarithm of the received power.

J3/F4-9
1140

AN ERROR ANALYSIS OF THE GREEN BANK INTERFEROMETER AS AN INSTRUMENT FOR MEASURING EARTH-ROTATION PARAMETERS

D.N. Matsakis and F.J.Josties
U.S. Naval Observatory
Washington, D.C. 20390

The connected-element interferometer at Green Bank, West Virginia, has been used for the determination of precise astronomical time (UT0-UTC) and the Earth's polar motion since 1979. The accuracy and precision of the system are examined with regard to instrumental errors, signal to noise, atmospheric modeling, and source motion. A quantitative method for the determination of these errors is described and results are compared to the actual observed data. A brief comparison with VLBI is given. Errors in the determination of source positions will also be described, and the published anomaly in the position of 3C345 is shown to be due to a small neighboring source.

A new method of reducing the data, which could remove the atmospheric component in the seasonal error of our determination of UT0-UTC, is described.

The merits of different source-observation strategies are assessed. In our current observation program, chosen to cover the sky as evenly as possible, about 10% of the observations make no significant contribution to our computation of either time or polar motion. New source strategies, under consideration at the USNO, are discussed.

TIME DOMAIN MEASUREMENTS
Commission A, Session 4, CR1-46
Chairman: M. Kanda, NBS, Boulder, CO

A4-1
1330

SOME RESULTS USING THE GUILLAUME-NAHMAN AUTOMATED DECONVOLUTION METHOD

N. S. Nahman, Senior Scientist, 723.03
Electromagnetic Fields Division
National Bureau of Standards
325 Broadway Boulder, CO 80303, U.S.A
M. E. Guillaume, Staff Scientist
Centre de Microelectronique de Grenoble
Centre National D'Etudes Des Telecommunications
Zirst BP 42, 38240 Meylan, France

The impulse response of a commercial low pass filter (3 dB attenuation at a nominal frequency of 3.5 GHz) was determined from time domain insertion measurements implemented by the NBS Automatic Pulse Measurement System (APMS). For these experiments the pulse source was a 50 ohm generator providing an unsymmetrical doublet-like pulse of 80 millivolts peak to peak and a nominal duration of about one nanosecond. The reference and response waveforms were acquired as 512 value sequences, each being obtained as the mean value of a one hundred waveform ensemble.

The filter impulse response was obtained through deconvolution using the automated version of an optimal deconvolution method (N. S. Nahman and M. E. Guillaume, National Bureau of Standards Technical Note 1047, 28-36, Boulder, CO 80303, Oct. 1981). The automated method has also been applied elsewhere to optical fiber measurements by the second author (M. E. Guillaume and J. Bizeul, Annales Des Telecommunications, 36, 179-186, 1981). Impulse response waveforms versus a range of values for the smoothing parameter γ were obtained using the manual mode. Also, for the automatic mode, a specific value of the smoothing parameter γ_0 was determined by iteration of the deconvolution process versus γ until the standard deviation σ of the imaginary part of the impulse response was minimized.

In principle, the imaginary part of the impulse response resulting from the inverse FFT of the optimally filtered transfer function should be zero. However, due to computation errors the imaginary part is a small random function. Contained within the computation random function is another random function due to the noise on the deconvolved result. As the smoothing parameter γ is varied, the standard deviation of the imaginary part passes through a minimum thereby providing a means for automating the deconvolution process by being able to select an optimum value of the smoothing parameter designated as γ_0. Impulse responses and their corresponding transfer function magnitudes versus γ are presented along with data on σ versus γ.

A4-2
1350

PERFORMANCE EVALUATION OF FREQUENCY DOMAIN DECONVOLUTION TECHNIQUES

Bidyut Paruck and Sedki M. Riad
Department of Electrical Engineering
Virginia Polytechnic Institute & State University, Blacksburg, Virginia 24061

This paper evaluates the performance of three methods of frequency domain deconvolution - Simple division, optimum compensation (B. Parruck, R. B. Stafford and S. M. Riad, Proc. of CPEM '82, Boulder, CO pp. G12-13, June 1982), Guillame-Nahman approach (NBS Tech note 1047, NBS, Boulder, CO October 1981). It compares these methods in terms of their capabilities of dealing with different classes of signals and their tolerance to the presence of noise. It, thereby, attempts to associate with each class of deconvolution problem, a method most suitable.

Let $x(t)$, $y(t)$ be the input and output of a system with impulse response $h(t)$. Let $x(jw)$, $Y(jw)$ and $H(jw)$ their corresponding frequency domain representations. The three methods of frequency domain deconvolution are -

(a) simple division: $H(jw) = \frac{Y(jw)}{X(jw)}$

(b) optimum compensation: $H(jw) = \frac{Y(jw)}{X(jw)} \cdot \frac{1}{1+[\lambda / |x(jw)|^2]}$

(c) Guillame-Nahman approach:

$$H(jw) = \frac{Y(jw)}{X(jw)} \cdot \frac{1}{1+[\gamma |c(jw)|^2 / |x(jw)|^2]}$$

where λ & γ are positive real numbers used as parameters and $e(jw)$ is frequency domain representation of the second-derivative operator.

In this comparison, a simple analytic transfer function $H(jw) = 0.5$ was assumed.

The different classes of signals considered are low pass, wide band, duration limited signals and signals with unlimited durations. The performance is evaluated in terms of the deviations of the deconvolution result from the ideal, analytical form. The signals are considered with and without an added White random gaussion noise λ-component to evaluate the techniques' noise filtering ability.

A4-3 1410 EXPERIMENTAL METHODS FOR OBTAINING THE SINGULARITY EXPANSION PARAMETERS FOR A CONDUCTING SCATTERER: Steven A. Dyer, R. L. Holbrook, Department of Electrical Engineering, University of Kentucky, Lexington, KY 40506; and L. Wilson Pearson, Department of Electrical Engineering, University of Mississippi, University, MS 38677

This presentation reviews an experimental methodology for obtaining the quantities necessary for characterizing the electromagnetic scattering properties of a conducting object by means of the singularity expansion of the object response. The methodology is based on the systematic application of systems identification algorithm methods to reduce transient waveforms derived from measurements of the object's scattering response to exponential series. By associating the coefficients in the idividual series according to their association with a common pole, the scalar-valued series can be associated into a single vector-valued series, which allows one to identify the singularity expansion quantities. The response quantity can, at least in principle, be the surface current density or the far-field scattering reponse, and determines, respectively, either the surface current density natural modes (L. W. Pearson and D. R. Roberson, **I.E.E.E. Trans. Ant. and Prop.**, AP-28, 182-190, 1980) or the far-field natural modes (K.S. Cho and J.T. Cordaro, **I.E.E.E. Trans. Ant. and Prop., AP-28,921-924,1980**)

A recently-developed optically-coupled head for a sampling oscilloscope obviates the symmetry requirement which was required in a previously-reported application of this scheme (L.W. Pearson and Y.M. Lee,**I.E.E.E. Trans. Ant. and Prop.**,AP-30,260-266, 1982). The sampling head provides a nominal two gigahertz bandwidth. Moreover, while the appeal to symmetry discards the prospect of recovering the natural modes for the symmetric object which correspond to a magnetic image plane, the free-field approach using the optically-coupled sampler recovers both symmetry classes of modes for a symmetric object.

The approach depends on the use of state-of-the-art transient measurement techniques and systems identification algorithms. The limitations which result from the interaction of these two tools remain the open question in judging the efficacy of the approach as a whole. These limitations are discussed and evaluated in the light of currently-available methods.

A4-4
1430 SOME RESULTS FROM A STATISTICAL SCATTERING EXPERIMENT, E. K. Miller, and J. T. Okada

Lawrence Livermore National Laboratory
P. O. Box 5504, Livermore, California 94550

The complex environments which characterize many electromagnetic systems (consider the antenna arrangements found on typical navy ships) make their analysis in any rigorous sense largely impractical. Yet it is important that the perturbing effect of such environments be somehow accounted for in evaluating system performance. The purpose of this paper is to present some results from a statistical experiment conducted in the time domain to measure the effects caused by N nearby identical scatterers on the receiving properties of a given antenna. It is found that the variance of the peak antenna current at first increases, and then decreases as N increases, with the environment changing from a discrete to an essentially continium or medium-like behavior. The mean peak current, on the other hand, decreases monotonically with increasing N. The impliations of these results for using a deterministic data base to estimate the currents induced by an incident EMP on an antenna located in a cluttered environment are also discussed.

Work performed under the auspices of the U. S. Department of Energy by the Lawrence Livermore National Laboratory under contract number W-7405-ENG-48.

A4-5
1450

CONSIDERATIONS OF RESONANCE EXTRACTION FROM TRANSIENT SCATTERING MEASUREMENTS:

M. L. VanBlaricum, Effects Technology, Inc.
and M. A. Morgan, Naval Postgraduate School

The singularity expansion methodology has been in existence for over a decade now and hence the mathematics and physical basis of the approach are well grounded. This grounding however has been based primarily in analytical and numerical work. The desire to represent the transfer function of a complex system in the closed singularity expansion representation led to the introduction of Prony's method and other resonance extraction procedures starting some eight years ago. The desire is to use these signal processing algorithms to determine the roles and associated residues of a system from measured transient data.

Many discussions and papers have been presented on the major aspects of this resonance extraction problem. Noise and rank uncertainty have been the primary issues discussed. However most work has been based on artificially generated data. When one looks at real measured data the considerations of noise and rank exist as well as other major problems. These include the problem of deconvolving the driving function from the measured response so that poles are extracted from only the smoothed impulse response. To perform this deconvolution requires that the driving function is adequately measured. Severe problems result if there is systematic error in the measurement. Another consideration is the spatial driving problem. When an incident field excites a target there is a time period in the resulting scattered field, even after the driving function has been deconvolved, in which the residues of the poles are time varying. This fact causes severe constraints on the way in which resonances are extracted.

This paper will present case histories of the above considerations, as well as others, as they have been encountered in analyzing transient scattering data from the Naval Postgraduate School scattering facility. Theoretical discussions will explain why these problems occur. Guidelines will be presented for both measurement and analytical techniques to insure that useful results can be obtained.

A4-6
1530

L_1- APPROXIMATION OF AN IMPULSE RESPONSE FROM A TIME LIMITED INPUT AND OUTPUT

Tapan K. Sarkar
Sadasiva M. Rao
Soheil A. Dianat
Department of Electrical Engineering
Rochester Institute of Technology
Rochester, New York 14623

A procedure is developed for a L_1approximation of the impulse response of a system for a finite time input and output waveforms. For the problems of interest the finite time input and output waveforms are decaying exponentials and hence they are not bandlimited. Since the input, output and the impulse response are not band limited functions, one should then have information about all the frequencies for a perfect characterization of the impulse response. For practical resons one cannot have access to the information about all the frequencies of interest. The object of this paper is to demonstrate that if we have information about the input and the output transfer functions up to a highest angular frequency ω_h, then the maximum error in the impulse response with respect to the maximum amplitude is given by $\frac{2\sigma}{\pi\omega_h}$ or $\frac{2\theta}{\pi\omega_h}$ depending on the nature of the decaying exponentials, i.e., whether h(t) is of the form $e^{-\sigma t}\cos\theta t$ or $e^{-\sigma t}\sin\theta t$. Numerical results have been presented to illustrate the results for the bounds.

A4-7 1550

A NEW CURVED-MOUTH TEM HORN FOR TIME DOMAIN DATA ACQUISITION

B.Z. Hollmann, Code F12
Naval Surface Weapons Center, Dahlgren, VA 22448

The time domain data acquisition system used at the Naval Surface Weapons Center (NSWC) has been previously described (B.Z. Hollmann, National Radio Science Meeting, 88, January, 1981). One of the problems associated with this system is clutter. A major source of clutter was found to be reflections between the mouth and throat of the TEM horn used to monitor the transient fields. In an effort to reduce these reflections, a curved-mouth TEM horn was designed and built. The idea was inspired by Burnside and Chuang (W.D. Burnside, C.W. Chuang, IEEE Trans. Ant. and Prop., AP-30, 790-796, 1982) who built a curved-mouth horn for use in frequency domain measurements.

This presentation describes the design and fabrication of a prototype curved-mouth horn and its time domain performance as compared with that of a conventional horn. The reception of a radiated Guassian pulse by the new horn is compared with that by the conventional horn. The results show clearly that clutter is reduced in the new horn. A time domain reflectometry experiment is described in which internal reflections by the horns are compared. The mouth reflection by the new horn is reduced in amplitude and spread out in time. The throat reflection is drastically reduced by a redesign of the connection to the groundplane stub. It is concluded that the new horn performs considerably better than the conventional horn in enhanced gain and reduced clutter. Ideas for further development will be briefly mentioned.

A4-8
1610

PROPAGATION CONSTANT OF THICK-FILM COPLANAR STRIPLINES

M. Ahmad, B. Parruck, A. A. Riad,
S. M. Riad, W. A. Davis
Department of Electrical Engineering
Virginia Polytechnic Institute and State University
Blacksburg, Virginia 24061

The paper describes a technique for measuring the propagation constant of thick-film transmission lines printed on alumina substrates. The method involves the characterization of the line using time-domain reflectrometry (TDR). Using the appropriate time windows, waveforms $e_1(t)$ and $e_2(t)$ reflected from Shorts at distances ℓ_1 and ℓ_2 respectively from the launch end are acquired. These waveforms are then transformed to the frequency domain using the fast Fourier transform (FFT) to yield $E_1(jw)$ and $E_2(jw)$ respectively.

Assuming the Shorts are identical deconvolution can be used to calculate the complex propagation constant $\gamma(jw)$.

$$\exp[-2\gamma(jw)(\ell_2-\ell_1)] = E_2(jw)/E_1(jw).$$

In the experiment, 50 ohm coplanar stripline (CPSL) are printed on alumina substrate. Each line is terminated in matched impedance on one end and is connected to the TDR line via a 3mm adaption at the other end.

The results of computation $\gamma(jw)$ for a number of lines are averaged to account for measurement inaccuracies as well as stripline variations.

A4-9
1630

THE MEASUREMENT AND DECONVOLUTION OF THE TIME JITTER IN EQUIVALENT-TIME WAVEFORM SAMPLERS:

W.L. Gans, National Bureau of Standards, Antenna Systems Metrology Group, Electromagnetic Fields Division, Boulder, CO 80303

The presence of time jitter between the trigger signal and the sampling strobe in an equivalent-time sampling oscilloscope can cause appreciable distortion of the recorded waveform. Under additive signal averaging conditions, a method has been developed to reduce this distortion. The method consists essentially of deconvolving a jitter-related effective impulse response from the recorded waveform data.

The NBS Waveform Metrology Group's Automatic Pulse Measurement System (APMS) is the primary system used for repetitive waveform measurements and calibrations in the time epoch range of 100 ps to 1 μs. It consists of a minicomputer system interfaced to a wideband (DC-18 GHz) equivalent-time sampling oscilloscope via a 14-bit D/A and A/D converter in such a manner that fast pulse waveforms may be acquired on the sampling oscilloscope screen and recorded into the minicomputer memory for subsequent processing and analysis.

As with any measurement system it is of great interest to be able to deconvolve (or otherwise remove) the distorting effects of that system from the measurement. The method described in this presentation consists of modeling or measuring an effective jitter-related time domain impulse response (jitter probability density function) and then using a deconvolution algorithm to remove the jitter related distortion from the recorded waveform data.

After the results of computer simulation studies indicated that the method was accurate and stable, experiments were conducted using actual pulse measurements on the APMS. For a given pulse measurement configuration, the jitter probability density function was measured and deconvolved from the measured pulse waveform. As with the simulated studies, the results of this technique appear to be very satisfactory.

Commission B Session 5

SCATTERING
Thursday afternoon, 6 Jan., CR2-6
Chairman: Dr. James Mink, U.S. Army Research Office,
Research Triangle Park, NC 27709

B5-1
1330

ANOMALOUS SCATTERING BY LAYERED MEDIA

C.W. Hsue and T. Tamir
Department of Electrical Engineering and
Computer Science
Polytechnic Institute of New York,
Brooklyn, N.Y. 11201

Recent work in integrated optics has stimulated considerable interest into the fields excited by realistic sources, such as laser beams, which are incident on configurations that usually involve one or more thin-film layers deposited on a thick substrate. The general features of such fields will be discussed and, in particular, it will be shown that the shape of the scattered fields is related to, and strongly affected by, leaky waves guided by the layered structure. For certain critical choices of the parameters involved, these fields may exhibit an anomalous behavior which, however, can be fully interpreted in terms of the guiding properties of the pertinent leaky waves.

To explore scattered fields, it is convenient to use a canonic configuration consisting of a dielectric layer having refractive index n_1 placed between two semi-infinite open regions with refractive indices n_0 and n_2. In contrast to symmetric ($n_0=n_2$) structures, for which a single type of leaky waves is known to occur, the more practical asymmetric ($n_0\neq n_2$) structures support both this type and a novel variety of leaky waves. In the integral representation that represents the scattered fields, the two sets of leaky waves account for poles and zeros in the integrand. When evaluating the integral in certain (visible) angular spatial domains, it is then found that the locations of these poles and zeros are qualitatively different for the two leaky wave types, but both of them may play an important role in determining the nature of the scattered fields. The particularly interesting case of incident Gaussian beams will be illustrated and it will be shown that, depending on the specific physical parameters of the layered structure, the reflected and transmitted fields may be quite different from those predicted by simple geometric optical considerations.

B5-2
1350 POLARIZATION CHARACTERISTICS OF SIMPLE EXTENDED TARGETS, Harry Mieras, Sperry Research Center, Systems Applications, 100 North Road, Sudbury, MA 01776

The dynamic polarization characteristics of simple targets which extend over several wavelengths are investigated. In particular, the loci of the polarization nulls as functions of aspect or frequency are displayed on the Poincare sphere. Null polarizations are used because these are inherent target descriptors, invariant under polarization basis transformations. The question is to what extent or in what sense are the null characteristics, or quantities related to them, invariant under aspect and frequency changes. The approach taken is to examine the null loci for dumbell target models and cylinders. It is found that even such simple targets exhibit complex null loci: The dependence of the polarization nulls upon the relative phase between the scattering centers may overwhelm the null characteristics of the individual scatterers. Some properties of the loci are: The locus is a smooth curve; if the amplitude of the individual scatterers remains constant as their relative phase varies, the locus is a closed curve; the locus may occupy a large or small area on the Poincare sphere depending on the relative strengths of the scatterers; it may be shaped as a local closed curve or circumnavigate the sphere in an undulating fashion. If the returns from the individual scatterers vary slowly with aspect, the closed curves spread into spirals. The complete polarization null history of a cylinder, for example, as aspect changes from 0° to 90°, occupies nearly the entire Poincare sphere.

B5-3
1410

Scattering From Randomly Rough Surfaces And The Far Field Approximation

Gary S. Brown, Applied Science Associates,
105 E. Chatham St., Apex, NC 27502

This paper derives rigorous results pertaining to the validity of the far field approximation for scattering from randomly rough, perfectly conducting surfaces having arbitrary statistics. The methodology employs the stochastic Fourier transform of the current induced on the infinite surface (G. S. Brown, IEEE Trans. Antennas & Propg., AP-30, 1982) by either a bounded or unbounded incident plane wave. The results are general in that no approximate simplifying forms for the current are employed. Exact expressions are obtained for the mean and variance of the scattered field for unbounded illumination and they are compared to the far field approximations to illustrate how the latter simplifications fail in this limit. Some of the pitfalls of the far field approximation in the case of beam illumination are discussed. When the incident plane wave is bounded, the conventional far field form for the mean scattered field can be rigorously derived for arbitrary surfaces, provided the cross sectional area of the incident beam is large compared to the square of the electromagnetic wavelength. The conventional far field result for the variance of the scattered field is shown to require the additional stipulation that the cross sectional area of the incident beam contains many decorrelation intevals of the surface roughness. The results obtained herein are important because they hold for arbitrary surface statistics. Whereas they appear to duplicate previous results, it must be remembered that the earlier results were only valid for a special class of surface statistics, i.e. surfaces for which single scattering theory holds.

B5-4
1450

FRESNEL SCATTERING FROM ANISOTROPIC IRREGULARITIES

Dusan S. Zrnic' and Richard J. Doviak
National Severe Storms Laboratory, NOAA
1313 Halley Circle
Norman, OK 73069

A theoretical formulation for backscattering from irregularities which have correlation length comparable or larger than the Fresnel length is developed. It is shown that the width of the spectral sampling function in the far field is inversely proportional to the antenna diameter and independent of range. The theory is applied to calculate the backscattered power from irregularities with correlation functions that consist of two parts: an isotropic part and a part that is isotropic in two dimensions. If the horizontal correlation lengths of tens of meters are assumed, the theoretical model reproduces very well the angular dependence of observed backscattered power (on the figure) as the radar beam axis is tilted away from the vertical (Röttger, J., J. Atmos. and Terres. Physics, 43, 277-292, 1981).

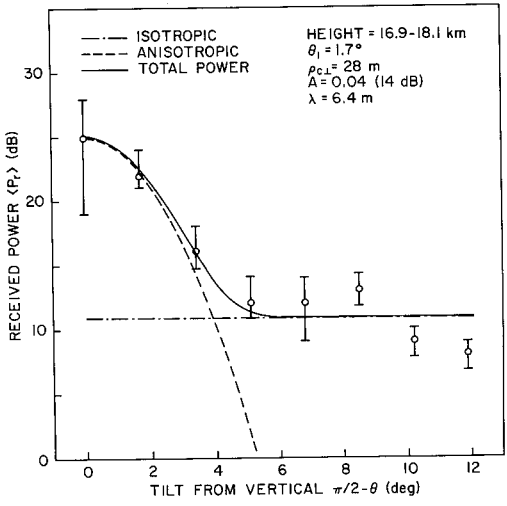

B5-5
1510

BACKSCATTER CROSS SECTIONS FOR RANDOMLY ORIENTED METALLIC FLAKES AT OPTICAL FREQUENCIES - FULL WAVE APPROACH

E. Bahar and Mary Ann Fitzwater,
U. of Nebraska, Lincoln, NE

The backscatter cross sections for randomly oriented metallic flakes are derived using the full wave approach. The metallic flakes are characterized by their surface height spectral density function. Both specular point and Bragg scattering at optical frequencies are accounted for in a self-consistent manner. It is shown that the average normalized backscatter cross sections (per unit area) for the randomly oriented metallic flakes are larger than that of a perfectly conducting sphere.

B5-6
1530

INTERACTION OF MICROWAVE INDUCED SURFACE CURRENTS ON FLAT PLATES WITH VARYING ELECTRICAL CONDUCTIVITIES

Donald A. Kelly, John P. Jackson, Robert W. Burton
Department of Electrical Engineering
University of Colorado, Colorado Springs, CO 80933

Using techniques previously developed, an infrared scanner has been used to detect surface current patterns on flat plates. These surface currents result from I^2R heating of conductive plates induced by electromagnetic radiation. In our case, square plates were irradiated with microwave frequency radiation (2-4GHz) at power density 10-30 m watts/cm^2.

It has been known that the amount of I^2R heating induced on a square flat plate is proportional to the electrical conductivity of the plate. A set of experiments are discussed which relate this heating with varying electrical conductivities. Along with these experiments, a model to theoretically calculate changes in maximum surface temperature rises due to varying surface conductivities is also presented so as to interpret experimental results.

Owing to boundary effects on the target, the surface currents induced through irradiation produce standing wave patterns. These patterns, which seem to be thermal analogues of expected current distributions, are detected by the infrared scanner. Studies to physically characterize how surface currents perform on high conductivity materials as well as how they produce detectable thermal radiation, are being conducted. Each pattern is examined as the conductivity of the individual plates is varied. These studies should yield insight as to the dependence of surface current distributions on electrical conductivity.

HIGH-SPEED DATA COMMUNICATION
Thursday afternoon, 6 Jan., CR1-42
Chairman: J. Salz, Bell Laboratories, Crawford Hill Laboratory, Holmdel, NJ 07733

C3-1
1330

HIGH-SPEED DATA TRANSMISSION OVER FADING RADIO CHANNELS

J. Salz, Bell Laboratories
Crawford Hill Laboratory
Holmdel, New Jersey 07733

A major contribution to system outage in a terrestrial digital radio channel is deep fading of the frequency transfer characteristic which in addition to causing a percipitous drop in received SNR also causes signal dispersion that can result in severe intersymbol interference. Because the temporal variation of the channel is slow compared to the signaling rate, the information theoretic channel capacity and the "Efficiency Index" in bits/cycle - a figure-of-merit we use for the communication techniques considered - can be viewed as random processes. Starting from an established mathematical model characterizing fading channels, we estimate the probability distribution of channel capacity and the distributions of efficiency indicies for different communications techniques. The repertoire of communication methods considered involves QAM modulation with adaptive linear and decision feedback equalization, and maximum likelihood sequence estimation.

C3-2 HIGH-SPEED DIGITAL TRANSMISSION ON SATELLITE CHANNELS:
1350 Douglas O. Reudink, Bell Laboratories, Crawford Hill Laboratory, Holmdel, NJ 07733

This talk will review the properties of the satellite channel at frequencies above 10 GHz and discuss techniques to achieve reliable, high-speed digital transmission.

Rain, especially in the form of thunderstorms, causes the major impairments to satellite-earth channels. The chief problems are signal attenuation and polarization crosstalk. To combat these impairments, high-gain satellite antennas, signal coding and space diversity can be employed. System performance considering weather impairments is determined for various hypothetical state of the art satellite systems.

C3-3 1430 HIGH-SPEED DIGITAL TRANSMISSION VIA OPTICAL FIBERS:

Tingye Li, Bell Laboratories, Crawford Hill Laboratory, Holmdel, NJ 07733

Optical fibers are well suited for high-speed digital transmission. Single-mode fiber systems using laser sources in the 1.2-1.6 μm spectral region can be made to operate at a data rate (per fiber) of several hundred Mb/s over repeater spans exceeding 100 km with an average transmission loss below 0.4 dB/km. Such high-performance systems are required for intercity and undersea-cable telecommunications applications. Multimode-fiber systems employing light-emitting diodes as sources can operate at 100 Mb/s over repeater spans exceeding 10 km at the wavelength of minimum dispersion near 1.3 μm. Such systems are suitable for intracity applications, including interoffice trunks, digital-carrier subscriber loops, and local area networks.

The state of the art and research progress concerning single-mode and multimode fibers, active devices, passive components, and systems will be reviewed with special emphasis on high-speed digital applications. The discussion on dispersion and loss spectra of fibers will focus on high-bandwidth graded-index multimode fibers, conventional single-mode fibers, and novel ultra-wideband single-mode fibers with minimal dispersion over a wide spectral range. Important properties of lasers and LEDs pertinent to high-speed operation will be considered, attention being paid to their transient spectra, noise behavior, and modulation bandwidth. The performance of p-i-n and avalanche photodiodes in optical receivers, with direct or heterodyne detection, will be compared. Passive components to be discussed include high-strength splices, low-loss connectors, and wavelength-multiplexers for extending the transmission capacity of fibers. Finally, encouraging recent results of high-speed systems experiments will be presented.

C3-4 1450 MODULATION COMPARISONS WITH A SATURATING AMPLIFIER CONSTRAINT: K. M. Clifford, P. Monsen, L. D. Tromp, and M. S. Wallace, SIGNATRON, Inc., Lexington, MA 02173

Uncoded and coded modulation techniques are compared in performance for a linear and nonlinear power amplifier model with the same saturation level. The nonlinear model is a third order nonlinearity typical of TWT amplifiers. The comparison is for high bit/second/Hz packing coupled with a stringent bandwidth constraint. The calculations include effects of the nonlinearities on performance and take into account an equalizer in the receiver to combat intersymbol interference. The coded systems use a combined coding/modulation approach. Coded systems are found to have potential for significant performance advantage over uncoded systems in both linear and nonlinear amplifier applications.

Commission F Session 5

REMOTE SENSING OF SURFACES - II
Thursday afternoon, 6 Jan., CR2-26
Chairman: R. K. Moore, Remote Sensing Laboratory,
University of Kansas Center for Research, Inc.,
Lawrence, KS

F5-1
1330

RADAR BACKSCATTER FROM ARCTIC SEA ICE

by
R.G. Onstott, R.K. Moore, Y.S. Kim and S. Gogineni
Remote Sensing Laboratory
University of Kansas Center for Research, Inc.
Lawrence, Kansas 66045

Measurements of the radar backscatter of sea ice conditions near Mould Bay, N.W.T., Canada, were made during the fall (October) of 1981 and during the summer (June) of 1982 as part of the FIREX/RadarSat Project. The data were acquired by the helicopter-borne University of Kansas microwave active spectrometer (HELOSCAT), operating over a frequency range of 1 to 18 GHz and an angle-of-incidence range of 5° to 70°. In this paper, a comparison of the radar cross-sections between ice types during fall, spring (previous experiments) and summer will be made and discussed in terms of the ability to discriminate among ice types. Also, the effect of small-scale surface roughness on radar cross-section will be addressed both empirically and theoretically. Data acquired under fall conditions shows a 4 dB spread in the average scattering cross-section for homogeneous first-year ice which has small-scale roughness which ranges from very smooth to rough.

F5-2
1400

PRELIMINARY RESULTS OF FM RADAR PROBING OF ARCTIC SEA ICE

by
R.G. Onstott, R.K. Moore and M. Fung
Remote Sensing Laboratory
University of Kansas Center for Research, Inc.
Lawrence, Kansas 66045

FM radar with broad sweep bandwidths can be used to probe volumes such as sea ice. An FM radar which was swept from 4.6 to 6.6 GHz and 8.6 to 10.6 GHz with angles of incidence from 0° to 35° was used to probe into an ice sheet so that an empirical examination may be made of surface roughness, penetration depth, location of scattering centers and layering. The results of this experiment will be discussed, as well as the design problems associated with short-range FM radars.

F5-3
1420

MEASUREMENTS AND MODELING OF SNOW DIELECTRIC PROPERTIES IN THE 4-18 GHZ BAND

M. Hallikainen, F. T. Ulaby, M. Abdelrazik
Remote Sensing Laboratory, The University of Kansas Center for Research, Inc.,
Lawrence, Kansas 66045

Microwave dielectric measurements of natural snow samples were made at eight frequencies between 4 GHz and 18 GHz using a free-space transmission method. The measured liquid water content covered the range between 0 to 0.12 cm^3/cm^3, and the density varied from 0.17 g/cm^3 to 0.37 g/cm^3. Dry samples were measured at temperatures between -4°C and -10°C, whereas all the wet samples were measured at 0°C. Samples were acquired from different fields and depths. The grain size varied between 0.5 mm and 1.0 mm. Most of the high wetness samples had a grain size of about 1 mm. No large clusters were observed in the samples. The measurements of wet samples were made 1 to 5 days after the snowfall. The wetness of the samples was determined with the freezing calorimeter method.

All measured quantities show a strong wetness-dependence. The dielectric constant ε' varies from 1.4 for dry snow to 2.9 for a volumetric wetness of 0.12 cm^3/cm^3 at 4 GHz, and to 2.1 at 18 GHz. The dielectric loss factor ε'' shows a relatively weak frequency-dependence, varying from practically 0 for dry snow to about 0.9 for m_v = 0.12 cm^3/cm^3. The measured attenuation constant α for the highest wetness is 180 dB/m at 4 GHz and 900 dB/m at 18 GHz.

The dependence of ε' and ε'' on snow wetness was examined through several empirical and theoretical models, including (a) simple linear and non-linear regression models, (b) the Polder and Van Santen mixing model (Physica, 12, 257-271, 1946), (c) the Tinga et al. confocal ellipsoidal model (J. A. Physics, 44, 3897-3902, 1973), and (d) a Debye-like model. The most satisfactory agreement between measured and calculated values was obtained from the application of the Polder and Van Santen and the Debye-like models, both of which yielded correlation coefficients of 0.94 or higher. Among these two models, the Debye model is preferred because it is easier to use and provides a unified approach for modeling ε' and ε'', while to fit the Polder and Van Santen model to the ε' and ε'' experimental data it was necessary that different shape factors be used to describe the water inclusions.

F5-4
1440

DIELECTRIC MEASUREMENTS OF SOILS IN THE 1.4 - 18 GHz FREQUENCY RANGE

F. T. Ulaby, M. Hallikainen, L. Wu, C. Dobson, M. El-Rayes, Remote Sensing Laboratory, University of Kansas Center for Research, Inc., Lawrence, Kansas 66045

An experimental program has been started to determine the dielectric behavior of soil-water mixtures in the microwave region. The experimental data will be used to develop a dielectric soil model, based on the physical characteristics of soils. Measurements at room temperature have been conducted between 1.4 GHz and 18 GHz on several soil types as a function of water content. In addition, preliminary measurements of frozen soils have been made in the 3-18 GHz region. This paper will present the experimental results and conclusions from the data.

A waveguide transmission method was employed at 1.4 GHz and in the 4-6 GHz range. Five different soil types, ranging from sandy loam to silty clay, were measured in both frequency ranges. In the 4-6 GHz region, two additional silt loam soils were measured. All measurements were conducted at room temperature as a function of water content. Polynomial expressions were generated for ε' and ε'' at 1.4 GHz and 5 GHz. The expressions depend on the water content and the fractions of sand and clay components of a soil in percent by weight. The linear correlation coefficients between the polynomial expressions and the experimental data are better than 0.99 for both ε' and ε''.

A free-space transmission system was constructed to cover the 3-18 GHz range. The system was tested against the waveguide method at 6 GHz, and the results were found to be in excellent agreement for both ε' and ε''. In the 3-18 GHz range, the same five soils, mentioned above were measured. In addition, pure sand, pure silt and silt with 10% of montmorillonite (clay) by weight, were measured. Preliminary measurements of frozen soils were made at temperatures between -10° C and -25° C. Polynomial expressions for ε' and ε'' up to 18 GHz are under development.

F5-5
1540

THERMAL MICROWAVE EMISSION FROM A SCATTERING MEDIUM WITH ROUGH SURFACES

R. T. Shin and J. A. Kong
Department of Electrical Engineering and Computer Science and Research Laboratory of Electronics,
Massachusetts Institute of Technology,
Cambridge, Massachusetts 02139

In the passive microwave remote sensing of earth terrain, scattering effects due to rough surfaces and terrain media play a dominant role in the determination of brightness temperatures. In this paper we develop a combined volume scattering and rough surface model by employing a Gaussian random surface and applying the small perturbation methods (SPM) which is modified with the use of cumulant techniques. The volume scattering effect of the terrain media is treated with both a discrete scatterer model where spherical scatterers are imbedded in a homogeneous background medium and a random medium model where scattering is accounted for by introducing a randomly fluctuating part in the permittivities. The coherent relectivity and transmissivity and the bistatic scattering coefficients are derived using the modified SPM and are shown to have wider regions of validity than the conventional SPM results. We make use of the radiative transfer theory to solve for the thermal microwave emission from an ingomogeneous layer bounded by rough surfaces at the top and at the bottom of the layer. We incoporate the rough surface effects into the radiative transfer equations by modifying the boundary conditions for the intensities with the rough surface scattering solution obtained using the modified SPM. The radiative transfer equations are then solved numerically using the Gaussian quadrature method and the results are illustrated and compared with experimental data.

F5-6
1600

MEASUREMENTS OF K BAND BRIGHTNESS TEMPERATURES OVER A MECHANICALLY GENERATED WAVE FIELD

P. M. Smith, Oceanography Division
Naval Ocean Research and Development Activity
Bay St. Louis, MS 39529

The emissivity of the sea surface at frequencies above 10Ghz is known to be strongly dependent on surface wind speed or some property of the sea surface which depends on wind speed. Hollinger (JGR, 75, 5209-5213, 1970) has shown how this wind dependence changes with incidence angle, frequency and polarization through measurements made from an ocean tower. The theory of Stogryn (IEEE Trans. on Ant. & Prop., AP-15, 278-286, 1967), which is based on the Kirchoff approximation, predicts the essential features of Hollinger's measurements, especially for vertical polarization. The emissivity measurements reported here were designed to provide a test of the assumptions on which Stogryn's and other emissivity theories are based and to determine which scattering mechanisms are most important.

Measurements of brightness temperature were made over a unidirectional, mechanically generated wave field. A 19 Ghz radiometer was positioned 1 meter from the mean surface of the water at various incidence angles and at both polarizations, looking both in the upwave and downwave directions. The antenna footprint was approximately 10 cm and the water wavelength approximately 1 meter. The amplitude of the waves were varied under zero wind conditions. The time series of T_B at vertical polarization can be explained, almost entirely, by assuming specular scattering from a smooth, undulating surface in spite of the observed presence of numerous small capillary waves. At horizontal polarization, however, the specular contribution was entirely absent even for extremely small amplitude waves. The horizontally polarized time series exhibited a component of radiation coherent with the wave field and an incoherent contribution having a mean temperature above the quiescent value for a flat surface. The phase coherent contribution may be related to Bragg scattering through the well known perturbation model of Rice. The water elevation was measured by a capacitance gauge and the wave slope was monitored using a fast-response laser slope gauge. A comparison of these measurements with the specular and perturbation theories is made.

F5-7
1620 SIGNIFICANT WAVE HEIGHT AND RADAR CROSS SECTION SIGNATURES ASSOCIATED WITH OCEAN RINGS, E. B. Dobson, Johns Hopkins Applied Physics Laboratory, Johns Hopkins Road, Laurel, Maryland 20707

Researchers have convincingly demonstrated that ocean rings can be detected and tracked using height data from satellite altimeters. Cold and warm rings exhibit elevations and depressions in the height data once the appropriate geoid has been removed from the altimeter measurements. The key to these vortex ring detections using height data is the geoid. Many areas of the world oceans where vortex rings are present do note have precisely known geoids. In these areas altimeters cannot be used to locate and track rings unless collinear passes are available.

This paper reports the interim results of a study to determine whether other altimeter measurable parameters such as significant waveheight ($H_{1/3}$) and radar cross section might be used in the location of rings. Various filters were applied to seven altimeter passes which were known to contain cold rings. The investigation shows wave height signatures which either increase or decrease in significant wave height from one edge of the ring to the other. Differences of up to 0.9 meters were noted between southern and northern edges. The position of highest rms wave height along the ring perimeter appears to be correlated with the wind. While $H_{1/3}$ shows promise as an aid in locating rings, radar cross section shows no consistent pattern in the rings studied to date.

F5-8
1640 SCR SYSTEM LIMITATIONS IN MEASURING BACKSCATTERED POWER AND DIRECTIONAL WAVE SPECTRA: E.J. Walsh, D.W. Hancock, III, D.E. Hines, NASA Goddard Space Flight Center, Wallops Flight Facility, Wallops Island, VA 23337, R.N. Swift, EG&G Washington Analytical Services Center, Inc., Pocomoke, MD 21851

The Surface Contour Radar (Kenney et al., IEEE Trans. Micro. Thy & Techniques, MTT-27, No. 12, 1080-1092, 1980) has demonstrated an ability to measure the Directional Wave Spectrum (DWS) of the sea (Walsh et al., Oceans '82 Conference Record, 1982). This paper undertakes an analysis of the effects on the accuracy of the DWS of the variation of the backscattered signal with wind speed, angle of incidence, and altitude. The SCR scans a pencil beam with $\pm$ 15° from nadir to measure the slant range to 51 evenly spaced points within the swath. The system always operates in a beam-limited mode at nadir and the backscattered signal level falls 6 dB with each doubling of altitude. But as the off-nadir angle increases the illuminated area eventually becomes pulse-limited and the signal falls off 9 dB when altitude is doubled. The rate of fall-off at a given altitude also varies with windspeed. At 200 m altitude the signal level is high and there is virtually no noise in the elevation measurements. As the altitude increases, the radar system noise increasingly contaminates the elevation measurements and corrupts the DWS. Using fewer than the 51 elevations computed by the SCR reduces the noise in the spectrum but also reduces the spectral resolution.

Commission G Session 4
Commission H Session 5

TOPICS IN IONOSPHERIC RESEARCH
Thursday afternoon, 6 Jan., CR2-28
Chairman: Erwin R. Schmerling, NASA Headquarters, Washington, D.C.

Dedicated to the Memory of
Arthur Henry Waynick (1905-1982)

It is with deep sorrow that we report the death of Dr. Arthur Waynick, on September 1, 1982 in London, England, while returning from a European Geophysical Union meeting.

Both directly and through his own work and indirectly through that of his many colleagues and students, Dr. Waynick has profoundly influenced the course of radio science and atmospheric research, both in the United States and abroad. His interest in these fields was established during a period of study at the Cavendish Laboratory from 1937-39. He returned to the United States in 1939 and worked in the Harvard University Underwater Sound Laboratory, transferring to the Pennsylvania State University in 1947. There he joined the Electrical Engineering Department, serving as its Head until his retirement in 1971, and as its first A. Robert Noll Professor.

In 1949 he founded the Ionosphere Research Laboratory at Penn State, serving as its director until his retirement and continuing an active participation until his death. Of particular note was his policy of engaging a group of outstanding international scientists as resident consultants to the Laboratory, a program which proved immensely productive in engaging both staff and students in cooperative research activities in important new fields of study.

He served as chairman of the U.S. National Committee for URSI in 1954, was a member of the U.S. National Committee for the IGY, of the NSF Advisory Panel on the IQSY, and of the National Academy of Sciences Geophysical Research Board Panel on the IQSY. He was a member of the National Academy of Sciences Space Science Board Committee on the Atmospheres of the Earth and the Planets, and also served as chairman of the NSF Advisory Panel on Atmospheric Sciences. He was a Fellow of the IEEE and a member of the National Academy of Engineering.

Art Waynick was a kind and considerate man. He was a continuing source of encouragement, support and counsel to his colleagues and to the many students he guided over the years, stimulating them to their best efforts. He will long be remembered with affection and respect.

Commission G Session 4
Commission H Session 5

G4/H5-1
1330 EARLY IONOSPHERIC RESEARCH AT PENN STATE:
Phillip W. Mange, Naval Research Laboratory, Washington, DC

Commission G Session 4
Commission H Session 5

G4/H5-2
1345 REMINISCING: George H. Millman, General Electric, Syracuse, NY

Commission G Session 4
Commission H Session 5

G4/H5-3
1400 THE ROLE OF DUAL POLARIZATION DIFFERENTIAL REFLECTIVITY RADAR MEASUREMENTS IN METEOROLOGY: Thomas A. Seliga, College of Engineering, Ohio State University

Commission G Session 4
Commission H Session 5

G4/H5-4
1430

A COMPARISON OF IONOSPHERIC PROPAGATION TO MICROWAVE MEASUREMENTS OF MESOSPHERIC WATER VAPOR:

Charles L. Croskey, Jack D. Carlson, Leslie C. Hale, John D. Olivero, Jung-Jung Taou, Ionosphere Research Laboratory, Penn State University; and Grace C. Joiner, Office of Naval Research, Washington, D.C.

Commission G Session 4
Commission H Session 5

G4/H5-5
1445

THEORETICAL AND LIDAR STUDIES OF THE MESOSPHERIC SODIUM LAYER:

C. F. Sechrist, Jr. and C. S. Gardner,
Aeronomy Laboratory,
Department of Electrical Engineering,
University of Illinois, Urbana, IL 61801

A 1.2-meter astronomical telescope located at the Goddard Space Flight Center Optical Test Site was used in conjunction with the laser and data collection subsystems of the University of Illinois lidar system to conduct steerable measurements of the vertical and horizontal density structures of the mesospheric sodium layer. Results of the lidar observations are being used to study the effects of atmospheric wave motions on the neutral sodium layer. In particular, wavelike features are ascribed to gravity waves in the background neutral atmosphere. Computer simulations reveal that a nonlinear model of the sodium layer response is required to describe the interactions between gravity waves and the sodium layer.

Commission G Session 4
Commission H Session 5

G4/H5-6 ION CHEMISTRY OF THE D-REGION: CURRENT STATUS
1500 W. Swider, AF Geophysics Lab., Hanscom AFB, MA 01731

The D-region long has been an active research area at the Ionosphere Research Laboratory (IRL) of the Pennsylvania State University. Professor A.H. Waynick was deeply interested in the effect of the D-region on electromagnetic wave propagation and contributed several papers to this subject. It was not until October 31, 1963, that a successful measurement of D-region positive ions was achieved, ironically by a Penn State graduate (Narcisi) at AFGL never associated with the IRL.

In 1945, Nicolet suggested that the ionization of NO by HLyα might be the source of the quiet D-region. A 1960 IRL paper by Nicolet and Aikin delved into all possible ionization sources for the D-region and gave a rudimentary ion model not compatible with the 1963 AFGL results, subsequently confirmed and added to by work at NASA, the MPI at Heidelberg and the U. of Bern. Laboratory work on the positive ions of the D-region, $H_3O^+ \cdot (H_2O)_n$, oxonium ions, has been accomplished by Kebarle and associates at the U. of Alberta, the NOAA team in Boulder, plus groups at the U. of Pittsburg and the U.S.Army (Aberdeen). For the quiet D-region, NO^+ is the precursor ion in a complex reaction scheme which yields oxonium ions. Theoretical models were given in 1977/6 papers by Reid and Thomas. For the disturbed D-region, O_2^+ is the initial ion, although its conversion to oxonium ions may be delayed where atomic oxygen is abundant. Swider and Narcisi, in a 1975 paper, obtained excellent agreement between theory and measurement. They also have shown that the clustering of oxonium ions and CO_2 may be an important mechanism hastening the formation of the heavier oxonium ions. For the quiet D-region, theory and measurements appear to agree qualitatively but detailed comparisons should be made to ensure complete agreement. An extensive winter-anomaly research program in Europe indicates that excessive NO is transported into a warm D-region which hinders oxonium ion formation according to papers by Offermann and colleagues.

More negative ion research needs to be done in both the laboratory and in situ. The U. Bern group only recently has observed the layer of heavy negative ions near 85 km measured in several AFGL flights. This layer cannot be explained by the conventional gas phase theory that the formation of negative ions begins with the attachment of electrons to molecular oxygen in a three-body process. Some progress has been made in modelling the negative ion distributions of the D-region using a simple theory, as will be discussed. Recent studies at Arecibo indicate that the ratio of negative ions to electrons is unity at about 70 km in the daytime, in line with much older D-region research.

Commission G Session 4
Commission H Session 5

G4/H5-7
1545

A REVIEW OF RADIO WAVE HEATING OF THE D-REGION:
Anthony J. Ferraro and Hai-Sup Lee, Ionosphere Research Laboratory, Penn State University

Commission G Session 4
Commission H Session 5

G4/H5-8
1600

ROCKET MEASUREMENT OF MAGNETOSPHERIC ELECTRON PRECIPITATION INDUCED BY CODED VLF TRANSMISSIONS:
Richard Goldberg and S.A. Curtis, NASA/Goddard Space Flight Center, Greenbelt, Maryland

G4/H5-9 1615 THE ITHACA AURORAL RADAR: INSTRUMENTATION, DATA ANALYSIS, AND A POTPOURRI OF RESULTS

By Wesley E. Swartz, Donald T. Farley, Jason Povidakes, and Bela G. Fejer, School of Electrical Engineering, Cornell University, Ithaca NY 14853

The auroral radar located in Ithaca NY (42.3° N, 76.4° W) has been evolving for several years. Currently the system operates at a frequency of 49.92 MHz and consists of a programmable controller, a 70 KW peak power transmitter, three 26 element co-linear dipole arrays which can be configured in various ways to provide phase interferometer information, two phase coherent receivers with quadrature base band outputs, a real time range-time-intensity (RTI) gray scale display, and a multi-channel analog tape recorder for off-line spectral analysis. The controller can be programmed to automatically cycle between up to eight different pulsing configurations and can provide unattended control of the recorder. It contains the logic for switching the RF drive to the transmitter and the transmit receive switch, and for generating the sample pulses used by the RTI. Single and multiple transmitter pulse configurations are possible. The unique real time RTI display is generated by a fast front end processor coupled to an 8080 micro-processor based system with self programming features for generating efficient inner loops. Integration time and a gain factor for the gray scale are selected via front panel switches. Over 130 ranges can be processed simultaneously and there is provision for noise subtraction.

Digitiztion of the analog tapes recorded at the radar site is done later using a new multi-channel analog to digital converter that simultaneously samples all four data channels while maintaining synchronization with the transmitter cycle. Usually raw samples are passed directly through the host computer (a Harris H123) to either a large capacity disc or tape. Processing is quite compute intensive but produces complete power spectra and cross spectra of the two receiver outputs for a large number of ranges with high time resolution.

The radar data exhibit a wide range of spectral features, some of which are similar to earlier electrojet results. Many spectra are quite broad, others are very narrow, and still others show mixtures. From the phase information in the interferometer cross spectra and the range dependence of some of the spectral features we can infer that separate scattering regions in both the vertical and azimuthal directions contribute distinct features to the total power spectrum of the signal. Some of these features do not yet have a satisfactory explaination.

G4/H5-10
1630

OBSERVATIONS OF SPACE SHUTTLE OPTICAL PHENOMENA

P. M. Banks
Space, Telecommunications & Radioscience Laboratory
Stanford University
Stanford, CA 94305

Photographic and TV observations made during darkness aboard the Space Shuttle reveal several interesting optical phenomena. The first, termed vehicle glow, results from a chemical interaction between the Orbiter surface materials and atomic oxygen of the upper atmosphere. Since the Orbiter moves at a supersonic speed with respect to the atmosphere, vehicle glow is seen only on the ram (or windward) side of the vehicle. Its physical manifestation is a bright (~10 kR) luminosity confined to a halo-like layer 5 to 10 cm thick above the vehicle surface. Spectral measurements of this glow indicate a short wavelength cutoff of 6300 A with a large increase in intensity towards the infrared.

A second source of optical emission occurs with the firing of the Shuttle reaction control jets. Large, luminous clouds of gas are seen in TV scenes. Simultaneous plasma particle and wave measurements show the excitation of broadband electrostatic noise in the ELF, VLF and LF frequency ranges as well as occasional bursts of energetic electrons and ions. Significant effects upon the potential of the Orbiter with respect to the background plasma are also noted.

Commission G Session 4
Commission H Session 5

G4/H5-11
1645 HORIZONTAL TRANSPORT IN THE F-REGION OF VENUS: John S. Nisbet, Ionosphere Research Laboratory, Penn State University

RADIO ASTRONOMY - GENERAL
Thursday afternoon, 6 Jan., CRO-30
Chairman: S. Gulkis, Jet Propulsion Laboratory,
California Institute of Technology, Pasadena, CA 91103

J4-1
1330 **MULTIFREQUENCY POLARIZATION MONITORING OF ACTIVE GALACTIC NUCLEI AT THE VLA**

L. A. Molnar and M. J. Reid
Harvard-Smithsonian Center for Astrophysics
60 Garden Street, Cambridge, MA 02138
R. C. Bignell, National Radio Astronomy
Observatory, P.O. Box 0, Socorro, NM 87801

We are pursuing a program of monthly observations of the 2 cm and 6 cm total and polarized flux densities of 17 variable extragalactic radio sources at the VLA. The sources (8 BL Lacertae objects, 7 quasars, 1 galaxy, and 1 unidentified source) were selected for their large degree of polarization position angle variability. Observations of constant sources indicate that the absolute position angle can be calibrated to within one degree at both wavelengths. Preliminary analysis indicates that one sigma errors in polarized flux densities are typically the greater of 5 mJy or 0.6% of the total flux density at 2 cm and 2 mJy or 0.3% at 6 cm. The first twelve months of data show a variety of variability behavior. They confirm the tendency for the variations in source polarization to be more rapid and have larger relative amplitude than the total flux density variations. The nature of the variations is most clearly shown in plots of the tracks of the sources in the plane of the Stokes polarization parameters Q and U. Several of the sources describe closed loops in this plane. The data will be discussed in terms of physical models of variability.

J4-2
1350 CALIBRATION OF THE VOYAGER PLANETARY RADIO ASTRONOMY RADIOMETERS ABOVE 4 MHZ:

J. J. Schauble, University of Florida Graduate Center, Eglin Air Force Base, FL 32542.
T. D. Carr, Department of Astronomy, University of Florida, Gainesville, FL 32611.

Our previously reported measurements of Jovian flux densities based on Voyager data in the 4 to 40 MHz range (Alexander et al., J. Geophys. Res. 86, 8529-8545, 1981) are incorrect because of inadequate calibration, the effect of antenna circuit resonances above 4 MHz not having been taken into consideration. We have subsequently made an improved calibration up to 7 MHz based on the impedance function presented by Sayre (E. P. Sayre, "Characteristics of the Planetary Radio Astronomy Antenna", Final Report, NASA Contract NAS5-24008, Avco Corp., June 15, 1976), calculated before the Voyager launchings from a computer-simulation model of the monopole-spacecraft combination. This model took into account the larger structural features of the spacecraft. Unfortunately, Sayre's impedance function does not extend beyond 7 MHz, because the model was considered too coarse for an adequate representation of the smaller structural details.

We have therefore developed an extrapolation of the Sayre impedance function to 40 MHz based on the thin-wire monopole function as presented by Schelkunoff, tempered by Voyager measurements of Type 3 solar burst dynamic spectra, and matched to Sayre's function at 7 MHz. We present plots of the spectral distribution of Jupiter's radiation from 40 kHz to 40 MHz based on the new calibration, for Voyager 1 and 2 data averaged over about a month before and after encounter.

J4-3
1410

A LOOK AT JUPITER'S DECAMETRIC S-BURST SPECTRA USING TWO SPECTROGRAPHS:

G. R. Lebo, W. B. Greenman, P. P. Gombola, Department of Astronomy, University of Florida, Gainesville, FL 32611; R. S. Flagg, Pan American World Airway, ASP MU 840 Bldg. 989, Patrick Air Force Base, FL 32925; J. J. Riihimaa, University of Oulu, Department of Astronomy, 90570 Oulu 57, Finland.

Jupiter emits short duration (S-Burst) decametric wavelength radio pulses which sweep downward in frequency at rates ranging from 5 MHz/sec to 50 MHz/sec, often interrupting other Jovian quasi-continuous radio events called L-Bursts. The sweeping S-Bursts seem to quench the L-Burst event already in progress, sometimes creating a V-shaped shadow (J. J. Riihimaa et al., Icarus 48, 298-307, 1981). Although a commonly acceptable theory explaining L-Bursts has yet to be presented it appears quite certain that the S-Bursts are due either to travelling electron bunches in Jupiter's magnetic field (R. S. Flagg, et al., Icarus 29, 477-482, 1976) or to a travelling exciter such as an Alfvén or magneto-acoustic wave (Staelin and Rosenkranz, JGR., in Press).

An electro-optical spectrograph having respective time and frequency resolutions of 15 msec and 200 kHz (J. J. Riihimaa, Astron. Astroph. 39, 69-70, 1975) and a real-time spectrograph having respective time and frequency resolutions of 300 msec and 3 kHz were used simultaneously to examine the S-Bursts details in more detail.

We discuss the interaction of L- and S-Bursts and examine the details of simultaneous S-Bursts having differing drift rates. The resulting crossing pattern suggests that either more than one exciter may be present at a given time or that more than one region can be simultaneously active.

J4-4
1430

MODEL JOVIAN DAM ARCS RESULTING FROM THREE-DIMENSIONAL RAY TRACING

J. D. Menietti, Southwest Research Institute, San Antonio, TX 78284
J. L. Green, NASA/MSFC, Huntsville, AL 35812
F. Six, Western Kentucky University, Bowling Green, KY 42101
S. Gulkis, JPS, Pasadena, CA 91103
D. A. Gurnett, University of Iowa, Iowa City, IA 52242

Three dimensional ray-tracing of the Jovian magnetosphere has been performed and model DAM arcs have been produced for source points along Io flux tubes at frequencies just above the R-X cutoff and initial wave normal angle, ψ, close to 90°. The model arcs extend for the full 360° of system III '65 longitude. The results indicate that the arcs so produced, which are low curvature, qualitatively match the V1 and V2 data when the angle between the spacecraft and Io is approximately 90° and the spacecraft distance is $\geq 50\ R_J$.

In order to model higher curvature arcs, the wave normal angle was allowed to vary at each frequency for source points along an Io flux tube until the model arc matched an observed arc. This technique resulted in an empirical $\psi(f)$ relationship. For the cases studied, this function is peaked around 10 MHz and falls off toward both higher and lower frequencies. We interpret these results as suggesting the higher curvature arcs, as viewed from distances $\geq 50\ R_J$, may be due to gyro-emission from electrons of higher energy than those producing the lower-curvature arcs.

FREQUENCY AND TIME STANDARDS FOR RADIO ASTRONOMY
Commission A, Session 5; Commission J, Session 5, CR1-46
Organizer: J. M. Moran

A5/J5-1 FREQUENCY STABILITY REQUIREMENTS FOR VLBI:
0840 A.E.E. Rogers, Haystack Observatory,
Westford, MA 01886

The total r.m.s. phase noise in the local oscillator system used for VLBI should be less than one radian for good coherence. VLBI experiments have been performed at frequencies up to 89 GHz and local oscillator systems with very high spectral purity and stability are needed. While a hydrogen maser frequency standard provides adequate stability on time scales greater than 100 milliseconds, the quartz crystal oscillator and multiplier chain must have adequate short term stability and freedom from line frequency phase noise. VLBI experiments at 89 GHz have shown that coherence times are limited to about 700 seconds by atmospheric phase fluctuations. Longer coherence times may be achieved in the future by using the interferometer simultaneously at a longer wavelength to calibrate the atmospheric phase. Such a calibration technique will place even more stringent requirements on local oscillator systems.

Commission A Session 5
Commission J Session 5

A5/J5-2
0900

HYDROGEN MASERS FOR RADIO ASTRONOMY

R.F.C. Vessot and E.M. Mattison

Since its inception, the technique of Very Long Baseline Interferometry has placed very stringent demands on frequency standards and has been one of the primary motivators for the development of hydrogen masers. The use of hydrogen masers in radio astronomy observatories has put a premium on ruggedness, reliability, and convenience in servicing as well as on frequency stability. Minimum size and weight are also desireable because applications in mobile VLBI terminals and the time sharing of masers among observatories still awaiting permanent maser installation make ease of transportation important. Development of SAO's VLG series of masers began in 1969 and was directed chiefly toward VLBI applications. These masers incorporate much technology learned from the development of a space maser for the 1976 Gravitational Redshift experiment and from the development more recently of improvements to cope with a wide range of environmental conditions and to reduce long-term drift. We will report data from an extensive series of tests conducted by a formal Maser Review Board at the Jet Propulsion Laboratories. Results of tests on a sorption cartridge pumping manifold to replace the ion pumps in all VLG-series masers will be reported, and progress in ongoing developments will be discussed.

A5/J5-3 HYDROGEN MASER PERFORMANCE AND FUTURE REQUIREMENTS
0920 FOR DEEP SPACE NAVIGATION

R.L. Sydnor, Jet Propulsion Laboratory
4800 Oak Grove Drive, Pasadena, CA 91109

The Jet Propulsion Laboratory (JPL) uses Hydrogen Masers for navigation, radio science and support of VLBI. The ever increasing requirements on the performance of the frequency standards of the Deep Space Network (DSN) which JPL operates for the National Aeronautics and Space Administration (NASA) necessitates the continuing evaluation, research and development on frequency standards. This paper reports on the latest evaluation of the latest hydrogen masers developed to date. These masers, which were developed by the Smithsonian Astrophysical Observatory and Goddard Space Flight Center, were tested for sensitivity to environmental effects (temperature, barometric pressure, magnetic field and humidity), long term drifts and Allan Variance and were evaluated for reliability and transportability. All the results of these tests will be included.

In the future, the performance requirements of the DSN increase by several orders of magnitude to meet the needs of outer planet navigation, gravity wave detection and VLBI. These new requirements are presented along with the technology with which it is felt that they will be met.

The research described in this paper was carried out by the Jet Propulsion Laboratory, California Institute of Technology, under contract with the National Aeronautics and Space Administration.

A5/J5-4
0940

NEW TECHNOLOGIES FOR BETTER FREQUENCY STANDARDS

D.J. Wineland, Time and Frequency Division
National Bureau of Standards
Boulder, Colorado 80303

With the increased need for better frequency standards, research is being pursued to explore new ideas which will eliminate or drastically reduce the fundamental limitations of existing standards.

Possible advances based on laser diode optical pumping (Rubidium and Cesium clocks), cryogenic techniques (H-maser), or the use of stored ions will be discussed.

A5/J5-5
1020

NEW TECHNOLOGICAL DEVELOPMENTS IN CRYSTAL OSCILLATORS

D. A. Emmons,
Frequency and Time Systems, Inc.
34 Tozer Road, Beverly, MA 01915

A brief review of recent progress in high stability crystal oscillators is presented. Among the developments which may have an impact on improved performance are:
New geometrical and mechanical designs;
Stess compensated cut angles for resonators; and
Improved oscillator circuit techniques.

Attention is specifically directed to the time domain characterization of frequency stability, for averaging times between 0.1 and 10^4 seconds. The best performance in currently available oscillators, typically for some τ between 1 and 100 seconds, is a few parts in 10^{13} (square root of the two sample variance.) Environmental and other influences which currently are limiting factors, may be circumvented by some of the new technological developments. The prospects for achieving performance approaching a few parts in 10^{14} will be discussed.

A5/J5-6
1040

LOW DRIFT DESIGN FOR SUPERCONDUCTING CLOCKS

G. J. Dick and J. E. Mercereau
Low Temperature Physics 63-37
California Institute of Technology
Pasadena, CA 91125

Atomic clocks have unparalleled frequency stability, but their low power of operation requires long integration times (1000 sec) for precise measurement. Superconducting cavity stabilized oscillators (SCSO's) have very much higher power capability, allowing optimum performance at times as short as 1 sec.

This paper will examine the optimum balance between resonator, oscillator, dimensional, and temperature stability for an all-cryogenic SCSO designed for low drifts and 10^{-16} frequency stability in the 10-1000 sec range. Sensitivity of the operating frequency to system parameters such as temperature and operating level is reduced by 100 to 1000 times compared to previous designs. The conclusion will present a ruby maser-superconducting, sapphire resonator design for a 3 GHz clock stable to 10^{-16} for 10^{3} sec.

A5/J5-7
1100 PRECISE TIME TRANSFER VIA RADIO INTERFEROMETRY:

K. J. Johnston, E. O. Hulburt Center for Space Research, Naval Research Laboratory, Washington, D.C. 20375

One of the byproducts of radio interferometry is the precise time synchronization of the bit streams of the received signals. This allows the relative time at the antennas receiving the signals to be synchronized to an accuracy proportional to a fraction of the inverse bandwidth. In search for higher angular resolution, radio astronomers have developed Very Long Baseline Interferometry (VLBI) where antennas have been separated by distances as large as the earth's diameter. In this technique the local oscillators are obtained from independent local oscillators whose frequency stability are derived from frequency standards such as hydrogen masers. In past experiments aimed at astrophysical, astrometric, and geodetic applications the relative time synchronization between antennas has been accomplished at the subnanosecond level.

The use and accuracy of VLBI for the synchronization of precise time will be reviewed in detail evaluating the limitations imposed upon VLBI by antenna geometry, radio source structure, frequency standards used to generate the local oscillators at the antenna sites, etc., as well as the difficulties encountered in transferring time from the Master Clocks to the antenna sites. The VLBI technique will also be evaluated versus other space-based techniques for time transfer such as the Global Positioning System (GPS) for future operational needs as well as the testing of precise time transfer systems.

Commission A Session 5
Commission J Session 5

A5/J5-8
1120

PRACTICAL EXPERIENCE IN CLOCK SYNCHRONIZATION USING LORAN C: A. T. Moffet, Owens Valley Radio Observatory, Caltech, Pasadena, CA 91125, and L. Beno, National Radio Astronomy Observatory, P.O. Box O, Socorro, NM 87801

In May, 1982, the NRAO Kitt Peak millimeter-wave antenna was used for the first time for VLBI. The VLBI clock, derived from a hydrogen maser frequency standard, was synchronized to UTC by use of LORAN C signals from stations at Searchlight, NV and Fallon, NV, using a commercially-available microprocessor-controlled receiver (Austron 2100). Estimates of the over-land propagation delays from the LORAN C stations to Kitt Peak were provided by the U.S. Naval Observatory. Clock offsets measured from the two stations agreed to within one micro-second. The Kitt Peak clock was also compared with clocks at Hat Creek and Owens Valley Observatories by means of the remote fringe verification capability in the Mark III VLBI terminals. For this real-time fringe search, 6cm receivers were used at each observatory, since no millimeter-wave source is sufficiently strong to yield detectable fringes with the ¼ second of data stored in the Mark III buffer. This comparison, later confirmend by the analysis of the tapes, showed that the Kitt Peak clock had been set up from a cold start to within 1.5 microseconds of UTC.

ANTENNAS
Friday morning, 7 Jan., CR2-6
Chairman: L. Wilson Pearson, Department of Electrical Engineering, University of Mississippi, University, MS 38677

B6-1
0850

THE RESONANT RECTANGULAR DIELECTRIC CAVITY ANTENNA

Mark W. McAllister, Stuart A. Long and
George L. Conway
Department of Electrical Engineering
University of Houston
Houston, Texas 77004

Dielectric resonators of various shapes have found a number of uses in microwave integrated circuit applications. The feasibility of utilizing similar resonant dielectric structures as radiating elements has been demonstrated recently for the case of cylindrical resonators (Long and McAllister, National Radio Science Meeting, Albuquerque, May 1982).

Materials typically used for resonators have very high permittivities (relative dielectric constants in the range of 100 to 300). If materials with lower values of dielectric constant (5 to 50) are used instead, proper geometrical design allows the radiated fields to be enhanced. A simple, first-order theoretical model using a magnetic wall boundary condition has been developed and the predicted fields and resonant frequencies calculated for several different sizes of resonant rectangular dielectric cavities. A dominant mode was found which was seen to provide a maxima in the far-field radiation patterns in the direction normal to the surface of the radiator.

An experimental investigation was also undertaken in which correspondingly sized antennas were fabricated and excited using a coaxial feed probe extending through a ground plane and into the dielectric. The input impedance was then measured using a network analyzer, and reasonable correlation was found between the theoretical and experimental values of the resonant frequencies.

B6-2
0910

THE FAR-FIELD RADIATION CHARACTERISTICS OF A RESONANT CONDUCTING RING ON A GROUNDED DIELECTRIC SUBSTRATE:

R.L. Holland, E.F. Kuester and D.C. Chang,
Electromagnetics Laboratory, Department of
Electrical Engineering, University of Colorado,
Boulder, CO 80309

Interest in the use of curved microstrip sections over grounded substrates as compact, circularly polarized radiators for integrated microwave circuit applications has encouraged a variety of attempts to derive an adequate characterization of the far-field radiation of such elements. However, to this point these attempts have fallen into a category of microstrip radiation estimates which account for the presence of the substrate through the use of the low frequency equivalent width of the microstrip line. The present paper discusses an approach to this problem which proceeds from a determination of the Green's function appropriate for a conducting ring over a grounded substrate of arbitrary thickness and refractive index to integral representations of the electric and magnetic fields associated with this configuration. Successive stationary phase evaluations of the field integral representations for parameter values consistent with far-field conditions provides a single finite Poynting integral with a closed form integrand.

A power pattern analysis shows that the ring element over a grounded substrate is capable of significant broadside radiation in its lowest mode of resonance, but that it exhibits more exaggerated endfire behavior as the order of resonance increases. Asymptotic analysis of the Poynting integral for rings of large radius relative to the radiation wavelength yields a favorable comparison with results obtained by the authors in a study devoted to determining the radiation loss from circular-arc-sections of microstrip by application of the local form of the radiation condition (as opposed to a Poynting integral analysis).

B6-3 0930 THE OPTIMUM FEED VOLTAGE FOR A DIPOLE ANTENNA FOR PULSE RADIATION: D. M. Pozar, R. E. McIntosh, and S. G. Walker, University of Massachusetts, Amherst, MA

A solution is presented for the time-domain voltage waveform which must be applied to the input terminals of a dipole antenna in order to maximize the amplitude of the radiated electric field at a specified time and far-field position. A constraint on the energy of the applied signal is used, and the applied signal is assumed to be bandlimited. The solution provides an upper bound on the maximum physically realizable electric field strength available from a dipole antenna, for fixed energy and bandwidth.

Briefly, an outline of the solution procedure is as follows:

1. The bandwidth of the applied voltage is specified, and then discretized into a set of frequencies suitable for later fast-Fourier transformation (FFT).

2. For each frequency in the band, Pocklington's equation is solved via the Moment Method for the current distribution along the dipole antenna. This "current mode" is normalized to 1 Amp at the dipole terminals.

3. A variational expression for the amplitudes of the current modes at each frequency is then used to extremize the electric field amplitude at a specified time t_o, and far-zone position, r_o and θ_o, subject to a constraint on the total input energy.

4. After the frequency domain terminal current has been found, the terminal voltage and radiated electric field (frequency domain) are easily derived.

5. The FFT is used to convert the frequency domain quantities of step 4 to time domain quantities.

Numerical examples are presented, and the effects of signal bandwidth, feed position, evaluation angle, and dipole length are shown. The optimum solution is also compared with the response of a Gaussian input voltage pulse, and improvements of 6 dB or more are noted.

The solution presented here is for the case of a dipole antenna. As will be seen, however, the solution is of such generality as to be capable of treating more sophisticated antennas, such as planar radiators and arrays, including mutual coupling. These problems may be considered in future work.

B6-4
0950

NEAR FIELD ANTENNA RANGES FOR ADAPTIVE ANTENNA ARRAYS:

A.W. Biggs, Remote Sensing Laboratory, CRINC
University of Kansas, Lawrence, KS 66045

The feasibility and implementation of a near field range for large antenna arrays are investigated. The investigation also includes adaptive antenna arrays at near field ranges. Advantages and disadvantages of near field over direct far field antenna pattern measurements are compared. Descriptions of the basic theory of probe compensated near field techniques and adaptive nulling are presented so that multiple usage of the near field range antenna arrays may be presented.

Analytical results by Arthur Yaghjian and Demetrius Paris and experimental verifications by Allen Newell and Paul Wacker are excellent background for near field ranges with conventional (non-adaptive)antenna arrays. With the development of extremely low sidelobe antenna arrays, the increase need is for precision in phase measurements. Similar problems occur with adaptive phased arrays, because a third antenna is introduced in the near field range. This added interaction makes a more interesting problem. Use of fast Fourier transforms (FFT) will also be applied with near field adaptive arrays.

B6-5 POLARIZATION MATCHING OF WIDE ANGLE, CONICALLY SCANNED
1030 PHASED ARRAY BEAMS: N. Amitay and M. J. Gans, Bell Laboratories, Crawford Hill Laboratory, Holmdel, NJ 07733

Multi-satellite communication may require coverage of a segment of the geosynchronous arc as large as 60°. A properly oriented ground station antenna can cover the above segment by means of a beam whose axis traces a conical surface (i.e., conically scanned beam). The antenna consists of two linear arrays feeding an imaging reflector arrangement through a polarization diplexer. This diplexer separates the incoming wave into two orthogonal polarizations without loss. In general, the polarization of the wave reflected by the diplexer does not remain the same as that corresponding to the feed array as the beam is scanned (polarization mismatch). This mismatch can cause an appreciable degradation of the antenna gain when the feed array is scanned in certain directions. For example, a ground station located at Seattle, Washington could experience 3.6 dB reduction in gain due to polarization mismatch when the antenna beam is scanned along a 60° segment of the geosynchronous satellite arc.

The above polarization mismatch loss can be substantially reduced by the use of two properly inclined polarization rotators. These devices are sufficiently broadband to cover the entire 12/14 GHz satellite communication band. Design formulas for the inclination angle between the polarization rotators are presented. Applying these formulas we have reduced the above-mentioned polarization mismatch loss to less than 0.01 dB.

B6-6 1050 DIRECTIVITY OF PLANAR ARRAY FEEDS FOR SATELLITE REFLECTOR APPLICATIONS:

Y. Rahmat-Samii, Jet Propulsion Laboratory, California Institute of Technology, Pasadena, CA 91109; and S. W. Lee, University of Illinois, Urbana, IL 61801

Array-fed reflector antennas are used extensively in today's contour and multiple-beam satellite antennas. To determine the directivity of these antennas theoretically, the total radiated power of the array feed must be accurately computed. In the initial design stage of an array-fed reflector antenna, it is necessary to approximate the element patterns with some simple functional forms which provide a convenient means of numerically analyzing the reflector performance. One such function is the $(\cos\theta)^q$ distribution which can be properly tailored to match the actual patterns of the most commonly used feed elements, such as open-ended waveguides, horns, etc. This match can be achieved in the forward hemisphere by using different q's in different pattern cuts (typically E- and H-planes).

In this paper, a closed-form expression for the radiated power is obtained for arrays with the $(\cos\theta)^q$ element patterns. The formulation which is a generalization of Forman's work takes into account polarization, non-symmetric, E- and H-plane element patterns, non-uniform element spacings and arbitrary complex excitation coefficients. The final results are expressed in terms of Bessel and Lommel functions which allow an efficient numerical evaluation. Selective numerical data are obtained to demonstrate the usefulness of these results. Comparisons are made with the available results obtained using direct numerical integration techniques, and with other available data based on less general formulations. Excellent agreement is observed for all cases. In particular, data will be presented on the directivity of seven-element cluster feeds used in multiple beam designs, and an array feed for producing a contour beam covering the Eastern Time Zone of the U.S.

B6-7
1110

ARRAY FEED SYNTHESIS FOR CORRECTION OF REFLECTOR DISTORTION AND VERNIER BEAMSTEERING:

S. J. Blank and W. A. Imbriale, California Institute of Technology Jet Propulsion Laboratory Pasadena, CA. 91109

This communication describes the on-going development of an algorithmic procedure for the synthesis of array feeds to simultaneously provide correction of reflector distortion as well as a vernier electronic beamsteering capability. This technique would be useful for correcting the gain-loss and beam pointing error which is caused by systematic reflector distortion. The distortions could be thermally induced on spacecraft antennas or gravity induced on large ground station antennas. Thus, the technique provides an electrical solution to the mechanical distortion problem. The algorithm uses the Jacobi-Bessel technique to calculate the secondary pattern of a reflector antenna having an arbitrary (i.e. distorted) shape together with a numerical search method to synthesize the parameters of an array feed in order to optimize the gain and beamsteering performance of the reflector system. A parametric study has been made using the algorithm with various array feed configurations (e.g. number and types of feed elements) and various magnitudes of distortion. Contour plots of the focal plane fields as a function of distortion have also been studied. Results obtained to-date indicate the effectiveness of the procedure.

B6-8 1130 AN INTERPOLATION TECHNIQUE FOR EFFICIENT COMPUTATIONS OF CASSEGRAIN SUBREFLECTOR PATTERNS: R. J. Pogorzelski, TRW Electronics and Defense, One Space Park, Redondo Beach, CA 90278

A recently developed algorithm (Pogorzelski, IEEE/AP-S Symposium Digest, June 1981, pp. 629-632) for computation of the physical optics integral applied to the subreflector of a Cassegrain system yields the results in a form which permits accurate interpolation. This reduces the required number of points at which the integral must be evaluated thus improving the efficiency of the overall computation.

In general, the field scattered from the subreflector may be thought of (and has very commonly been thought of) as consisting of two parts, which might be termed the specular part and the edge contribution. It is the edge contribution which gives rise to the familiar ripples on the scattered pattern. These rapidly varying ripples make straightforward interpolation difficult. However, if the two parts of the physical optics field are computed separately, the specular part, being quite smooth, may be interpolated easily and need therefore be computed at only a sparse set of points. The edge contribution may subsequently be combined with the densified specular data. Although the edge contribution must be computed at many more points than the specular part, it is much more rapidly computable. Thus, a significant reduction in overall computation time is realized.

Although the scheme is presented in the context of the new algorithm alluded to above, it is equally readily applicable to the widely used Ludwig algorithm (A. C. Ludwig, IEEE Trans, AP-16, Nov. 1968, pp. 767-769). Thus any existing computer program using the Ludwig algorithm may be modified to take advantage of the present interpolation scheme with very minimal effort.

Commission C Session 4
Commission E Session 2

SATELLITE SERVICE COORDINATION
Friday morning, 7 Jan., CR1-42
Chairman: A. Giordano

C4/E2-1
0850

Computer Software for Analyzing Scenarios of Space Communication Services

Hiroshi Akima
Institute for Telecommunication Sciences
Natl. Telecomm. and Information Adm.
U.S. Department of Commerce
325 Broadway, Boulder, CO 80303

Use of the limited resources of geostationary orbit and frequency spectrum by the space communication services including the BSS (broadcasting-satellite service) and FSS (fixed-satellite service) must be optimized. Regardless of whether or not the optimization process is automated, one must have a tool for analyzing inter-system interference of a proposed scenario (orbit and frequency use plan) of the space communication services. Since such a scenario generally involves many variables, analyzing the scenario by the use of a computer seems highly desirable. The computer software for that purpose must be reliable, efficient, flexible, upward compatible, portable, and well-documented.

A computer software capability has been developed at ITS to analyze BSS scenarios. It provides analysis results using appropriate combinations of several antenna patterns, antenna pointing tolerances, and propagation models. It includes many subroutines, each of which performs a unit procedure of the analysis. It also includes many data files of various nature. A special emphasis has been made to arrange the data files in such a way that the user of the software needs to give only essential data that uniquely specify the scenario. How to arrange the data files is one of the keys to successful development of the software.

Modification of the software is under way. The modified software will be able to analyze an FSS scenario as well as a BSS scenario. It should therefore be able to analyze not only the radio-frequency carrier-to-interference ratios but also the baseband characteristics of a desired signal interfered with by interfering signals of different modulation types. It should include a new propagation model developed by the CCIR (International Radio Consultative Committee), shaped-beam antenna patterns, and actual antenna patterns to be given numerically.

C4/E2-2
0910

BROADCAST SATELLITE EARTH STATION INTERFERENCE FROM FIXED TERRESTRIAL MICROWAVE

H.M. Gates, Institute for Telecommunication Sciences,
Boulder, CO 80303
D.A. Hill, National Bureau of Standards,
Boulder, CO

Contention for spectrum between satellites and fixed terrestrial microwave continues to pose problems for planners. Currently there are approximately 2000 private (non-common carrier) microwave transmitters deployed in the continental. United States which operate between 12.2 to 12.7 GHz. This same frequency band has been allocated for the use of broadcasting satellite services in the International Telecommunication Union Region 2 (Western Hemisphere). This domestic sharing issue will be resolved in part or in total as part of the United States preparation for the Regional Administrative Radio Conference which is to convene in mid 1983.

This research compares the operating levels of these two diverse systems and expands on selective conditions for domestic sharing while minimizing interference and concludes that sharing is possible but only under several restrictive conditions.

C4/E2-3
0950 MARGIN ESTIMATES FOR CORRELATED SATELLITE COMMUNICATION GROUND SITES (30/20 GHz)

Paul Christopher, MITRE Corporation
Bedford, MA. 01730

The 30/20 GHz satellite band will be expected to provide reliable trunking at a nominal 0.9999 availability. Extra transmitter power will be required to overcome rain and gaseous attenuation to achieve this high level of availability. Recent attenuation models, such as a 1980 Crane model, offer excellent insights into single site attenuation. A nominal 18dB margin (30 GHz) has been used recently by NASA to represent single site attenuation at 0.999 availability in some parts of the United States. However, dual diversity will be available at trunking stations and should offer relief from severe margin requirements.

Recent diversity gain relations from the United States and Japan are examined. A new bivariate exponential density function is used to calculate margin requirements at correlated ground sites. Autocorrelation functions for rainfall rate (Y. Furuhama and T. Ihara, URSI Commission F Symposium, May 1980) supply the needed correlation coefficient between separated ground sites. A correlation coefficient equal to 0.2 (perhaps 8 km separation) and 0.9999 availability yield typical margins at 30 GHz and 100°W as 8.3dB (Miami) and 3.6dB (Seattle).

Optimum orbital positions are also discussed.

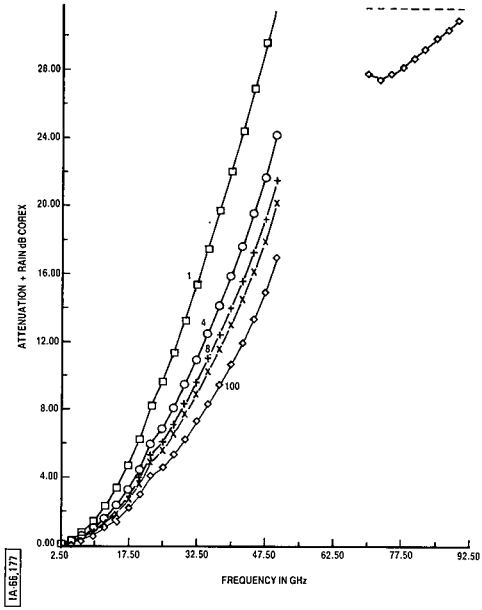

Figure M-2. ATMOSPHERIC ATTENUATION RELATIVE TO FREE SPACE FOR MIAMI — 100°W 0.9999 AVAILABILITY, DUAL DIVERSITY AT 1, 4, 8, 12, 100 km.

C4/E2-4
1010

A NEW ANALYSIS FOR RAIN ATTENUATION AT CORRELATED SATELLITE COMMUNICATION GROUND SITES

Paul Christopher, MITRE Corporation,
Bedford, MA. 01730

Valuable analysis has appeared (K. Morita, et al., Trans. of the IECC of Japan, E61, No. 6) which can relate bivariate exceedance probability to lognormal rain attenuation. This analysis, however, is exceedingly difficult to revert: Rain attenuation has not been exactly expressed as a function of exceedance. The difficulty in analysis appeared at the outset with the choice of a lognormal density function. Here, an exponential density function is chosen to represent most of the extreme attenuation of interest. A univariate density function of form

$$p(A_1) = \frac{\phi}{\beta} \exp - \frac{(A_1 - \lambda)}{\beta}$$

where

A_1 = rain attenuation at first site, dB
ϕ = fraction of time noticeable rain attenuation occurs, ~0.01
λ = lowest attenuation of interest
β = standard deviation of attenuation

The bivariate density function, with arbitrary correlation coefficient ρ, can be approximated for exceedance probability, P_e. Further, this exceedance probability relation can be reverted to find rain attenuation (switched diversity) as

$$A_r = ((1 - \rho\sqrt{1-\rho^2} + \frac{1}{\sqrt{1-\rho^2}})/\beta) \ln(C/P_e)$$

where C is also a function of ρ and β. The results give close agreement to Hodge's "diversity gain" experiments if $P_e \leq 0.0001$.

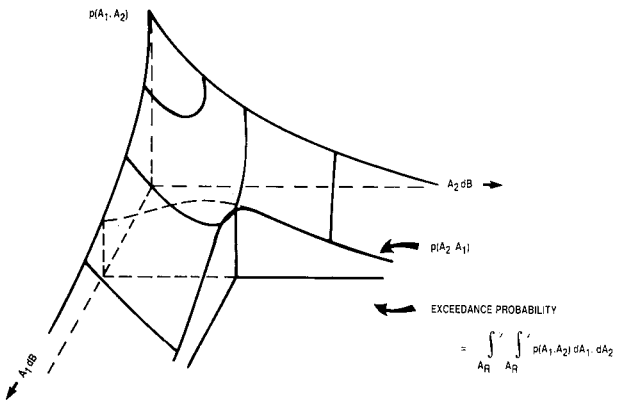

OPTICAL AND MICROWAVE STUDIES OF VEGETATIVE SURFACES - I: THEORETICAL INVESTIGATION
Friday morning, 7 Jan., CR2-26
Chairman: Jin A. Kong, Laboratory of Electronics, MIT, Cambridge, MA

F6-1 0830 BACKSCATTERING FROM A VEGETATION LAYER - A MULTIPLE COMPONENT MODEL: R. Lang, Department of Electrical Engineering and Computer Science, George Washington University, Washington, DC; and D. M. LeVine, Goddard Space Flight Center, Greenbelt, MD

Electromagnetic backscattering from a layer of vegetation over a flat ground is studied using a discrete scatter model. The vegetation is assumed to consist of leaves and stems. The leaves are modeled by flat circular dielectric discs, while the stems are replaced by circular dielectric rods of finite length. Using the dyadic scattering amplitude of these elements, the distorted Born procedure is used to calculate the backscattering coefficients from a slab of vegetation.

The distorted Born procedure is applied by first computing the mean field in the slab region due to an obliquely incident plane wave. From the viewpoint of the mean field, the slab region of discrete scatterers can be replaced by an equivalent deterministic dielectric constant. The backscattering coefficients are then calculated by employing single scattering theory where scatterers are assumed to be embedded in the equivalent dielectric medium. In performing the necessary averaging, both leaves and stems are assumed to have orientation statistics that are azimuthally symmetric with respect to the slab normal.

The scattering amplitudes for the discs and rods have been obtained by employing a physical optics technique which is valid when the leaf thickness and rod diameter is small compared to wavelength. The models are valid in the low frequency, resonant and geometric optic regions if the thinness criterion is satisfied.

Results are obtained for vegetation layers which consist of leaves only or of stems only or of both leaves and stems. These results are then interpreted geometrically by using single scattering in an equivalent dissipative medium.

F6-2
0900

SCATTERING FROM A LAYER OF ARBITRARILY ORIENTED CIRCULAR DISCS WITH APPLICATION TO VEGETATION

H.J. Eom, M.A. Karam and A.K. Fung
Remote Sensing Laboratory
University of Kansas
Lawrence, KS 66045

A vegetation layer is modeled by a collection of randomly oriented circular discs above an irregular ground plane. The backscattering coefficient from such a layer is computed using the radiative transfer theory. It is shown that significantly different results are obtained from this theory as compared with some earlier investigations using the same modeling approach but with restricted disc orientations. In particular, the backscattered cross-polarized returns cannot have a fast increasing angular trend which is inconsistent with measurements. In addition, it is possible to have the vertically polarized return higher or lower than the horizontally polarized return depending on the assumed disc distribution which is in agreement with what one might expect intuitively. Comparisons are shown with measurements taken from milo, corn and wheat and good agreements are obtained for both polarized and cross-polarized returns. Upon comparing with calculations of scattering from a vegetated half-space, it is found that the half-space case has a significantly faster angular drop-off.

F6-3
0920

REMOTE SENSING OF SOIL MOISTURE AND VEGETATION

J. A. Kong, S. L. Lin, S. L. Chuang, and R. T. Shin
Department of Electrical Engineering and Computer Science and Research Laboratory of Electronics,
Massachusetts Institute of Technology,
Cambridge, Massachusetts 02139

In the microwave remote sensing of soil moisture and vegetation fields, we may model the soil ground as a random rough surface or a periodic surface when the field is plowed in a regular manner. The vegetation may be modelled as discrete scatterers with disk, needle, spherical, and ellipsoidal shapes; or as a random medium described by correlation lengths characterizing the vegetation structure and a variance characterizing the random fluctuations. In the study of rough surface scattering and emission for both the active and passive remote sensing, the development of a theory that preserves both the principles of energy conservation and reciprocity has been proven to be a difficult and challenging task. In this paper we show that by applying a rigous modal theoretical approach to periodic surfaces, both these two fundamental principles are satisfied. We shall illustrate the theory with a sinusoidal profile for the surface although it applies to all surfaces describable by single valued functions. The results are shown to include shadowing effects and account for multiple scattering. A detailed discussion will be made by considering the behavior of each individual mode. The results for the periodic surface are then applied to the interpretation of experimental data collected from vegetation fields. The angles of observation can be arbitrary with respect to the parallel direction of the plowed field. Several combined volume scattering and rough surface models are now under active development.

F6-4
0940

AN RTE PHASE FUNCTION DESCRIPTION OF VEGETATION CANOPIES

J. A. Smith, M. H. Randolph, and D. Winder
Department of Forest & Wood Sciences
Colorado State University
Fort Collins, CO 80523

Radiative transfer theory has previously been applied to calculate optical reflective behavior patterns of such terrain media as vegetation canopies. However, most models developed have been primarily from a phenomenalogical viewpoint employing average scattering and absorption coefficients and simple canopy geometry arguments to calculate appropriate parameters in such formulations as the Duntley equations. Where more complex media abstractions have been made, Monte Carlo techniques have been employed.

In contrast, the availability of well-defined Rayleigh and Mie scattering phase functions in the atmospheric domain has led to the application of numerous and well-understood numerical solution approaches to the radiative transfer equations which are then available as benchmarks for alternative developments. In this paper, the vegetation canopy case is united with the mainstream of radiative transfer theory by the presentation and analysis of example canopy phase function formulations based on various canopy geometric and optical abstractions.

Overall characteristics of the phase functions for different canopy types are examined in terms of traditional agronomic descriptors and finally, example classical RTE solution methods are applied and compared with some of the existing canopy reflectance models.

F6-5 1040 MODELING THE REFLECTANCE OF A DISCONTINUOUS FOREST CANOPY:

Alan H. Strahler, Department of Geology and Geography, Hunter College, New York, NY; and Li Xiaowen and Janet Franklin, Department of Geography, University of California, Santa Barbara, CA

A mathematical model of the reflectance of a discontinuous coniferous forest canopy allows the direct calculation of the height and spacing of trees from remotely sensed reflectance values. The model is geometric-optical in character, treating trees as randomly positioned green cones on a contrasting background, and is driven by estimates of the proportion of each pixel in green canopy, shadow, and understory. Because the model is directly invertible, parameters of tree height and spacing can be directly inferred from spectral reflectance ratios. Field measurements from the Klamath National Forest in northeastern California show that compound Poisson models, such as the Neyman Type A distribution, are needed to describe tree spacing accurately. With correction for covariance between height and density, as well as other second-order effects, mean height and a Poisson spacing parameter can be calculated to within ten percent of true values using the model on Landsat data.

F6-6
1100

MONTE CARLO MODELING OF REMOTE EARTH SENSING WITH VARIGATED GROUND ALBEDOS

William A. Pearce, EG&G Washington
Analytical Services Center, Inc.,
6801 Kenilworth Avenue, Riverdale,
MD 20737

A Monte Carlo radiative transfer code has been developed which is capable of modeling a remote earth sensor in the visible and which takes into account horizontal variations in the earth's albedo as well as vertical atmospheric inhomogeneities and multiple scattering and/or absorbing species. The code, tracking photons backward from the sensor along their path through the atmosphere, economically models sensors with arbitrary fields of view and viewing direction. It has the capability of simultaneously modeling results for several different maps of Lambertian ground albedos, several solar incidence directions and several atmospheric profiles.

The capabilities of the code have been exploited to study the effects associated with one and two dimensional Lambertian ground albedo patterns. Our initial studies focus on three wavelengths: 0.47, 0.55 and 1.65 μm and include atmospheric profiles whose aerosol component varied from zero to moderately heavy. Results for a nadir-pointing sensor scanning across a single linear albedo boundary showed both long and short range scattering effects extending one km. or more from the boundary. When the ground albedo pattern is allowed to become two dimensional, the longer range scattering effects act to reduce overall contrast. This is illustrated by comparing the scan across a boundary between two semi-infinite regions with a scan across a boundary of a checkerboard pattern. As the dimension of the checkerboard pattern shrinks, longer range effects are further damped but contrast is reduced; i.e., the intensity gradient in the vicinity of the boundary is decreased but the overall contrast is reduced leading to signature shift effects. In addition to field-like albedo configurations, it was also useful to study albedo patterns which were sinusoidal in one dimension. These permitted direct computation of a one dimensional modulation transfer function and, hence, the atmospheric line spread function.

The results from our current efforts will also be presented.

F6-7
1120

ATMOSPHERIC EFFECTS IN SATELLITE-SENSED VEGETATIVE SURFACE FEATURES:

S.A.W. Gerstl, Theoretical Division, T-DOT,
MS B279, Los Alamos National Laboratory,
Los Alamos, New Mexico 87545

To gain a deeper understanding of the process of remote sensing we describe it mathematically as a radiative transfer problem of solar radiation through a coupled system of atmosphere and vegetation canopy. The detailed problem formulation requires therefore the solution of the radiative transfer equation and a system description in terms of all possible interaction processes of solar radiation with given system components. Algorithms that solve the radiative transfer equation have been developed in the past to varying degrees of complexity and accuracy. However, a complete systems description in terms of differential scattering and absorption cross sections is complicated due to the large number of systems components and their variable nature.

We are reporting initial results of numerical experiments applying the highly-developed discrete-ordinates finite-element method to solve the radiative transfer equation. Extending the SUITS concept of horizontal and vertical leave projections we derive expressions for photon interaction cross-sections that describe the canopy architecture in terms of measured leaf angle distributions, height-dependent leaf area index, and individual leaf reflectance and transmittance functions. Thus, to a 10-layer canopy model we added a 5-layer description of a realistic atmosphere containing rural aerosols of variable visual range in a 2-km tropospheric boundary region. Radiative transfer calculations were then performed with this coupled 15-layer canopy/atmosphere model. Computed radiances exiting a soybean canopy with LAI=2.9 compare favorably with field measurements. This agreement is improved when certain assumptions are made about the anistropy of the individual leaf scattering. In addition, comparing the radiance above the canopy with that above the atmosphere allows us to quantify the effects of the atmosphere. Our model calculations show clearly that multiple scattering effects in the atmosphere (Rayleigh and Mie scattering) dominate the satellite signal in the visual region (0.45 $\mu m \leq \lambda \leq 0.7$ μm, covered by Landsat bands 1 and 2), while in the near infrared (0.7 $\mu m \leq \lambda \leq 1.1$ μm, Landsat bands 3 and 4) the vegetation signature is perturbed typically by about 10% for rural aerosols with a surface visual range of 10 km. Other aerosol conditions have also been considered.

F6-8
1140

THE APPARENT SPATIAL RESOLUTION OF NON-UNIFORM SURFACE IMAGERY: Yoram J. Kaufman, University of Maryland and NASA/Goddard Space Flight Center, Greenbelt, MD 20771

CLEAR AIR SCATTERING, PROPAGATION AND DUCTING
Friday morning, 7 Jan., CR1-40
Chairman: J. H. Richter, Naval Ocean Systems Center, San Diego, CA

F7-1
0830

RADAR CROSS-SECTION OF MEASUREMENTS OF WINGTIP VORTICES

R.B. Chadwick and J. Jordan
NOAA/ERL/Wave Propagation Laborabory, Boulder, CO 80303

Wingtip vortices trailing behind large jet aircraft in landing and take-off configurations constitute a major hazard to small aircraft at major airports. Because of this hazard, planes must be spaced at least 3 to 6 nautical miles depanding on the type of planes involved. This spacing rule, called the 3, 4, 5, 6 rule, is a major source of delay and reduces the capacity of our large airports. Deregulation of the airline industry has increased the traffic at large airports and has changed the mix of aircraft so that large and small planes regularly use the same runways. Commercial aviation is projected to double by the end of the century without a significant increase in the number of airports. Clearly the wake vortex problem must be solved before then.

Research into wingtip vortices dates back to 1907 and public monies were first expended on the problem in 1950. During the 1970's there was a great deal of work done on the wake vortex problem and currently a large amount of literature exists on the subject. However, even with all of the effort that has been directed at this problem, an accepted, operationally oriented solution has not emerged. It appears that to be widely accepted a solution must include direct measurement of the vortices in the approach zone of the runway. Presently, indirect techniques involving measurement of the ambient wind would not be acceptable to the Canadian Aviation Administration or to the Airline Pilots Association.

A major problem over the past decade has been the lack of an all-weather sensor that can detect wake vortices to significant ranges. It was thought by people directing wake vortex research that microwave radar could not detect vortex returns. Our experiments with a short-range clear air radar have proven beyond doubt that 10 cm radar can detect and locate vortices of large commercial jet aircraft (737 and larger) at ranges of 1 km. This presentation shows our measurements of radar cross section of vortices and projects that modest radars such as ours should be able to detect vortices at ranges of 2 km. Also a discussion of vortex detection algorithms will be presented.

F7-2
0900

FEASIBILITY OF USING ASYMPTOTICS FOR TROPOSPHERIC DUCT PROPAGATION MODELING

R.A. Pappert - G. B. Baumgartner
Electromagnetic Propagation Division
Naval Ocean Systems Center, San Diego, CA 92152

A recent tropospheric propagation modeling effort directed particularly at speeding up field calculations for tropospheric ducting environments will be discussed. The modeling effort was initiated because of the fact that in the GHz range elevated tropospheric layers can support hundreds of modes and practical field calculations for anything beyond case studies require simplified procedures. These simplified procedures could involve approximations directed towards speeding up waveguide calculations or could take the form of replacing waveguide methods by ray techniques or by a hyrid mixture of waveguide and ray concepts. Involved in each of these alternatives and within the context of the modified refractivity formalism is the need for calculating plane wave reflection coefficients, or their equivalents, from layered media. This paper deals with the question of the feasibility of using asymptotic forms of the plane wave reflection coefficients for the purpose of waveguide analysis for a trilinear ducting environment.

F7-3 0920 EVAPORATION DUCTING EFFECTS AT 3 GHz AND 18 GHz: K. D. Anderson, EM Propagation Division, Naval Ocean Systems Center, San Diego, CA 92152

The results of recent one-way, fixed terminal, propagation measurements at 10 and 1.7 cm wavelengths confirm that the evaporation duct is an effective trapping mechanism to ranges exceeding twice the standard radio horizon range. A brief overview of the experiment is presented and a comparison of theoretical predictions to the observed measurements is examined in detail. Particular emphasis is placed on the discrepancies between theory and measurements noted during stable conditions.

F7-4
0940

SYSTEM ASPECTS OF ATMOSPHERIC PROPAGATION AT EHF

Jerry D. Hopponen and David M. Theobold
Lockheed Missiles and Space Company, Inc.
Sunnyvale, California 94086

Transatmospheric EHF links are susceptable to amplitude and phase effects caused by the propagation medium and not encountered in lower frequency bands. One approach to the design of systems employing such links is the use of a computer model which integrates the atmospheric filter into a simulation of the hardware performance. Although the air mass is highly variable, certain effects in clear air can be assessed to provide useful guidance in system conception and development.

Absorption by molecular oxygen and water vapor causes dispersive attenuation, phase delay, and noise due to random emission. These effects may be predicted for specific bands and atmospheric conditions by use of a computer program for calculating the complex refractive index of air and for ray tracing, and then used to generate an atmospheric filter in the system simulation. Examples of the variation of these effects illustrate the dependence on frequency ray path elevation, and season. The characteristics of the atmospheric transfer function are of particular importance to questions regarding modulation distortion in high data rate systems, where the resulting signal distortion is quantified by predicting bit error rate degradation. Specific examples calculated for BPSK communication show that phase effects may may play a major role in system performance in the band near 60 GHz, and that consideration of the multitude of absorption lines in this band is crucial to estimating system performance at various heights above the earth's surface. A summary of the atmospheric absorption model, ray tracing techniques, and communication simulation language is presented along with the examples.

F7-5
1040

MIXED-PATH PROPAGATION IN FOREST ENVIRONMENTS:

D. A. Hill, U.S. Department of Commerce,
National Bureau of Standards,
Boulder, Colorado 80303

The integral equation approach which was previously applied to propagation over irregular terrain (R.H. Ott, Radio Science, 6, 429-435, 1971) has been extended to include the effects of forest cover along the path. The forest is modeled as a lossy, anisotropic slab, and the slab parameters (thickness, permittivity, and conductivity) are allowed to vary along the path. The surface impedance boundary condition for grazing incidence on a layered medium is applied at the top of the slab. The vertical electric dipole source and the observer can be located either within or above the slab, and the height dependence is approximated by the height-gain functions for a uniform slab (J.R. Wait, Radio Science, 7, 747-750, 1967). The numerical solution of the integral equation becomes less efficient and loses accuracy for long paths at high frequencies, but the computer code has been found useful at HF for paths up to 100 km in length.

The special case of a transition from forest to bare ground has been examined in detail. An analytical solution has been obtained by performing a Kirchhoff integration over a vertical aperture at the forest transition. This method is an extension of an earlier mixed-path treatment (G.D. Monteath, Application of the Electromagnetic Reciprocity Principle. Section 4.5, 1973), and is valid when the source and observer are located far from the transition. The Kirchhoff approximation and the integral equation have been compared and are in excellent agreement away from the transition. An analytical continuation solution (T. Tamir, IEEE Trans., AP-25, 471-477, 1977) to the same geometry agrees with the Kirchhoff and integral equation solutions only when the constitutive parameters of the slab are very close to those of free space.

F7-6
1100

RAPID CALCULATION OF ATMOSPHERIC ATTENUATION

John F. Cavanagh, Code F405
Naval Surface Weapons Center
Dahlgren, VA 22448

A closed form expression has been developed for the attenuation due to atmospheric gases. This expression can be used for any elevation angle and path length. The basic assumptions underlying the derivation of the expression were an exponential height variation of the attenuation coefficient and an effective earth's radius model to account for refractive effects.

The attenuation values obtained with this model are compared with calculations made with a large main-frame computer a model consisting of the 1976 U.S. Standard Atmosphere, computed attenuation coefficients (Liebe and Gimmestad, Radio Science 13(2), 245-251, 1978) and a ray trace procedure.

F7-7 ANALYSIS OF PHASED ARRAYS ON FADING MICROWAVE LINKS:
1120 Steen A. Parl and Mark S. Wallace, SIGNATRON, Inc., Lexington, MA 02173

Multipath fading on line-of-sight links is an important factor in the design of microwave radios. The performance is strongly dependent on how the antenna couples to the propagation medium, and it is of interest to determine analytically this performance for some antenna systems. This is accomplished here by modeling the multipath with a three ray model based on ray tracing from a simplified refractivity profile. The analysis of several different arrays provides a comparison with conventional space diversity.

F7-8 1140 A STUDY OF TROPOSPHERIC SCINTILLATION AT 6 GHz USING SIGNALS FROM COMMUNICATION SATELLITE: C. N. Wang, F. S. Chen, and C. H. Liu, University of Illinois at Urbana-Champaign, Urbana, IL 61801; and D. J. Fang, COMSAT Labs, Clarksburg, MD 20871

Amplitude scintillations were observed in a 6 GHz uplink - 4 GHz downlink INTELSAT circuit between Si Racha, Thailand and Hong Kong. Approximately one year's data during 1979 have been analyzed. It will be shown that the scintillation events studied are due to tropospheric effects on the 6 GHz uplink signal. These events were characterized by slow fades with fading rates from a few tens of seconds to a few minutes. The fluctuations were in general not more than 2 db peak to peak, but reached 5 db level for several occasions. Diurnal and seasonal variations of the scintillation events will be presented. Pronounced afternoon peaks and equinoctial maxima are observed. Signal statistics including scintillation index, power spectrum and intensity distribution will be discussed. Model propagation computations have been carried out on special events with nearly periodic variations in signal amplitudes. Attempts will be made to relate the observed data to tropospheric dynamic processes such as clear air turbulence and gravity waves.

Commission H Session 6

NOVEL TECHNIQUES FOR EXCITING ULF/ELF WAVES FROM SPACEBORNE SYSTEMS
Friday morning, 7 Jan., CR2-28
Organizer: Mario D. Grossi

H6-1
0840 A REVIEW OF NOVEL TECHNIQUES FOR EXCITING ULF/ELF WAVES FROM SPACEBORNE SYSTEMS:

M.D.Grossi, Radio & Geoastronomy Division,
Harvard-Smithsonian Center for Astrophysics,
Cambridge, Massachusetts 02138

With the advent of space transportation systems, such as the Shuttle Orbiter, it will be possible to perform experiments of injection of ULF/ELF waves by using techniques that were unfeasible or impractical with smaller size spacecraft.

Very long wire antennas (with length of 100 Km or even larger) are a distinct possibility, based on the use of NASA electrodynamic tethers of the Shuttle-borne T.S.S. (Tethered Satellite System) facility. Spaceborne loops, of the cryogenic and non-cryogenic variety, are also feasible and they are being studied at present. For long wire configurations, an interesting opportunity is represented by the $\underline{v} \times \underline{B}$ mechanism: the antenna itself can now function as source of primary electric power, available for the excitation of ULF/ELF waves. Therefore, in principle, there is no need of a conventional electric primary power source (such as batteries, solar cells, thermoelectric converters, etc.) for energizing ULF/ELF injection experiments, when using long wire antennas.

Several issues still require detailed study in order to ascertain the chances of success for such experiments as the attempts at receiving on the Earth surface, above background noise, the ULF/ELF waves emitted by the spaceborne antennas. Will, for instance, the primary power generated by a 100 Km long T.S.S. electrodynamic tether be at the 50 KW level ? And will the power radiated by the wire, as Alfven waves in the ULF/ELF band, be at the 1 KW level ? Some authors put forward estimates that are close to these values. Other investigators expect lower levels, about 10 dB smaller. Additional open issues are the extent of power losses in reaching the E-layer from above, in crossing it, and in exciting long-range propagation modes in the Earth-Ionosphere cavity (or, in illuminating a bright spot on the Earth surface). From the theoretical and experimental work now under way, or under planning at this stage, it can be expected that some of the spaceborne ULF/ELF wave generation techniques mentioned above will eventually emerge as useful approaches for novel geophysical experimentation, as well as for new system applications.

H6-2
0900

EXCITATION OF VLF AND ULF WAVES BY A TETHERED SATELLITE SYSTEM

C.E. Rasmussen, Radioscience Laboratory,
Stanford University, Stanford, CA 94305

The wave equation has been solved for an arbitrary current source moving in a cold plasma. The results have been applied to a shuttle-borne tethered satellite system orbiting at approximately 250 km. The wave spectrum and therefore the radiation pattern, depends primarily upon the spacial extent in the direction of motion of the terminating bodies. Large bodies, those whose size is greater than 40 m, excite primarily the shear Alfven wave which travels along the magnetic field lines. Calculations show that wave amplitudes as high as several V/m for the parallel electric field and .01 gauss for the magnetic field can be excited. Also associated with the wave is a parallel current on the order of tens of milliamperes per m^2. However, if the size of the terminating bodies is less than 40 m, the frequency of the excited waves increases and the waves begin to spread perpendicularly to the field lines. The dependence of the excited wave modes, the radiation pattern, and the wave amplitude upon the amount and the distribution of the current flowing in the tether is discussed.

H6-3
0920 WAVE PHENOMENA ASSOCIATED WITH TETHERED SATELLITE SYSTEMS IN THE IONOSPHERE

M.Dobrowolny, Istituto di Fisica dello Spazio Interplanetario, CNR, Frascati, Italy

We consider the possibilities of wave excitation associated with the motion of a very long metallic tether in the ionosphere. The tether, up to 100 km long, is supposed to be deployed from the Shuttle and having a conducting subsatellite or balloon at the other end. The interaction of the tethered satellite system with the ionosphere is considered from two different points of view. First, results on current-voltage characteristics of the tether from models of charged particle collection from the ionospheric medium are recalled; secondly, we outline the picture of the overall ionospheric perturbation produced by the tether and, in particular, the current system associated with its motion in the ionosphere. Basic analogies with the electrodynamic interaction of Io with the Jovian magnetosphere are pointed out. Referring to the case of a conducting tether covered by an insulator, estimates are given of the power in low frequency Alfvén waves which can presumably be transmitted along the intercepted flux tubes in the case of a tether terminating with a balloon of large dimensions.

H6-4 WAVES EMISSION BY LONG ANTENNAS MOVING IN THE IONOSPHERE:
0940 Pierluigi Veltri and Vincenzo Belcastro, Dipartimento di Fisica, Universita della Calabria, Cosenza, Italy; and Marino Dobrowolny, Instituto di Fisica dello Spazio Interplanetario, C.N.R., Frascati, Italy

In connection with the presently developed TSS (Tethered Satellite System) project, we have considered the problem of radiation of both electrostatic and electromagnetic waves from long conducting tethers moving in the ionosphere. In particular we have calculated the radiation resistance with respect to low frequency plasma waves emission, from ULF up to the electron cyclotron frequency.

Both the case of an infinitely long wire and the case of a wire of finite length have been studied. In the last case the current structure of the associated Alfven wings has been explicitly obtained and the power injected in such wings has been calculated.

H6-5
1020

CHARGE: A TETHERED MOTHER/DAUGHTER ROCKET PAYLOAD

W.R. Raitt, A.B. White, CASS, UMC 34,
Utah State University, Logan, UT 84322
P.R. Williamson, P.M. Banks; SU, Stanford, CA
N. Kawashima, K. Oyama; ISAS, Tokyo
W.E. Sharp, SPRL, U of M, Ann Arbor, MI

In early 1983 it is planned to fly a tethered mother/daughter sounding rocket payload as part of the NASA sounding rocket program. The payload will be launched from White Sands missile range, and will make observations to study vehicle charging, beam plasma interactions, and the behavior of an electrically conducting tether system in the ionosphere.

The paper will describe experiments to measure the vehicle charging and beam plasma interaction on a time scale of 100 nS; to study the wave emission from the beam; to modulate the tether current; to study the energy distribution of the vehicle return current; to study photon emission from the beam and the vehicle sheath; to study the background plasma; and to study the electrical characteristics of the vehicle charge sheath.

The measurements will take place during the deployment of 400 m of electrically conducting, insulated tether. The mother attitude will be controlled to perform a stepped roll to cover pitch angles from 0 - 305^{o} for a variable beam current electron gun. The overall instrument mode changing for the complete flight necessary to meet the functional objectives of the experiment will be controlled by a microprocessor.

H6-6
1040

A LOOP ANTENNA FOR A VLF SATELLITE TRANSMITTER

H. C. Koons, M. H. Dazey, D. C. Pridmore-Brown, and A. Lu, The Aerospace Corporation, P. O. Box 92957, Los Angeles, CA 90009

The Space Sciences Laboratory of The Aerospace Corporation is presently defining an experiment to test a loop antenna configuration as a VLF transmitter in the ionosphere. The experiment is sponsored by the Naval Air Systems Command. The primary objectives of the experiment are to validate existing models for radiation by a loop antenna and to study the performance of the antenna in the ionospheric plasma.

The antenna will be carried into orbit in the payload bay of the space shuttle. During the radiation tests it will be deployed above the payload bay by the remote manipulator system. A VLF receiver aboard a subsatellite will be used to map the radiation pattern of the antenna by measuring the field intensities at distances from 1 to 100 km from the transmitter. Calculations predict that the antenna impedance will only be slightly modified by the plasma and that the link to the receiver can be closed at distances well beyond 100 km in the main lobe of the antenna pattern.

A one-third scale model of the antenna has been constructed. Impedance measurements will be made on the model in a 5-m diameter space plasma simulation chamber at NASA Lewis Research Center.

H6-7 1100 A VLF TRANSMITTER ON THE SPACE SHUTTLE: EXCITATION OF VLF WAVES USING A LONG ELECTRIC DIPOLE ANTENNA: U. S. Inan and T. F. Bell, Stanford University, Stanford, CA 94305; and R. W. Fredericks, TRW Defense and Space Systems, Redondo Beach, CA 90278

The characteristics of the VLF transmitter system designed for the Waves in Space Plasmas (WISP) project are examined. The unique aspects of such a space-born system for active studies of interactions between energetic radiation belt particles and coherent waves are discussed. Current models of emission triggering and particle precipitation that result from these interactions are used in order to assess the feasibility of the experiment. In studying the power budget of such a VLF transmitter system, the radiative element is the determining factor. The results of new model calculations of the terminal impedance and radiation efficiency of a biased dipole antenna in the magnetospheric plasma will be presented.

H6-8
1120 "Orbiter-Excited Electrostatic Emission",
Stanley D. Shawhan, Gerald B. Murphy, and Donald A. Gurnett, Department of Physics and Astronomy, The University of Iowa, Iowa City, Iowa 52242

The Plasma Diagnostics Package (PDP) on the STS-3/OSS-1 Space Shuttle Mission in March 1982, measured broadband electrostatic noise of up to 0.1 V/m electric fields. Detailed wideband measurements showed that the electric field spectrum in the 0-30 kHz range was "white" with no discernible magnetic field. The 16-channel spectrum analyzer indicated a spectrum slightly peaked at ~ 0.3 kHz with a fall-off at 30 Hz on the low end and ~ 100 kHz at the high end. Throughout the flight, the overall intensity varied ~ 70 dB with maxima at times when the plasma was rammed into the payload bay. When the payload bay doors were closed, the noise completely disappeared indicating that the noise is generated external to the Orbiter--possibly in the Orbiter wake. When the thrusters fire, the upper frequencies disappear and lower frequencies seem to be enhanced.

One interpretation of this noise phenomena is that the Orbiter motion through the ionosphere excites ion acoustic waves with wavelengths as short as $2\pi\lambda_D \sim 3$ cm which are doppler shifted up to ~ 100 kHz. The low frequency limit would then be at a wavelength characteristic of the Orbiter size (~ 20m). Total power dissipation by this mechanism is on the order of tenths of watts to tens of watts depending on assumptions about the volume in which the waves exist.

INVERSE SCATTERING
Commission B, Session 7, CR2-6
Chairman: Jerry Harris, Exxon Products Research, Houston, TX 77001

B7-1
1330 TOMOGRAPHIC AND PROJECTIVE RECONSTRUCTIONS OF 3-D IMAGE DETAIL IN INVERSE SCATTERING

N.H. Farhat, C.L. Werner and T.H. Chu
University of Pennsylvania, The Moore School of Electrical Engineering, Philadelphia, Pa., 19104

It is known from *inverse scattering theory* that multi-aspect monostatic or bistatic frequency response measurement of the far field scattered by a 3-D conducting or nondispersive body under conditions that satisfy the *physical optics* and Born approximations can be used to access the Fourier space of the scatterer. Correction of the data collected in this fashion (by wavelength and angular diversity) for range-phase, and in practice for clutter and system response, yields knowledge of a finite region of the 3-D Fourier transform of the object *scattering function*. The scattering function can be viewed as representing the 3-D geometrical distribution and strengths of those scattering centers or differential scattering cross-sections on the body that give rise to the measured field. The size and shape of the accessed Fourier region depends on geometry and on the extent of the spectral and angular apertures utilized. Reconstruction of a *diffraction and noise limited* image of 3-D object detail can then be obtained by Fourier inversion of the acquired Fourier space data.

In this paper it will be shown, using both computer generated and realistic experimentally obtained data, that high resolution *tomographic images* and *projection images* of prominent scattering centers of a 3-D body can be obtained from a limited amount of realistic data using the *projection-slice theorem* stemming from the multidimensional Fourier transform. Specifically it is demonstrated that given the data over a slice or surface of finite extent instead of within a given volume of the Fourier space, it is possible to reconstruct a high resolution recognizable image of the 3-D distribution of prominent characteristic scattering centers of the object. Because for a fixed spectral range, the number of angular observation points required to access a finite extent slice or surface in Fourier space is less than the number required to access a volume, appreciable saving in the number of elements needed to form a high resolution wavelength and angular diversity imaging aperture can be achieved. This has significant implications in the implementation of cost-effective, very broad-band, imaging radar networks capable of resolving 3-D detail on distant objects with near optical resolution. Examples of the tomographic imaging of two conducting spheres and projection imaging of a scaled model of a B-52 will be presented.

B7-2
1350

AN ESTIMATOR OF THE EFFECTIVENESS OF PRONY'S METHOD FOR RADAR TARGET DISCRIMINATION:

J.R. Auton, M.L. Van Blaricum, Effects Technology, Inc., 5383 Hollister Avenue, Santa Barbara, California 93111

This paper begins to answer the question of: How accurately can two different radar targets be discriminated based on natural resonance information present in the backscattered field from the targets. Specifically, a technique is developed for estimating the accuracy of Prony's method in extracting the natural frequencies (SEM poles) of the targets from noisy measurements of the backscattered fields. The estimator is developed so that the full resonance extraction procedure does not have to be implemented each time a Monte Carlo trial is run. Estimators of this type will be necessary in the simulation and design of future noncooperative radar target identification systems based on natural target resonances. Numerical examples are used to demonstrate the effectiveness of the estimator.

B7-3
1410 COMPUTER MODELING OF SUBSURFACE PROBING USING ELECTROMAGNETIC FIELDS, E. K. Miller, G. J. Burke, C. G. Dease, E. M. Didwall, W. A. Johnson
Lawrence Livermore National Laboratory, P. O. Box 5504, Livermore, California 94550

The radiating and scattering behavior of conducting objects buried in the ground are of interest in such diverse areas as hardened communication systems, EMP simulation, geophysical exploration, and underground construction. Our attention in this paper is directed to the latter two applications, wherein electromagnetic fields provide a means for probing into a half space such as the ground. The approach is to use an integral equation for wire objects located on either side of, or penetrating, the interface between two electrically dissimilar media. Solution of the integral equation is achieved via the moment method, and the Sommerfeld integrals are evaluated using an interpolation procedure.

Results are shown from representative computations for two different scenarios, passive probing and active probing. In passive probing, the sensing field is due to a background source, for example, the field of a broadcast station or the earth's natural electromagnetic field. Detection is then based on the local variation in the background field which is caused by scattering from a buried object. In active probing, the sensing field is produced by the probing system itself and an object's presence detected via a change in self or mutual impedance. Because the environment is a noisy one, both approaches can benefit from signal processing to improve the effective signal-to-noise ratio and reliability of detection, a subject which is also discussed.

Work performed under the auspices of the U. S. Department of Energy by the Lawrence Livermore National Laboratory under contract number W-7405-ENG-48.

B7-4
1450

THE RESOLUTION OF AN APERTURE FOR COHERENT IMAGING, RADAR, AND HOLOGRAPHIC APPLICATIONS, REVISITED: THE DEFINITION OF RESOLUTION, AND SOME EXPERIMENTAL CONFIRMATION:

W. Ross Stone, IRT Corporation,
1446 Vista Claridad, La Jolla, CA 92037

There are many instances in which a field is recorded over a finite aperture and this data is then used to reconstruct information about the source of the field: This is one class of inverse scattering problems. This is also a basic process in radio frequency "imaging" systems, such as radar (including SAR), holographic, and radio telescope systems. The process of recording the field over a finite aperture introduces a fundamental limitation on the reconstruction, often expressed in terms of the lateral resolution limit of the aperture. The classical incoherent value for this limit is $K\lambda z/D$, where λ is the wavelength, z is the perpendicular distance between the source of the field (or the scatterer or the object being imaged) and the aperture, and D is the size of the aperture. The value of K depends on the resolution criterion chosen (e.g., K = 1.22 for the Rayleigh criterion). Four years ago the author showed that the lateral resolution for such a coherent imaging system should be given, in the Fresnel approximation, by $\Delta\phi/2\pi$ times the above expression, where $\Delta\phi$ is the accuracy with which the phase of the field can be measured across the aperture. Because phase measurements at radio frequencies can typically be made to accuracies small compared to 2π radians, this often implies that a resolution which is a power of 10 or more smaller than the classical value should be obtained. It was also shown that $\Delta\phi$ is related in a simple way to the signal-to-noise ratio of the measurement, and similar results were derived for the longitudinal, or depth, resolution.

These results were apparently not obviously applicable in many potential applications because of the definition used for resolution used in deriving them. There was also no experimental demonstration of the results, and no obvious procedure for obtaining this improved resolution. A definition directly applicable to imaging and self-cohering radars is used to rederive these previous results, obtaining the same basic expressions. It is then shown how these results have recently been independently verified in an experiment by H. D. Collins et.al., which also suggests a straightforward procedure to obtain this improved resolution.

Acknowledgement: Many helpful and enlightening discussions and suggestions from B. D. Steinberg and A. K. Luthra contributed significantly to this work.

B7-5
1510

WAVE EQUATIONS FOR RADIATING AND NONRADIATING SOURCES, AND SOME RESULTS ON UNIQUENESS AND RESOLUTION FOR INVERSE SOURCE AND INVERSE SCATTERING PROBLEMS

W. Ross Stone, IRT Corporation
1446 Vista Claridad, La Jolla, CA 92037

Nonradiating sources are sources which produce fields that vanish everywhere outside a sphere of finite radius. The determination of the source term in the inhomogeneous Helmholtz wave equation from knowledge of the fields due to that source over a closed surface exterior to the support of the source distribution is termed the inverse source problem. When the source consists of sources induced by the interaction of an incident field with the inhomogeneity of a medium, this becomes an inverse medium problem. Bleistein and Cohen (J. Math. Phys., 18, 194-201, 1977) have shown that the inverse source problem has a unique solution if and only if the source has no nonradiating components. Using their expansions for the radiating and nonradiating portions of the source, this paper shows that the radiating portion satisfies an inhomogeneous wave equation, while the nonradiating portion satisfies the homogeneous wave equation. The implications of these results for the physical (vis-a-vis mathematical) realizability of nonradiating sources are discussed, as well as the implications regarding the uniqueness of the inverse source problem.

The analogue of a nonradiating source for the inverse medium problem is a nonscattering potential (or refractive index). It is known that such potentials exist for a single, monochromatic plane wave incident field. By contrast, it is also known that a potential is uniquely determined by the fields scattered by an infinite set of incident plane waves (see H. P. Baltes (ed.), Inverse Source Problems in Optics, Springer-Verlag, 1978, Chap. 3 and references therein for a discussion of these concepts). A very important practical case falls between these two extremes: Given a finite number (>1) of incident plane waves, over what set of potentials can uniqueness be achieved? This question is investigated in light of the new results obtained above, and a relationship between spatial resolution and uniqueness is obtained. The consequences of this result for the inverse source problem are pointed out, in terms of obtaining at least a limitation on the set of nonradiating sources which can be associated with a set of scattering data.

Commission F Session 8

OPTICAL AND MICROWAVE STUDIES OF VEGETATIVE SURFACES II: OBSERVATIONAL INVESTIGATIONS
Friday afternoon, 7 Jan., CR2-26
Chairman: D. S. Kimes, NASA/Goddard, Greenbelt, MD

F8-1 1330 MICROWAVE IN-SITU MEASUREMENTS OF THE DIELECTRIC PROPERTIES OF TERRAIN: J. Jian, R. K. Moore, R. Swanson, and R. Zoughl, Remote Sensing Laboratory, University of Kansas Center for Research, Inc., Lawrence, KS 66045

In this paper a simple, in-the-field, real-time dielectric measurement technique is described. It is shown that a monopole antenna, together with a reflecting plate, may be used as a probe for measuring both the real and the imaginary parts of the dielectric constant. The measurement of the real part of the dielectric constant ε_r' is performed by measuring the resonant frequencies of both free space and the sample. Then, by measuring the Q-factor for both cases we can define the imaginary part of the dielectric constant ε_r''. Several results of measurement of the dielectric constant of rocks and soils are given. Comparison between the dielectric values obtained with this technique and those obtained using conventional methods show good agreement between the measured values.

F8-2
1400

MEASUREMENTS OF THE MICROWAVE DIELECTRIC AND ATTENUATION PROPERTIES OF PLANTS

R.P. Jedlicka and Fawwaz T. Ulaby
Remote Sensing Laboratory
University of Kansas, Lawrence, Kansas 66045

To relate the microwave propagation properties (absorption and scattering) of vegetation canopies to their physical properties, such as volumetric moisture content, vegetation density, and plant geometry, two types of experimental measurements were conducted. The first consisted of measurements of the attenuation due to propagation through soybeans and corn canopies at each of several stages of growth. The second set of experiments involved measurements of the complex dielectric constant of leaves and stalk materials as a function of moisture content. The measurements were made at several frequencies in the 1-8 GHz band. The results of these measurements will be presented, together with a discussion of how dielectric mixture theory may be used to relate the dielectric properties of the plant parts to that of the canopy.

F8-3 1420 EFFECTS OF VEGETATION CANOPY STRUCTURE ON MICROWAVE BACKSCATTER: Jack F. Paris, Earth Resources Research Division, NASA Lyndon B. Johnson Space Center, Houston, TX 77058

Electromagnetic wave scattering by discrete elements depends on the dielectric constant and the size and shape of the elements. A vegetation canopy is a polydispersive collection of discrete scattering elements. In the case of coherent microwaves, the interactions of the waves with the canopy and the underlying surface is complex. It is important that the fundamental nature of these interactions be well understood in order to lay the proper foundation for the specification of remote sensing systems for particular vegetation applications such as crop identification and crop canopy condition assessment using synthetic radar aperture imagery.

Several observational studies have shown that the backscattering coefficient of some crops is affected significantly by changes in the wavelength used. In some cases, backscattering is enhanced when the wavelength is close to the size of the plant parts that interact with the incident waves. Also, changes in the orientation of plant parts due to natural differences in plant morphology or due to the effects of the wind have been observed to cause significant changes in the backscattering properties of the canopy.

In an effort to understand this phenomenon better, mathematical models were formulated to predict the backscattering coefficient of typical vegetation canopies. The Monte Carlo approach was used with various distributions of plant part sizes and orientations. The paper reports the results of such modeling investigations.

F8-4 1440 ATMOSPHERIC INFLUENCE UPON OBSERVATION OF SURFACE BIDIRECTIONAL REFLECTANCES

D. J. Diner, 183-301, Jet Propulsion Laboratory
4800 Oak Grove Drive, Pasadena, CA 91109

Sources of error in surface reflectance property measurements due to atmospheric contamination are being investigated. Modification of intrinsic angular and spectral reflectances at the "ground truth" level can arise due to illumination of the target by diffuse skylight in addition to direct (although attenuated) sunlight. Further attenuation and modification of the signal occurs during transmission through the atmosphere to space. Another source of contamination is the "adjaceny effect", or influx of scattered photons from a neighboring surface of possibly different angular and spectral reflectance.

The magnitudes of these effects are calculated quantitatively using several radiative transfer algorithms. The relative proportions of photons with varying histories (e.g., direct vs. diffuse reflection, atmospheric path radiance) for a homogeneous surface boundary are studied using the Grant-Hunt matrix operator method. For studies of the adjaceny effect and influence of a non-uniform ground, a new calculational method has been introduced. The essential and unique aspect of this method is a spatial Fourier transformation of the three-dimensional radiative transfer equation and solution for the diffuse radiation field in the Fourier domain. The spatial field is then reconstructed from the individual components. The technique is applicable to any surface albedo distribution with non-Lambertian bidirectional reflectances. Sample calculations for several test cases will be presented.

This work is funded under contract NAS7-100 with the National Aeronautics and Space Administration.

F8-5
1540

SPECULAR AND DIFFUSE REFLECTANCE OF TWO WHEAT CANOPIES MEASURED AT MANY VIEW ANGLES:

V.C. Vanderbilt, L. Grant, L.L. Biehl, B.F. Robinson, Laboratory for Applications of Remote Sensing, Purdue University, West Lafayette, IN 47906

This paper reports research to understand how visible light is scattered - both diffusely and specularly reflected and linearly polarized - by wheat as a function of sun-view directions, two crop development stages, and wavelength. The analysis is based on 200 spectra taken continuously in wavelength from 0.45 to 0.72 μm in 33 view directions using an Exotech model 20C spectroradiometer six meters above two wheat canopies in the boot and fully headed maturity stages.

The results of this analysis demonstrate a technique involving polarization measurements for separating the canopy reflectance factor into two fractions - one due to specular reflection of sunlight by canopy foliage and the other due to diffuse reflectance of light by canopy foliage. The results show that the amount of specularly reflected sunlight from the two canopies is greatest in the blue spectral region and decreases gradually with increasing wavelength. The results show that in a particular direction the ratio of specularly reflected sunlight to the total (specular and diffuse) reflected light is generally large viewing toward the sun azimuth. Yet the results also show that as a fraction of solar irradiance the amount of specularly reflected light is minimum in the solar azimuthal view direction.

The results show that the portion of the reflectance factor attributed to diffusely reflected light from foliage varies with wavelength, crop development stage, and view directions. The total variation and the variation as a function of view direction were significantly greater for the headed wheat canopy.

To separate the diffuse and specular components of the reflected light, it is necessary to correctly orient a polarization analyzer on the radiometer used to acquire the data. The sun-view directions define a plane of incidence of sunlight specularly reflected to the radiometer. The results demonstrate that for acquisition of data during clear sunny conditions, regardless of view direction, the polarization analyzer should be oriented parallel to this plane of incidence.

F8-6 1600 DYNAMICS OF DIRECTIONAL REFLECTANCE FACTOR DISTRIBUTIONS FOR VEGETATION CANOPIES: D. S. Kimes, Earth Resources Branch, NASA/Goddard Space Flight Center, Greenbelt, MD 20771

Directional reflectance factors that span the entire exitance hemisphere were measured for homogeneous vegetation canopies and row crops in red and near IR bands. Other supporting measurements included leaf orientation distributions, row height and width, percent ground cover, leaf area index, and the optical properties of the leaves and soil. For each cover type these data were collected at different solar zenith angles during a clear day.

These data and literature data were used to study the dynamics of the directional reflectance factor distributions of plant canopies as a function of the geometric structure of the canopy, solar zenith and azimuth angles, and the optical properties of the leaves and soil. The data were used to validate a radiative transfer model for heterogeneous three-dimensional scenes. The paper reports the results of the measurement and modeling investigations which provide insight to the physical interactions involved in the dynamics of directional reflectance.

F8-7 1620 UNDERSTANDING THE TEMPORAL REFLECTANCE BEHAVIOR OF CULTIVATED CROPS USING POPULATION BIOLOGY MODELS: G. D. Badhwar, NASA Johnson Space Center, Houston, TX 77058

It is known that various biological systems undergo differing developmental sequences, and consequently have different growing lengths. These developments manifest themselves in reflectance changes over time, called a temporal profile. These changes have proven to be the key for separation and unique identification of several crops. A model of this temporal file, for the Kauth-Thomas Greenness, G, is suggested to be of the form

$$\frac{dG}{dt} = k(t)G(1 - \frac{G}{G_m})$$

where G_m, is the carrying capacity ('saturation valve') of the plant population and k(t) is a complicated function of time. We show that this model describes the known properties of many cultivated crops. Attempts to relate k(t) to the Leaf Area Index as a function of time will be discussed.

F8-8 1640 ANALYSIS OF SAR DATA WITH EMPHASIS ON POLARIZATION AND LOOK ANGLE EFFECT OVER A FOREST-RELATED SCENE: S. T. Wu, NASA/NSTL/ERL, NSTL Station, MS 39529

The Seasat L-band and the aircraft X-band dual polarized SAR data acquired over a forested-related scene were examined, preprocessed and analyzed in conjunction with ground truth data to gain a basic understanding of the measurements and data characteristics in the microwave regions of the spectrum associated with specific surface materials and cover types. The forest related scene contains large stands of deciduous (oak-tupelo), coniferous (pine) forest, agricultural fields, pasture, shrubs, barren land, urban areas, clearcuts and open water. Count value and histogram analysis of the four polarization X-band SAR with two look angle configuration data sets and the one polarization one look angle Seasat L-band SAR result in the following findings: The Seasat L-band SAR data contain the smallest range of count value variation while the aircraft X-band SAR VV polarization the largest. The aircraft X-band SAR HV and VH polarization data contain the same type of count value distribution. HH polarization data from both aircraft and Seasat SAR are sensitive to the wetness or water content in the surface while VV and HV data are not. This is in agreement with the finding reported by Elachi et. al. Using land cover types in the study area, it may be concluded that VV polarization data is good for vegetation detection, HH polarization data is good for surface wetness detection and HV polarization data is good for very rough surface detection. Comparison of the two look angle data set suggests that the change of radar return from vegetative surface such as deciduous, forest, pine forest, clearcut, pasture, cropland and wet field are insignificant when the incidence angle is changed from 35 to 55 degrees.

Commission G Session 5
Commission H Session 7

IONOSPHERIC MODIFICATIONS
Friday afternoon, 7 Jan., CR2-28
Chairman: J. S. Nesbitt

G5/H7-1
1340

EXCITATION OF ULF HYDROMAGNETIC WAVES BY MODIFICATION OF IONOSPHERIC CONDUCTIVITY

P. B. Morris and T. J. Rosenberg,
Institute for Physical Science and Technology
University of Maryland, College Park, MD 20742
and
L. J. Lanzerotti, Bell Laboratories, Murray Hill
NJ 07974

In a recent paper, Rosenberg et al. [Phys. Rev. Lett., 47(18), 1343-1346, 1981] reported observations of geomagnetic field pulsations in the frequency range ∿0.01-0.02 Hz (i.e., Pc4) associated with solar x-ray events. The characteristics of these ULF pulsations, as observed on the earth's surface at magnetically conjugate locations, were consistent with those expected for eigen-oscillations of the geomagnetic field. The magnetic field oscillations were identified as magnetospheric hydromagnetic (Alfvén) waves, presumably excited by the flare-associated changes in ionospheric conductivity. Several additional events have now been analyzed which further support this identification. An analysis is presented of the relative spectral power in subsets of the 30-300 sec band as a function of time during pre-flare, flare, and post-flare periods, the relative spectral power for the dominant frequency component(s) within the Pc4 band, and the spectral development of the horizontal field components in conjugate regions. Estimates of the solar flare-induced ionosphere conductivity variations in these events are obtained based on satellite x-ray flux data. These results suggest that artificial techniques capable of producing substantial sudden conductivity enhancements or depletions on a local scale (e.g., chemical releases, HF heating, electron beams) might excite magnetospheric hydromagnetic waves. The solar-flare-induced changes in conductivity are not periodic, indicating that sudden conductivity changes are sufficient for the excitation of waves; periodic modulations of the conductivity, as suggested in several recent proposals, are not necessary.

G5/H7-2
1400 NONLINEAR GENERATION OF WHISTLER WAVES BY BEAT OF TWO HF-PUMP WAVES IN THE AURORAL IONOSPHERE*:

G.J. Morales, M. Shoucri, and J.E. Maggs (Physics Department, University of California at Los Angeles, Los Angeles, CA 90024).

An analytic study is made of the excitation of whistler waves in the frequency range $\omega/2\pi \gtrsim 5$ KHz by high-power HF ($\omega/2\pi \sim 5$ MHz) pulses launched into the auroral ionosphere from the ground. The physical principle consists of generating an in situ nonlinear antenna located between the reflection layers of two HF-pump waves of frequency ω_1, ω_2 and radiating a whistler wave of frequency $\omega = \omega_1 - \omega_2$. The nonlinear antenna results from the electromagnetic beat ponderomotive force which produces an oscillatory ambipolar electric field that drives the whistler wave. By properly choosing the frequencies ω_1 and ω_2, one can selectively adjust the overlap between the two Airy patterns such that a localized antenna is created with an effective wavenumber matching that of a whistler at frequency $|\omega_1 - \omega_2|$.

The generated whistler is radiated along the magnetic field lines in a head-light pattern. One part of the signal is earth bound, the other is ducted along the magnetic field lines away from earth. The efficiency of the process has been calculated from first principles and although it is found to be quite small, detectable signals appear to be possible at HF powers compatible with present auroral ionosphere heating facilities (HIPAS in Alaska and HEATER in Norway).

*Work supported by ONR.

Commission G Session 5
Commission H Session 7

G5/H7-3
1420

STIMULATED HF TO ELF DOWNCONVERSION IN THE IONOSPHERIC E-REGION: K. Papadopoulos, C. L. Chang, K. Ko, A. Reiman, and V. Tripathi, Science Applications, Inc., McLean, VA 22102; and P. Palmadesso, Naval Research Laboratory, Washington, DC 20375

A novel scheme for generating ELF waves in the E-region of the ionosphere by nonlinear stimulated downconversion of HF is presented. The dominant nonlinear force driving the ELF wave is due to the ohmic heating nonlinearity, while the force on the pump and the sideband is controlled by the collisionless ponderomotive force. It is shown that for pump powers above threshold the interaction is spatially localized and leads to pump depletion. The efficiency of power transfer from HF to ELF for the hybrid collisional-collisionless coupling exceeds by more than two orders of magnitude the efficiency for a purely collisionless system given by the Manley-Rowe relations. Computational results for pump threshold and downconversion efficiency for parameters appropriate to communication schemes and ELF magnetospheric probing will be presented.

G5/H7-4 1440 ELF RADIATION FROM AN ARTIFICIALLY MODULATED AURORAL ELECTROJET:

H.G. James, Communications Research Centre,
Department of Communications,
P.O. Box 11490, Station 'H',
Ottawa, K2H 8S2, Canada
R.L. Dowden, University of Otago,
Box 56, Dunedin, New Zealand.

During a collaborative scientific campaign in Dec. 1981, the ionospheric heater of the Max-Planck-Institut für Aeronomie (P. Stubbe et al., J. Geophys. Res., 86, 9073-9078, 1981) located near Tromso, Norway transmitted on a carrier frequency of 2.8 MHz. The carrier was square-wave amplitude modulated using a format of four frequencies between 525 and 4125 Hz. ELF waves were radiated by the modulated auroral electrojet and were received at an altitude of 1200 km by the ISIS-I spacecraft. Signals were received along a 450-km stretch of the orbit centred south and west of the heated region. All signal frequencies were above the gyrofrequency of the dominant ion, O^+, and below the lower hybrid resonance frequency, at spacecraft height. Harmonics of the fundamental modulation frequencies, present because of the square wave spectrum, were also observed.

The observed spatial limits of the radiation zone agree with computed three-dimensional ray paths for the right-hand-polarized wave mode in a O^+-e^- plasma. The observed group dispersion with frequency indicated that the ionospheric E- and F- region densities were low in comparison with median values. The radiated power fluctuated on time scales of the order of a fraction of a second. Received power varied over several orders of magnitude. The effective ac current of the electrojet can be estimated on the basis of the short-dipole theory for a cold plasma.

Commission G Session 5
Commission H Session 7

G5/H7-5
1520

CHARACTERISTICS OF IONOSPHERIC EFFECTS OF ELF RADIATION GENERATED BY MODULATION OF THE CURRENT SYSTEM

R. Allshouse, K. Carroll, H.S. Lee,
and A.J. Ferraro
Ionosphere Research Laboratory
Department of Electrical Engineering
Pennsylvania State University
University Park, PA 16802
R.G. Joiner
The Office of Naval Research
Arlington, VA

This paper describes recent measurements of ELF radiation created by modulating the dynamo current system with the high power HF "heater" facility of the Arecibo Observatory, NAIC. The authors have observed the generation several times but this paper explores some newer observations and their ionospheric features. Discussed will be the correlation of intensity of ELF generation with heating as measured with the cross-modulation equipment, the strength of ELF generation due to daytime and night-time dynamo current magnitudes, the polarization of ELF waves as related to the overhead dynamo current direction and the measurement of the mean height of the ELF source. Finally stepped frequency data are presented and a simplified model of the ELF antenna is discussed.

Commission G Session 5
Commission H Session 7

G5/H7-6 1540 LONG PATH PROPAGATION AND DETECTION OF ELF RADIATION GENERATED BY MODULATION OF THE EQUATORIAL ELECTROJET

A.J. Ferraro, H.S. Lee, R. Lunnen, K. Carroll, and R. Allshouse
The Ionosphere Research Laboratory
Dept. of Electrical Engineering
Pennsylvania State University
University Park, PA 16802
R.F. Woodman
Instituto Geofisco Del Peru, Lima, Peru

ELF radiation can be generated by modulating the dynamo current system, polar electrojet or equatorial current system with a high power HF heater facility. Briefly discussed are past results using the Arecibo and Tromso facilities.

New observations at 1.0 Khz are described in which the Jicamarca radar was used as the heater with ELF receiving equipment located at Arecibo, Puerto Rico. Future experiments are to be discussed.

G5/H7-7
1600 IONOSPHERIC MODIFICATION USING HIGH POWER HF-WAVES IN THE AURORAL REGION*: M. Shoucri, G.J. Morales, and J.E. Maggs (Physics Department, University of California at Los Angeles, Los Angeles, CA 90024).

A model is presented showing effects of heating the polar ionosphere by high-power high-frequency waves launched from a ground-based transmitter. The transport equations are approximated by two coupled nonlinear equations of the diffusion type which are numerically solved for the electron density and temperature. The results are pertinent to on-going ionospheric heating experiments located in the auroral region (HIPAS in Alaska and HEATER in Norway).

The analysis has shown the existence of localized large scale density cavities produced by ohmic heating near the HF-wave reflection layer, where absorption is highest. The mechanisms governing the deformation of both the density and temperature profiles are explained. Their time evolution and spatial scalelengths are estimated for different modes and frequencies of the HF-waves.

*Work supported by ONR.

G5/H7-8
1620

RF HEATING EFFECTS ON THE ARECIBO D-REGION, FROM DYNASONDE OBSERVATIONS:

J.W. Wright, The Cooperative Institute in Environmental Sciences, University of Colorado, Boulder, CO 80309
L.M. Duncan, Los Alamos National Laboratory Los Alamos, New Mexico 97545
S. Ganguly, Rice University, Houston, Texas

A half-hour episode of 10-sec. ON/OFF heating of the daytime ionosphere shows clear phase path effects on four Dynasonde diagnostic frequencies reflected in the E and F regions. The heating itself is shown to be confined to the upper D-Region and well below the heater reflection altitude of 114 km. The data suggest a prompt electron density modulation of about 5%.

Condensed Technical Program (cont.)

THURSDAY, 6 JANUARY

0830-1200

A-3 Microwave and Field Measurements	CR1-46
B-4 Transients	CR2-6
C-2 Information Thoery	CR1-42
F-3 Remote Sensing of Surfaces-I: The Sea	CR2-26
F-4 (See J-3)	
G-3 Ionospheric Propagation	CR1-40
H-4 Wave Emissions From Artificial Electron Beams	CR2-28
J-3/F-4 Atmospheric Effects and Radio Astronomy	CR0-30

1330-1700

A-4 Time Domain Measurements	CR1-46
B-5 Scattering	CR2-6
C-3 High-Speed Data Communication	CR1-42
F-5 Remote Sensing of Surfaces-II	CR2-26
G-4/H-5 Topics in Ionospheric Research	CR2-28
J-4 Radio Astronomy	CR0-30
CCIR Study Group 5	OT8-6

1700

Commission B Business Meeting	CR2-6
Commission J Business Meeting	CR0-30

1730

Commission G Business Meeting	CR2-28

2000

Executive Council Meeting	OT8-6

FRIDAY, 7 JANUARY

0830-1200

A-5/J-5 Frequency and Time Standards for Radio Astronomy	CR1-46
B-6 Antennas	CR2-6
C-4/E-2 Satellite Service Coordination	CR1-42
F-6 Optical and Microwave Studies of Vegetative Surfaces-I: Theoretical Investigation	CR2-26
F-7 Clear Air Scattering, Propagation and Ducting	CR1-40
H-6 Novel Techniques for Exciting ULF/ELF Waves From Spacebourne Systems	CR2-28

1330-1700

B-7 Inverse Scattering	CR2-6
F-8 Optical and Microwave Studies of Vegetative Surfaces-II: Observational Investigations	CR2-26
G-5/H-7 Ionospheric Modeling	CR2-28